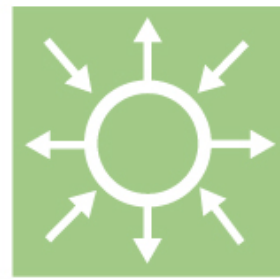# Cable System Transient Study

Vindforsk V-110. Experiments with switching transients and their mitigation in a windpower collection grid scale model

Elforsk report 09:05

Muhamad Reza and Henrik Breder   January, 2009

Cable System Transient Study

Vindforsk V-110. Experiments with switching transients and their mitigation in a windpower collection grid scale model

Elforsk report 09:05

Muhamad Reza and Henrik Breder   January, 2009

Preface

The purpose of this project was to study and quantify switching transient in a cable collection grid system by measuring real transients in a laboratory scale with the possibility of control and variation of parameters, configurations and switching cases including abnormal states.

The work was carried out by the laboratory staff at ABB Corporate research as a project within the Swedish wind energy research programme "Vindforsk II". The report is the final report for project V 110 Cable System Transient Study. The report is written by Muhamad Reza and Henrik Breder. Further, the work has been carried out by Muhamad Reza and Henrik Breder with involvement of Lars Liljestrand, Ambra Sannino, Leif Hederström, Lars Nordin, Kenneth Johansson and Frans Svendsen at ABB Corporate Research.

Vindforsk – II is funded by ABB, the Norwegian based EBL-Kompetanse, E.ON Sverige AB, Falkenberg Energi AB, Göteborg Energi, Jämtkraft AB, Karlstad Energi AB, Luleå Energi AB, Lunds Energi AB, Skellefteå Kraft AB, Svenska Kraftnät, Swedish Energy Agency, Tekniska Verken i Linköping AB, Umeå Energi AB, Varberg Energi, Vattenfall AB and Öresundskraft AB.

Comments on the work and the final report have been given by a reference group with the following members:

Sture Lindahl	Gothia Power
Michael Lindgren	Vattenfall
David Söderberg	Vattenfall
Ola Carlson	Chalmers
Stanislaw Gubanski	Chalmers
Torbjorn Thiringer	Chalmers
Philip Kjær	Vestas
Lars Gertmar	ABB

Stockholm January 2009

Anders Björck

Summary

Large cable-based systems such as collection grids for wind parks emerge worldwide. Transient overvoltages (tov.), appear, e.g., at grid energizing, de-energizing and fault handling. IEC test standards do not consider cable characteristics or repetitive re-strikes. This needs a clarification of transients in wind park cable collection grids with respect to causes, prevention, and mitigation.

A laboratory environment has been created at ABB Corporate Research to enable measurements on typical apparatus within well-defined circuits and controlled parameters. Worst-case conditions can be tested with limited risks in terms of possible hazard and cost.

Results from experiments on characterizing transient overvoltages in a cable system are presented. This is made along with theory and the verifications and comparisons of commonly used surge protection methods, namely: surge arresters, surge capacitors and RC-protection.

 ❖ The experiments verify the consistent occurrence of repetitive pre-strikes and re-ignitions in a cable system. The occurrence is determined by the electrical circuit and the point-on-wave of switching operations.

 ❖ Surge arresters always limit the maximum voltage magnitude but voltage steps with a magnitude twice the protective level could occur while the voltage can swing within a band in magnitude below the surge arrester protection level from negative to positive polarity.

 ❖ Surge capacitors and the RC-protection show mitigation effects although not removing the repetitive transients completely.

The selection and application of such mitigation methods still requires engineering with a basic understanding of physical phenomena.

Mixing up different causes of transient overvoltages could lead to wrong decisions regarding the surge protection. Transient overvoltages caused by voltage escalation due to multiple re-ignitions, for instance, has been very little discussed today. Common knowledge of such is also limited.

 • This investigation concludes and quantifies the occurrence of repetitive transients with high steepness compared with IEC standard impulse tests.

 • The results also show that a few repetitive pre-strikes frequently occur during closing operations with inductive load, which are known to occur with all most commonly used types of breakers.

It is not within the scope of this work to determine what is a dangerous (respectively, a safe) level of steepness of tov. This is expected to be different for different components depending on type of insulation and electrical design. However, when considering:

- the fact that an insulation failure starts with a discharge avalanche due to local initial e-field stress

- the fact that ac voltage magnitudes in high order of frequency content distribute locally different from the fundamental frequency case

these quantified transients must be considered in the dimensioning of the related components. It is therefore recommended to further investigate the insulation coordination of the components within large cable-based systems such as collection grids for wind parks.

Sammanfattning

Stora system av kablar i form av insamlingsnät för vindparker ökar i antal världen över. Transienta överspänningar förekommer exempelvis vid spänningssättning och bortkoppling av insamlingsnätet samt i samband med hantering av elektriska fel. IEC standard tar hittills inte hänsyn till varken kabelkaraktäristik eller repetitiva återtändningar, viket påkallar behov av en förklaring av transienternas uppkomst och eventuella möjliga åtgärder.

En laboratoriemiljö har skapats hos ABB Corporate Research för att möjliggöra mätningar med typiska komponenter i väldefinierade kretsar med tillhörande parametrar och där svåra fall kan provas med begränsade kostnader och risk för skador.

Resultat från experiment med karaktärisering av transienta överspänningar i kabelsystem har presenterats. Jämförelse mellan teori och mätningar har gjorts samtidigt som effekter av olika lindrande åtgärder har studerats.

❖ Experimenten verifierar ett konsistent uppträdande av repetitiva för- och återtändningar av brytare i kabelsystem. Villkoren för uppträdande bestäms av den elektriska kretsen och det aktuella ögonblicket/ elektriska fasvinkeln i vilken brytaren manövreras.

❖ Ventilavledare begränsar alltid spänningens amplitud, men spänningssteg av storlek av dubbla skyddsnivån, dvs. från plus till minus, kan förekomma inom ett område som bestäms av skyddsnivån.

❖ Skyddskondensatorer och s.k. RC-skydd visar mildrande effekter men eliminerar inte transienterna.

Val och applikation av skyddsmetoder kräver dock ingenjörsarbete under insikt och förståelse av grundläggande fenomen.

Hopblandning av olika källor och orsaker för transienta återvändande spänningar kan leda till felaktiga beslut om skyddsåtgärder. Transienta överspänningar orsakad av spänningsstegring genom repetitiva återtändningar diskuteras numera mycket sällan. Allmänna kunskaper om dessa fenomen är begränsade.

• Denna undersökning konkluderar och kvantifierar förekomsten av repetitiva transienter med hög branthet jämfört med IEC standard test.

• Resultaten visar också att få repetitiva återtändningar uppkommer under slutning med induktiv last vilket är vanligt för samtliga förekommande kopplingsapparater.

Arbetet som redovisas i denna rapport omfattar ej någon bedömning av riskerna med de uppmätta transienterna vilka kan skilja sig avsevärt mellan olika objekt med hänsyn till isolationens material, uppbyggnad/geometri.

Dock gäller:

- ett isolationsfel i form av en "avalange" initierad av en lokalt hög elektrisk fältsyrka, såkallad initial fältstyrka

- en överspänning med högt frekvensinnehåll fördelar sig olika från en motsvarande överspänning med huvudsakligt grundtonsinnehåll (50Hz)

dessa transienter måste beaktas vid dimensionering av aktuella komponenter i större kabelsystem som fallet med insamlingssystem för vindkraftparker.

Table of Contents

1 Introduction

The main contribution of this work is the experimental verification of the occurrence of tov. phenomenon in cable systems. An attempt is made to characterize this phenomenon in terms of magnitude, number of re-ignitions and the rate of voltage step, and to verify these parameters in order to compare mitigation methods.

1.1 Project Description

A major part of the Vindforsk project namely "V-110 Analys av transienter i kabelsystem" is the establishment of a laboratory environment resembling the collection grid in a wind park which has been created at ABB Corporate Research and used to enable measurements on typical apparatus within well-defined circuits and controlled parameters.

The work was carried out in cooperation with two other Vindforsk projects: Chalmers V-220, namely: "Analys av högfrekventa elektriska svängningar i vindparker" and with Vattenfall Power Consultants (VPC) V-108, namely "Design av elsystem för havsbaserade vindkraftparker".

An overview of tov. caused by switching operations is shown in below[1].
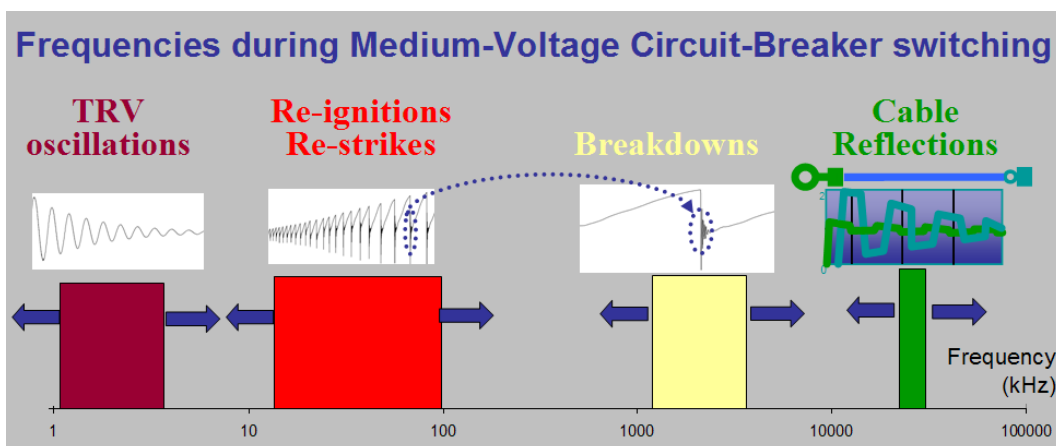
Figure 1: An overview of transient overvoltages, tov., caused by switching operations

---

[1] Modified from Glinkowski, Electrical Environment of Transformers, Open Workshop, CIGRE JWG 12/13/23.21,
http://cigre1.avenda.fr/WG12132321/workshopparis02/FinalPackageR5.ppt slide #61 (no longer available at internet), Paris, August 2002, Reported in prepared by CIGRE JWG A2-A3-B3.21. A similar picture can be found as Fig. 7
www.e-cigre.org/Search/download.asp?ID=ELT_218_2.pdf in
www.esat.kuleuven.ac.be/electa/publications/fulltexts/pub_954.pdf

The ABB Corporate Research group has also during decades made on-site measurements in several industrial facilities, in which some results have been published [1], [2].

1.2 ABB Wind Cable Laboratory

1.2.1 Laboratory Experiments vs. Field Measurements

Actual measurements from field installations are basically the best source of information for studying complex phenomena in large grids. When doing field measurements, the measurements are made on an actual circuit with all real conditions. However some limitations exist such as:

- Difficulties to isolate the causes of specific phenomena.
- Space limitation for measuring equipment and sensors and limited time on site.
- Commercial aspects, also concerning responsibility for the live operating system.
- Safety aspects as well as risks of damaging equipment.

On the other hand, laboratory experiments have the following advantages:

- Different apparatus can be tested in well-defined electrical circuits in controlled environment.
- Possibility to change parameters and measured variables.
- Possibility to create conditions that can be difficult to achieve in real networks, such as faults.
- Worst-case conditions can be tested with limited risks and costs.
- Repeatability of tests.

A combination of field measurements and laboratory experiments if possible is then the best option. In this report, however, investigation on tov. phenomena in cable system is done by means of laboratory experiment only. Furthermore, it is verified that the measurement results can be verified satisfactorily to qualitative analysis.

1.2.2 Wind Park Representation in the Wind Cable Laboratory

Due to limitations of the laboratory arrangement, a small section of a wind park is reproduced within the laboratory setup. The illustration of the wind park section reproduced within the ABB wind cable laboratory can found in Figure 2 in which the schematic diagram (single line diagram, SLD) is shown in Figure 3.

Figure 2: The part of wind park reproduced in the laboratory setup (grayed area)

Figure 3: ABB Wind Cable Laboratory system line diagram (SLD)

1.2.3 Remark on the Wind-Cable-Laboratory Experimental-Setup

The radial fork structure of the test laboratory presented in Figure 3 was intended to enable studies of reflection phenomena[2]. However, hundreds of recurrent surges from re-ignitions in combi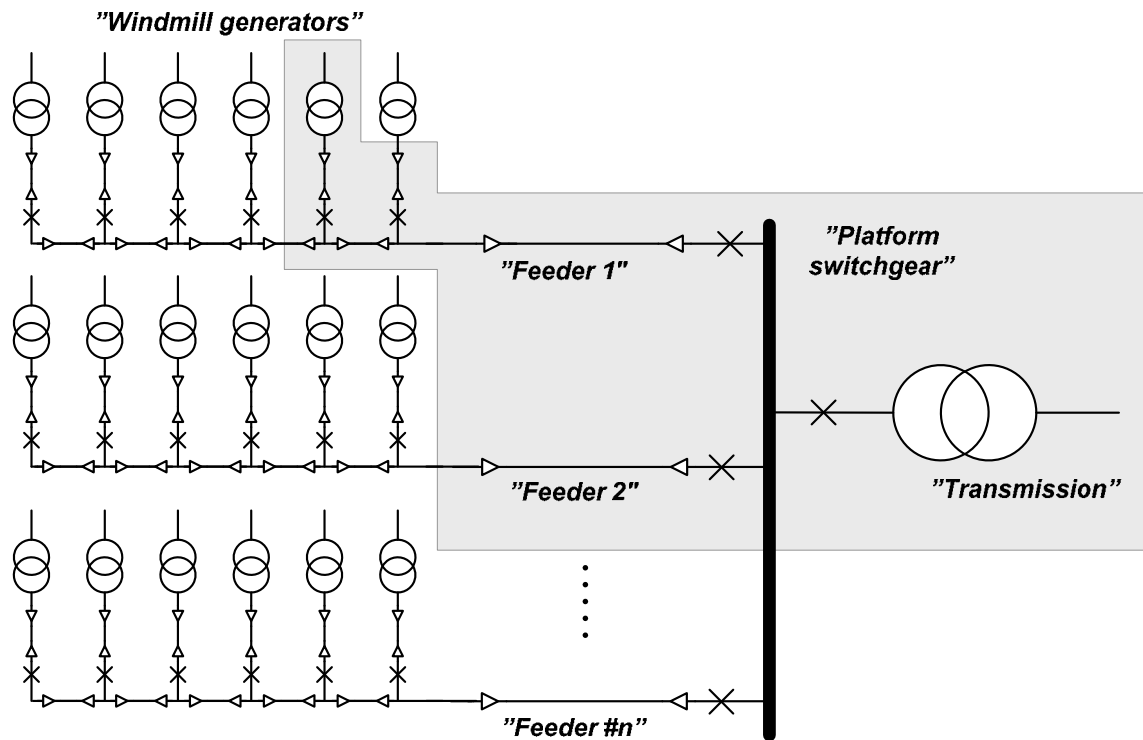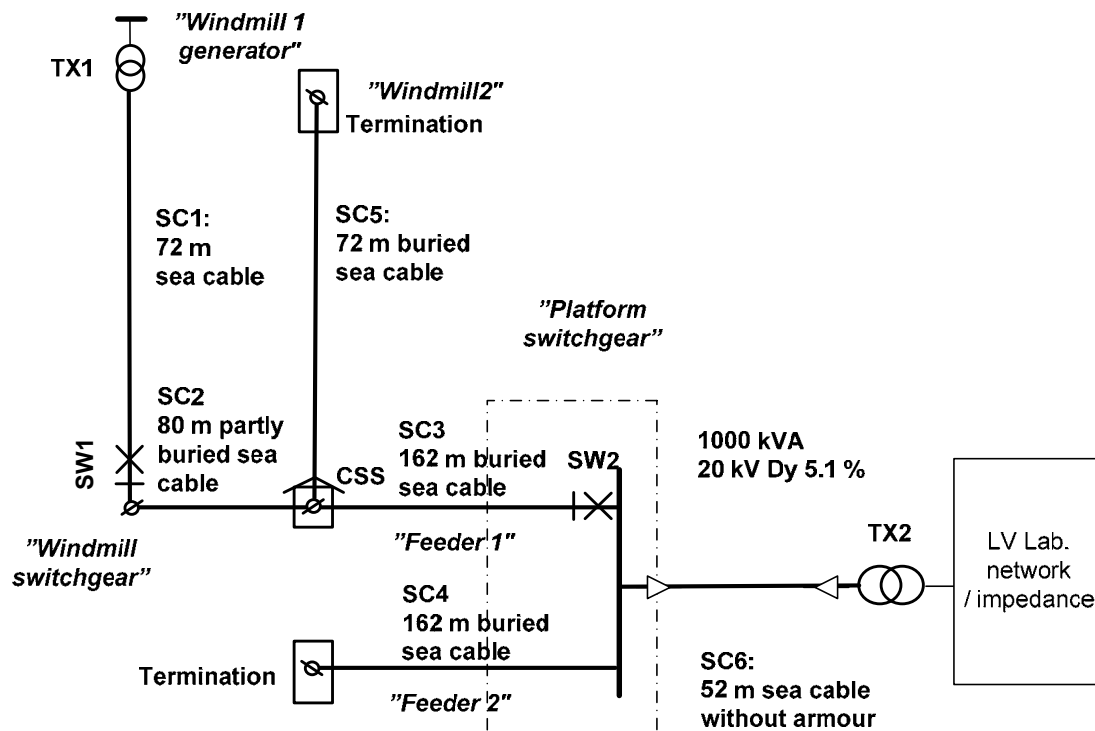nation with multiple reflection points dramatically complicate the evaluation of the studies. Therefore, in order to evaluate models, to identify and compare the consequences of parameter changes as well as to understand the physical behavior of the switching devices used within this study, it was necessary to reduce the number of wave reflection points. Consequently the extra feeder SC4 and the extra windmill tee-off SC5 (Figure 3) were disconnected during the evaluated laboratory experiment presented in this report. The details of the laboratory setup with these two extra feeders disconnected will be presented later in Section 3.

1.3 Scope

The scope of this report is to cover the experimental verifications in the laboratory and supporting the Vindforsk projects V-108 and V-220, hereby focusing the scope of tov. in wind power parks.

- The experimental part has been defined as the characterization of measured transients in terms of voltage level, time-derivative and repetition frequency in actual cases.

The results have been obtained from laboratory experiments within an environment that was created at ABB Corporate Research enabling experiments with actual apparatus in a controlled environment.

---

[2] Multiple Reflection Points and Repetitive Surges

   Every point in a cable system which provides a discontinuity in terms of wave impedance causes wave reflections. Given an extensive cable system with a large number of feeders and cable terminals, a number of reflections will occur corresponding to the discontinuities and respective reflection points. Reflection points with different travel distance to the source and to any other points will cause a time difference corresponding to the travel speed over the different lengths. Consequently a number of reflection points cause a complicated pattern of reflections while the wave is propagating throughout the system while reflected back and forth from every point, until each wave finally arrives at a certain terminal at different time-points. However, wind mill collection grids are usually regular in shape with a large number of equidistant sections which make a large number of reflections coincide.

   Simulations of rectangular structured grids also show a clear pattern of multiple waves appearing from reflections with equal and consistent time intervals.

   Each surge current also induce voltages in the adjacent phases creating secondary waves in every possible propagation mode in the three-phase system between the three line conductors, equipotential grounding and earth. Combining all wave reflections of each single wave and adding hundreds of recurrent wave pulses from repetitive re-ignitions propagating in at least four modes, give a high dignity of complexity derived from the number of reflection points in a three-phase cable system.

Switching medium voltage system for energizing, de-energizing and fault handling differ very much between

- OHL for which many MV components are made, and

- MV collection cable systems in wind power.

The intention is to use traditional MV components and apparatuses to stay cost-effective.

The results of the transient overvoltage characteristics in a cable system and the verification of commonly utilized surge protection devices, namely surge arresters (e.g., ZnO), surge capacitors and RC-protection on mitigating the tov. are presented.

It is not within the scope of this work to determine what is a dangerous (respectively, a safe) level of steepness of transient overvoltages. This is expected to be different for different components depending on type of insulation and electrical design and the component manufacturers.

1.4 Definitions

a	Reflection coefficient when a traveling wave reaches a termination
b	Refraction coefficient when a traveling wave reaches a termination
BRK	Circuit Breaker (Breaker)
C, C#	Capacitor, Capacitor with capacitance equal to #-nF
Cap	Capacitor
C_{load}	Load Capacitance
COV	Continuous Operating Voltage
$C_{surge-cap}$	Surge-Capacitor Capacitance
Emf	Electromotive force
ID	Identity (in "Case ID")
IEC	International Electrotechnical Commission
I_{BRK}	Current recorded across breaker
L	(Stray-) Inductance
LIWL	Lightning Impulse Withstand Level
LV	Low Voltage
l	Length of (grounding) wire for calculating the stray inductance
MV	Medium Voltage
OHL	Overhead Line
PSCAD	Power Systems Computer Aided Design
R, R#	Resistor, Resistor with resistance equal to #-Ω
RC-Protection	Resistor-Capacitor Protection
$R_{protection}$	Resistance part (in Ω) of the RC-Protection
r	Radius of (grounding) wire for calculating the stray inductance
SC#	Submarine Cable. Six submarine cable (24 kV, 240 mm^2) sections are installed in the laboratory: SC1-SC6.
SLD	System Line Diagram
SW	Switching apparatus
t	Time
t_{delay}	Time delay

tov.	transient overvoltage
t_{rise}	Rise time, time taken by a voltage step from its 10% to reach its 90% of the maximum value
TX1	Transformer at the node representing the "Windmill Generator" in the laboratory circuit
TX2	Transformer at the node representing the "Feeding Grid" in the laboratory circuit
$t_{10\%}$	The instant when the voltage (of a strike) is at its 10% of the step
$t_{90\%}$	The instant when the voltage (of a strike) is at its 90% of the step
t_{max}	The instant when the voltage (of a strike) is at its maximum value
t_{min}	The instant when the voltage (of a strike) is at its minimum value
$U_{10\%}$	The voltage point (of a strike) with the value equals to 10% of the step
$U_{90\%}$	The voltage point (of a strike) with the value equals to 90% of the step
ΔU	Voltage step magnitude when a strike occurs
ΔU_{limit}	Minimum level of the magnitude of voltage-step change to be identified as a strike
U_m	Maximum voltage (for cable rating)
U_{max}	Maximum voltage (of a strike)
U_{min}	Minimum voltage (of a strike)
U_n	Rated voltage
U_{peak}	Supply peak voltage
U_{TX1}	Voltage recorded at transformer TX1 terminal
U_{BRK}	Voltage recorded at breaker terminal (towards the load/transformer TX1)
$\dfrac{\Delta U}{\Delta t}$	Rate of voltage step in a positive-strike from the time when the minimum voltage is recorded to the time when the maximum voltage is recorded; or rate of voltage change in a negative strike from the time when the maximum voltage is recorded to the time when the minimum voltage is recorded
$\dfrac{dU}{dt}$	Rate of voltage step in a strike at a certain instant

$\left(\dfrac{dU}{dt}\right)_{10\%-90\%}$	Rate of voltage step in a strike from the time when the voltage point reaches its 10% value to the time when the voltage point reaches its 90% value, of the strike's voltage step
$\max\left(\dfrac{dU}{dt}\right)$	The maximum rate of voltage step in a strike
XLPE	Cross-linked polyethylene (a.k.a. PEX)
ZnO	Zinc-Oxide surge arrester
Z_{surge}	Surge impedance of Cable
μ	Permeability of (grounding) wire
τ	Time constant
τ_2	Time constant after a transient protection device (e.g. surge capacitor) is installed

1.5 Structure

This report has the following structure.

Section 1 Introduction (this section) describes the purpose and scope for this report as well as terms, abbreviations and acronyms used. The introduction to the ABB Wind Cable Laboratory is also presented in this section.

Section 2 Problem Description describes the potential for the occurrence of tov. in cable systems, the risk objects subjected to tov. and some commonly known surge protection devices. In the end of the section, some considerations regarding the potential tov. worst cases are highlighted.

Section 3 Laboratory Setup and Test Scenarios describes the details within the laboratory experiment reported throughout this document. This section covers the description of the laboratory circuit, the types and parameters of the circuit apparatuses, the surge protection devices to be tested, the types and parameters of the devices used within the measurement system and the type and parameter of the load used in the laboratory circuit as well as the description of the test scenarios, the selection of test cases, the list of the tested cases and the test routines performed to each test case.

Section 4 tov. Analysis Method describes the background and logics of the attempt to characterize tov. phenomenon in terms of magnitude, number of re-ignitions (strikes) and the rate of voltage step. Ways for presenting the tov. indicators obtained from the tov. analysis method are also described in this section.

Section 5 Base Case (ZnO Only) Results and Analysis presents the results and detail analysis of the laboratory base case, when surge arresters (ZnO) are installed without any other surge protection devices added (implemented). The basic phenomena of traveling waves obtained from the laboratory experiment are presented and verified in this section.

Section 6 Experiment and Verifications of tov. Mitigation Methods presents the results and detail analysis of the laboratory cases where mitigation methods are implemented in addition to surge arresters. The mitigation methods tested are surge capacitors, RC-protection and point-on-wave control.

Summary of Results, **Section 7**, summarizes the results obtained from the laboratory experiment in general.

Section 8 Conclusions concludes this report.

In S**ection 9** Remark, the authors state their awareness on research ongoing within IEEE and CIGRE communities in similar area: studies on tov. in cable systems.

Section 10 Future Works points some potential continuations of this project.

In **Section 11** References, source material and further reading are specified.

In **Enclosure A, Section 12,** a detail explanation of the impact of stray-inductance loop on surge capacitors is given.

Enclosure B, Section 13, some concerns related to the worst cases highlighted earlier in **Section 2** are presented in more details.

Finally in **Enclosure C, Section 14** presents tables with all tov. steepness indicators defined in 4.2.4.

2 Problem Description

2.1 Transient overvoltages in Cable Systems

In overhead line, OHL, systems the transient overvoltages (tov.). are often related to lightning induced over voltages and therefore electrical apparatus is currently tested with a standard lightning impulse – lightning impulse withstand level (LIWL) – of 1.2/50 μs surge. Surge arresters are used as common protection agains tov.

There are significant differences between cables and OHLs. While tov. in OHL systems are often caused by lightning, tov. in cable systems can be caused by circuit breaker (breaker) operations: closing and opening breakers and switches.

Furthermore, the surge impedance for OHLs is typically 300-400 Ω while it is less than 40 Ω for cables. The lower surge impedance may result in the higher time derivative of the tov. This is because the time constant for the voltage across a load like a transformer when hit by a step voltage propagating along a transmission line (cable or OHL), depends proportionally on the surge impedance of the cable and the capacitance of the load.

- The consequence is that the same transformer will see at least 10 times higher time derivatives of the tov. if connected to a cable system than to an OHL when exposed to the same overvoltage source.

- The tov. in cable systems may have high rate-of-rise and repetitive nature.

Current test specified in the IEC standards however do not yet consider cable characteristics or the repetitiveness of tov.

- Consequently attention is drawn to characterize the transient phenomena that can occur in a cable system and to investigate the effectiveness of commonly utilized protection devices for mitigating this high-time-derivative tov.

The investigation covered by this report is focused on tov. caused by switching phenomena due to the interaction of different electrical apparatuses in a cable system, such as the transformer, the cables, the switching apparatus and the surge protection devices, which is normally found in a windmill farm collection grid. There, the cables act as transmission lines for propagating waves with voltages appearing across the switching contacts or current flowing through the contacts. Switching transients in three-phase systems can be extremely complex [3], [4]. However, generally while opening and closing electrical contacts of any apparatus there is a time interval when the voltage withstand in the apparatus is low enough to allow re-ignitions during voltage variations.

The voltage variations can be

- Transients initiated by pre-striking.

- Transients initiated by current chopping.

- Any transient enhanced by wave return after reflection in one or several points of reflection due to wave impedance discontinuity.

The time interval corresponds to the motion of the contacts where also the voltage withstand-level is a function of the contact travel, i.e. contact opening gap, and the actual insulation medium.

2.2 Risk Objects Subjected to transient overvoltages

It is not within the scope of this work to determine what is dangerous or complementary as safe level of steepness nor magnitude or step.

The resulting impact due to tov. is expected to differ between different components depending on geometry, type of insulation and the electrical design.

Potential risks of failures due to electrical transients have been suspected for transformers [5], [6]. Even if the tov. does not immediately break down fresh and healthy insulation, the potential risk of electrical insulation failures will increase later due to factors such as:

- The state of the health of the insulation.
  Any defect or cavities in moulds can degrade the health-status of a transformer, as well as history of stress and partial discharges.

- Environmental impact.
  Humidity and contamination (salt) will impact the insulation strength.

- Voltage distribution over the transformer as load object.
  The electrical geometry around the incoming leaf and along the winding leg has influence on the voltage distribution.

- Heat in running conditions.

Steep and high-magnitude strikes could occur in some cases depending on the system design, type of the electrical apparatuses and the load or fault circuit to be switched. The creation of strikes is probabilistic and stochastic in nature. When tov. are caused by breaker operation, e.g., It depends on both the probabilistic instant-of-contact-opening/closing when the breaker is operating as well as the stochastic behavior of the breaker itself (e.g. the behavior of arc quenching in the breaker) [7]. Especially, the instant of contact opening is really crucial. Without a point-on-wave control, the instant of contact opening/closing of the breaker will happen at random, thus, cases with no strike as well as cases with steep overvoltages can be expected.

The potential risks of failures due to electrical transients on transformer have been recognized by ABB. In ABB Handbook on Distribution Transformers [8] some precautions on this issue have been addressed where some explanations are given. Some potential protections have also been proposed as described below.

2.3 Commonly Utilized Mitigation Methods

In the ABB Handbook on Distribution Transformers [8], surge capacitors and point-on-wave control have been mentioned. RC-protection has been known also as a derivative of surge capacitors for surge protection purpose. Moreover, surge arresters have been utilized since long as protection devices against overvoltages. Therefore in this laboratory experiment, these surge protection devices are investigated, whose main characteristics are presented as follow:

2.3.1 Surge Arrester (ZnO)

A surge arrester presents a momentary path to earth, draining over-charge from the line [9]. It is connected in shunt to the circuit. ZnO surge arrester is composed of non-linear resistors where overvoltage impulses can be diverted into current surges while the energy of the wave is discharged. In this way, surge arresters limit the amplitude of the tov. Surge arresters are preferably located close to the equipment to protect – in this case at the terminal of the transformer TX1 (See Figure 4). The protection level of the ZnO arrester is set with sufficient margin to the temporary overvoltages depending on the system grounding and operating conditions.

2.3.2 Surge Capacitor

A surge capacitor is connected in shunt to the circuit as a termination of the cable. Surge capacitors are used to decrease the rate of rise of the steep fronted tov. caused e.g. by pre-strikes and re-ignitions. In addition surge capacitors also reduce the resonance frequency of the recovery voltage across the circuit breaker and this way reducing the number of repetitive pre-strikes and re-ignitions.

2.3.3 RC-Protection

RC-Protection (a series connected resistor and capacitor) is used to prevent reflected waves and to damp high frequency oscillation caused by a steep voltage. The RC-protection is connected in shunt to the main circuit. High frequency current-zero-crossing through a breaker is prevented from causing pre-strikes or re-ignitions and from having a number of re-ignitions following the first one. RC-protection should be tuned to effectively prevent any reflected wave and to damp any high frequency oscillation when it is connected at the end of a cable. Generally the resistance of the resistor should equal the surge impedance of the cable (Z_{surge}) and the capacitance of the capacitor should be much larger than the capacitance of the cable. The first requirement is to prevent any reflected wave and the latter is to damp the oscillating current through the breaker caused by pre-strikes or re-ignitions.

2.3.4 Point-on-Wave Relevance

Strikes resulted from the operation of the breaker are stochastic in nature. They depend to a large extent on the instant of opening/closing of contacts of

the breaker and the probabilistic of the breaker parameters itself (e.g. probability of arch quenching, etc.). E.g. breaking a load or fault, no strikes at a phase will be obtained when contacts are opened at either the exact instant of current zero crossing or sufficiently out of the critical time window around the zero-crossing. Pre-strikes can be prevented by closing at minimum voltage across the breaker.

In this experiment, within the test routines, the operation (opening/closing) of the breaker is performed by theoretical approach and scanning the instant time of the opeing/closing the contacts in such a way that the worst case results. For examples, opening an inductive load when the current chopping level is at its highest or closing a no-load (more capacitive) case when the voltage is at its peak.

2.4 Potential Transient Overvoltages, Worst Cases

Potential tov. worst cases have been found to be switching load side short cables with some amount of current and an extensively longer cable on the supply side. While energizing the load side, the effective voltage step will depend on the surge impedances of the cables and the numbers of feeders in parallel, holding up the supply side voltage. The tested case with one cable on the source side of the breaker and one equal cable (same surge impedance) on the load side will cause a maximum voltage step with the value of half the maximum supply voltage peak. Multiple cable feeders and sections on the supply side will also cause a number of reflection points, adding up returning reflected waves accordingly.

The switching point denoted SW1 in Figure 3 represents the switchgear operation in the bottom of a windmill tower where the length of the cable SC1 corresponds to the tower height, i.e. the effective cable distance between a transformer located in the nacelle and the switchgear located lower down inside the tower. Consequently the switching point SW1 provides the basic conditions for the occurrence of high frequent transients during closing and opening of the circuit, and in the laboratory setup that point will closely represent the worst case. The focus of this experiment is on this switching point SW1.

Moreover, some concerns can also be related to these worst cases, such as:

- Operation Cases and Load Conditions.
- Phase Opposition between Network and Generator.
- Interruption of Transformer Inrush Currents.
- Ground Fault Cases.
- ZnO Protection Level.
- Open Arcs and Intermittent Earth Fault Situations.

Details of these concerns can be found in Enclosure C in Section 13.

3 Laboratory Setup And Test Scenarios

3.1 Description of the Laboratory Circuit

As explained earlier in Section 1.2.3, in order to reduce the number of wave reflection points during each test, the extra feeders SC4 and SC5 in Figure 3 were disconnected. As a result, the schematic diagram of the test circuit used throughout the laboratory experiment ceomes the one shown in Figure 4. A remark should be given that the cables and the transformers (the high voltage-side) are rated up to 20-24 kV. However, due to some practical reasons, during this test the nominal voltage level of the medium voltage (MV) cable grid is set at 12 kV.
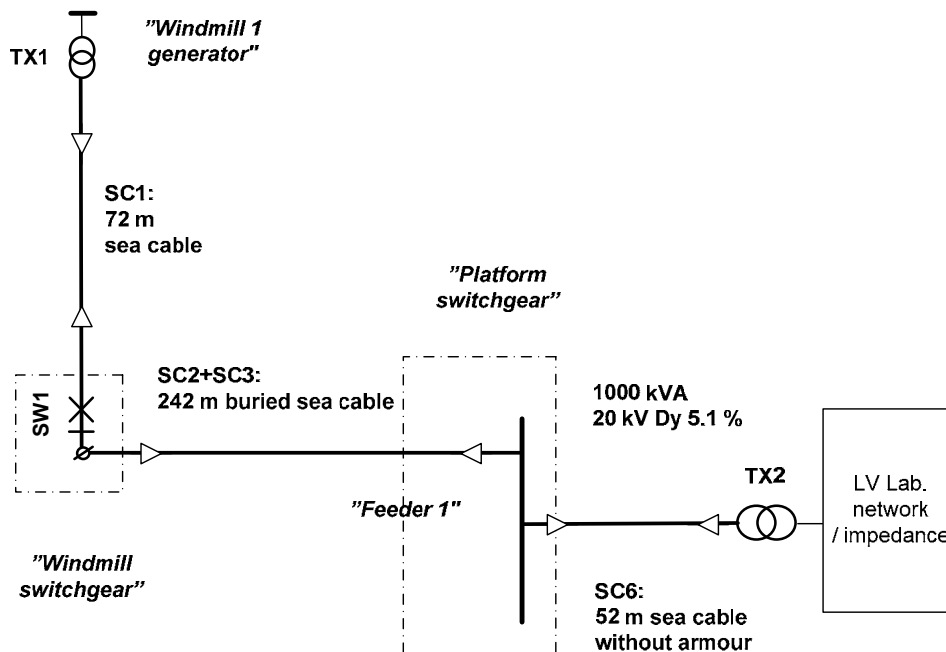

Figure 4: Schematic diagram of the laboratory setup

3.2 Description of the Circuit Apparatus

An XLPE Cable with 240 mm^2 cross-section of aluminum conductor rated at nominal voltage 20 kV in trefoil formation has been used. The cable parameters can be found in Table 1.

Table 1 Cable Parameters [9]

Single-core cable, nominal voltage 20 kV (U_m = 24 kV)												
Cross-section of con-ductor	Diameter of con-ductor	Insula-tion thick-ness	Diameter over insula-tion	Cross-section of screen	Outer diameter of cable	Cable weight (Al-con-ductor)	Cable with (Cu-con-ductor)	Capaci-tance	Charging current per phase at 50 Hz	Induc-tance (trefoil)	Induc-tance (flat forma-tion)	Surge impe-dance
mm^2	Mm	mm	mm	mm^2	mm	kg/m	kg/m	µF/km	A/km	mH/km	mH/km	Ω
240	18.1	5.5	30.7	35	40.0	1.9	3.4	0.31	1.1	0.35	0.60	24.8

The surge impedance of the cable is 24.8 Ω, which was obtained from laboratory measurement and verified with PSCAD simulation. Figure 5 shows the physical cross-section of the cable used within the laboratory setup and the corresponding PSCAD model used in the simulation.
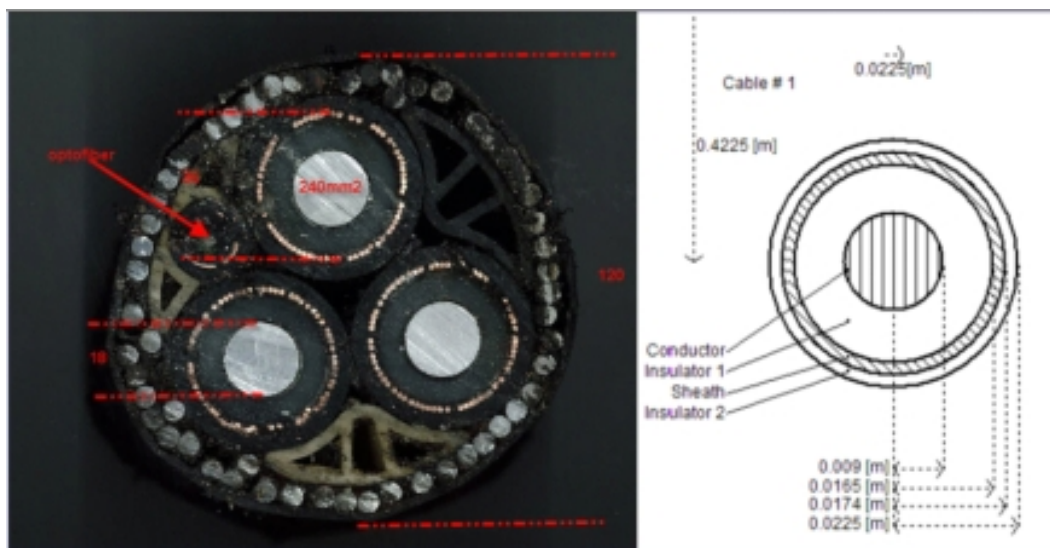

Figure 5: Cross-section of the cable used in the laboratory setup and the PSCAD model used in the simulation (only one phase is shown in the simulation model)

The two transformers used, TX1 and TX2 are rated 1.25 MVA and 1 MVA respectively. The pictures and the corresponding parameters of the transformers, TX1 and TX are shown in Figure 6 and Figure 7 respectively.
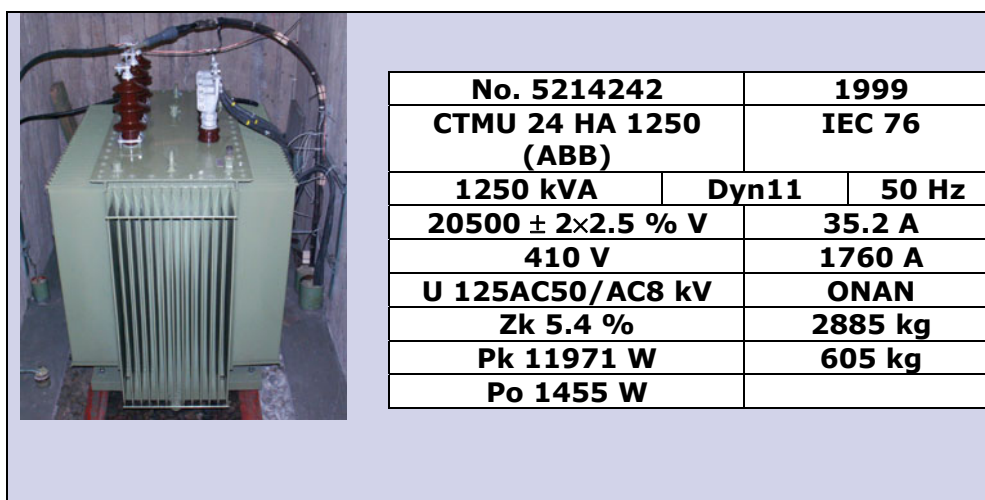
No. 5214242		1999
CTMU 24 HA 1250 (ABB)		IEC 76
1250 kVA	Dyn11	50 Hz
20500 ± 2×2.5 % V		35.2 A
410 V		1760 A
U 125AC50/AC8 kV		ONAN
Zk 5.4 %		2885 kg
Pk 11971 W		605 kg
Po 1455 W		

Figure 6: Transformer TX1 (photo left) and the parameter plate

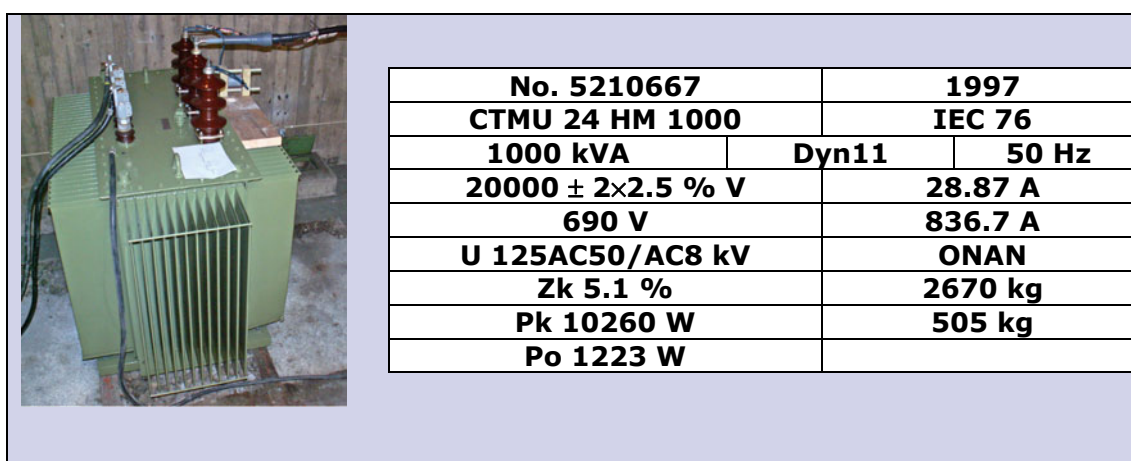| No. 5210667		1997
CTMU 24 HM 1000		IEC 76
1000 kVA	Dyn11	50 Hz
20000 ± 2×2.5 % V		28.87 A
690 V		836.7 A
U 125AC50/AC8 kV		ONAN
Zk 5.1 %		2670 kg
Pk 10260 W		505 kg
Po 1223 W		

Figure 7: Transformer TX2 (photo left) and the parameter plate

The windmill transformers used under test are delivered with delta connected medium voltage windings. Consequently an artificial neutral point has been provided in order to provide a system defined neutral point and to prevent dc charge of the test system. The artificial "grounding transformer" was made of three 24 kV rated voltage transformer primary windings connected in wye, consequently with a practically negligible admittance. They were connected at the "platform switchgear" (see Figure 4).

For the switching apparatus, the ABB VM1-type breaker with nominal rating of 12 kV has been used. The parameters of the breaker are shown in Figure 8.

Technical data

Rated voltage	kV	12
Rated power frequency withstand voltage	kV	28
Rated lightning impulse withstand voltage	kV	75
Rated current	A	...3150 [1]
Rated short-time current, 3s	kA	...50
Rated short-circuit breaking current	kA	...50
Rated short-circuit making current	kA	...125
Mechanical operating cycles		
Operating mechanism		...100 000
Vacuum interrupter		...30 000
Operating cycles at rated current		...30 000
Operating cycles at short-circuit current		...100
Power consumption		
At rest	W	≤ 10
After an autoreclosing cycle	W	≤ 100
Operating time		
ON, approx. [2]	ms	45...60
OFF, approx. [2]	ms	35...50
Pole centres [2]	mm	150/210/275
Distance between upper and lower contact terminal [2]	mm	205/310
Height [2]	mm	475/598/620
Depth	mm	424
Width [2]	mm	450/570/600/750
Weight [2]	kg	90-148

[1] Breakers for 4000 A with fan cooling
[2] According to rated values

Figure 8: The switching apparatus used during the laboratory experiment (photo of the product upper-left and photo of the laboratory installation lower-left) and the technical data

3.3 Description of Protection Devices

Three surge protection devices, namely: surge arresters (ZnO), surge capacitors and RC-protections are investigated.

A base case is defined as the case with only surge arresters (ZnO) installed at the terminals of transformer TX1. The surge arresters are always installed at the transformer TX1 also when other surge protection devices are tested. This approach is based on two considerations:

1. ZnO-type surge arresters are well known to always limit the maximum voltage magnitudes of tov. but have no effect on reducing the steepness of the tov.

2. The surge arresters are primarily used to protect the test transformers i.e. to avoid transformer damage during tests due to high tov. magnitudes.

The installed ZnO protection has a Continuous Operating Voltage COV = 14.3 kV with the characteristic points of 1mA @ 17.2 kV; 10kA @ 28.5 kV, see Section 0 in Enclosure C.

Figure 9 shows the surge arresters installed throughout the laboratory experiment and the corresponding setup of the protection level. Figure 10 illustrates the installation of the surge arresters for protecting the transformer TX1. The other surge protection devices tested: the surge capacitors and the RC-protection are shown in Figure 11. Remarks should be given that during the laboratory experiment:

- Two sets of 3 x capacitors are available with the values of 3 x C = 83 nF and 3 x C = 130 nF, and

- Two sets of 3 x resistors are available with the values of 3 x R =20 Ω and 3 x R = 30 Ω.

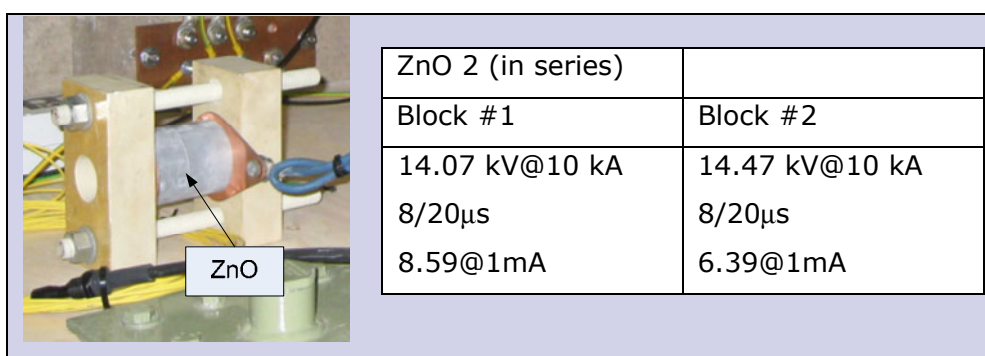| ZnO 2 (in series)	
Block #1	Block #2
14.07 kV@10 kA	14.47 kV@10 kA
8/20μs	8/20μs
8.59@1mA	6.39@1mA

Figure 9: Surge arresters (photo left) and the setup used throughout the laboratory setup for protecting transformer TX1
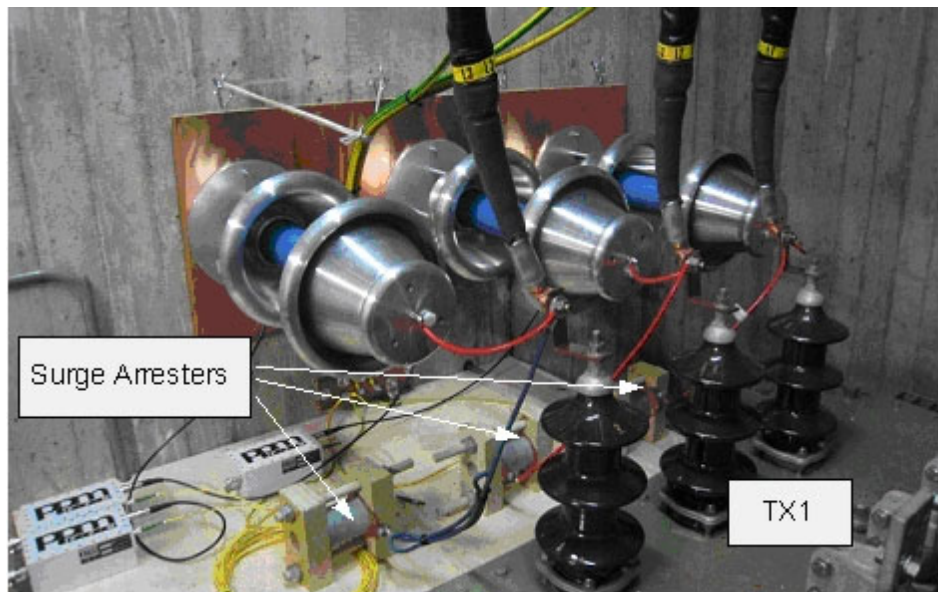
Figure 10: Installation of surge arresters for protecting the transformer TX1 throughout the laboratory experiment
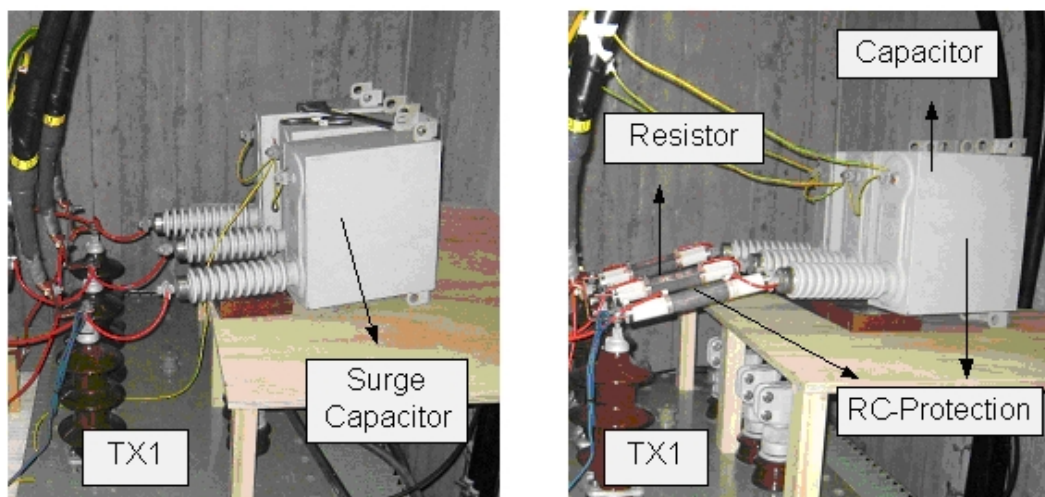

Figure 11: Surge protection devices: the surge capacitors (left photo) and the RC-protections (right photo)

Three potential locations for implementing the protection devices are considered (the schematic diagram of these potential locations is shown in Figure 10 where the details around the protection devices locations are highlighted):

1. At transformer TX1 terminal– "node 2" in Figure 10.

2. At BRK terminal (towards the windmill generator) – "node 3" in Figure 10.

3. At transformer TX2 terminal – "node 4" in Figure 10.
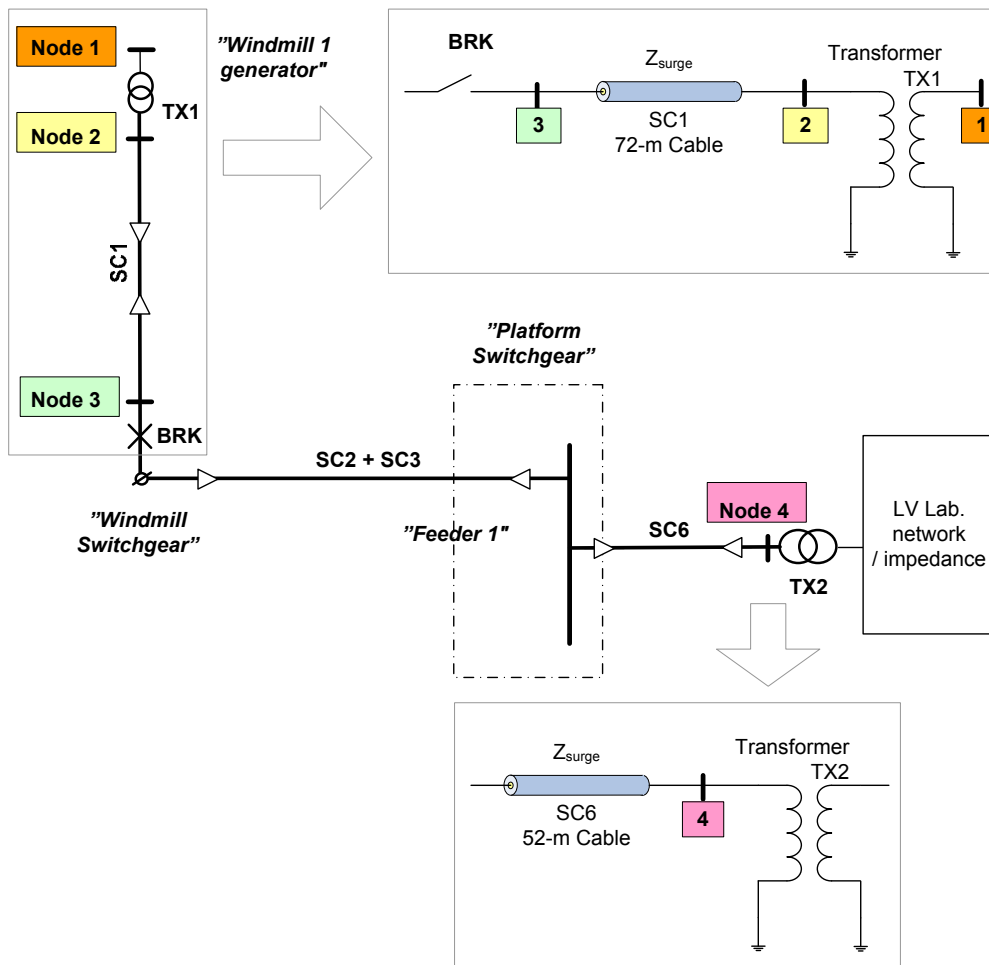
Figure 12: Schematic diagram showing the potential locations for implementing (combinations of) the protection devices

The illustrations of the implementation of surge protection devices in these locations are shown in Figure 13.
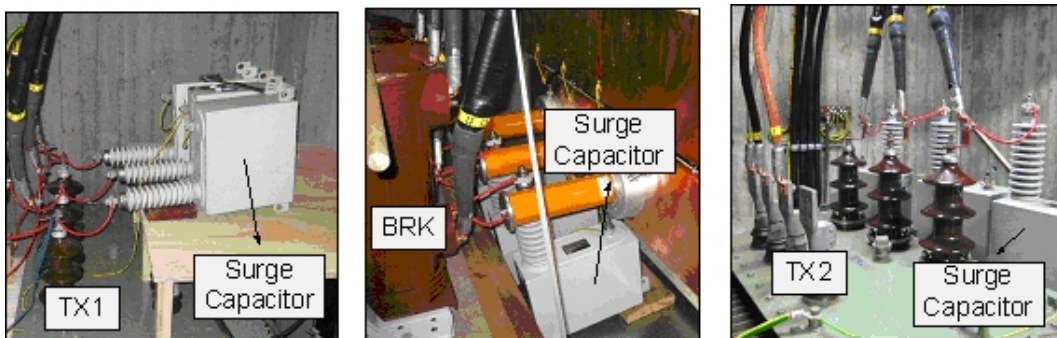

Figure 13: illustrations of the implementation of surge protection devices in the potential locations: at TX1 terminals – node 2 (left photo), at BRK terminals – node 3 (mid photo) and at TX2 terminals – node 4 (right photo)

3.4 Measurement Setup

Figure 14 shows the schematic diagram of the measurement device arrangements. The voltages are measured at the TX1 (Node 1) and BRK (Node 3) terminals. For this purpose, voltage dividers are implemented at each phase of the TX1 terminals (of "NorthStar" type) and each phase of BRK terminals (of "HILO" type). Currents (all three-phases) through TX1 and BRK are also measured. For this purpose, current transformers (of "Pearson Current Monitor" type) are installed at the outgoing terminals of BRK towards the transformer TX1 (Node 3). Each of the voltage dividers and current transformers are connected via optical links to two transient recorders "TRA 800s". Thus, a total of nine channels of the two transient recorders are used (six channels for voltage measurement and three channels for current measurement). Pictures of the measurement devices, the optical data transmitters and receivers as well as the transient recorders are shown in Figure 15. The detail parameters of the voltage dividers, current monitors and transient recorders, shown in Figure 15, are presented more in detail in Figure 16 to Figure 19.
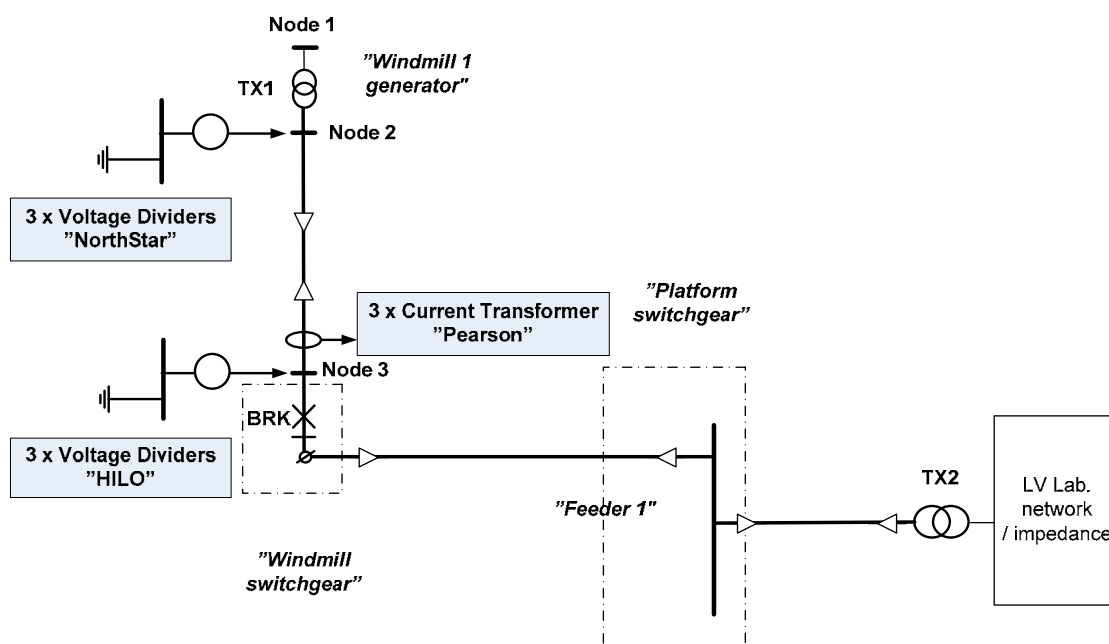

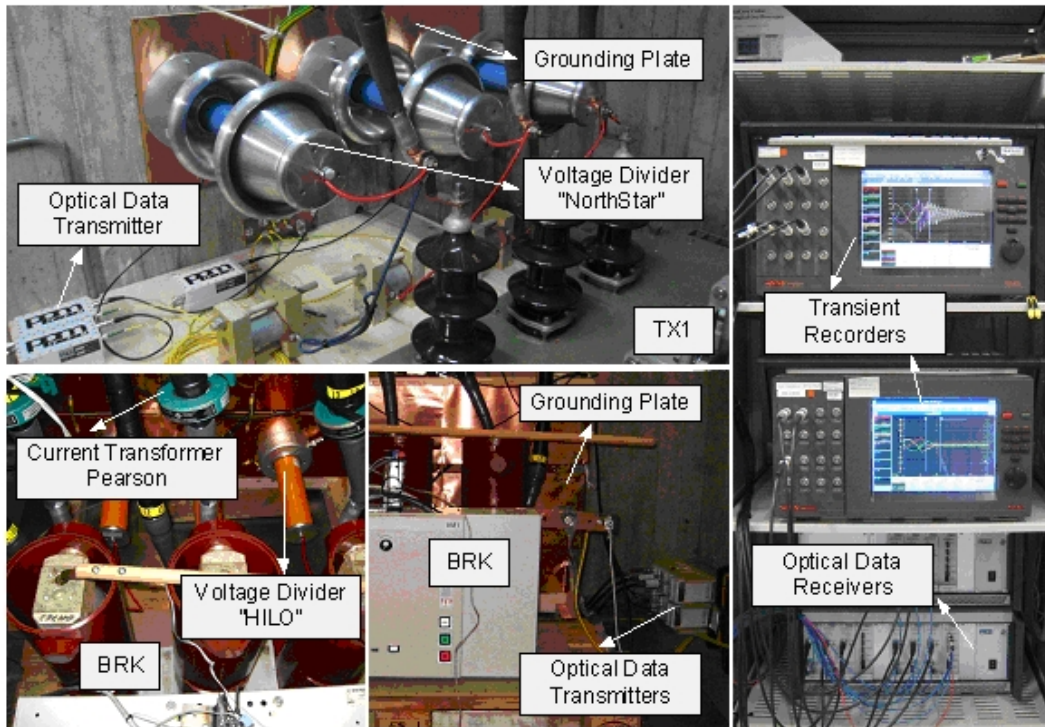*Figure 14: Schematic diagram of measurement device arrangement*

Figure 15: Measurement device arrangements within the laboratory environment; From the upper-left graph clock wise until the lower-left graph: the voltage divider and the optical data transmitter at TX1 cell, the transient recorders and the optical data receivers at operator and control room, the optical data transmitter at BRK cell, as well as the voltage dividers and current transformers at the BRK cell

Model Number	VD-100
Max DC/Pulsed V (kV)	100/180
Max Frequency (MHz)	20
Cable Length (ft)	30
DC Accuracy	<0.1%
10Hz - 1MHz Accuracy	1%
1MHz - 20MHz Accuracy	3%
Resistance (Megohms)	1600
Height (inches/cm)	24/60
Diameter (inches/cm)	11/28
Capacitance (approx pf)	25
Base Diameter (inches/cm)	10/25
Standard Divider Ratio	10,000:1

Figure 16: Voltage divider North Star Type VD-100 (photo left) and the parameters

	HVT40RCR
rated input voltage:	
dc voltage	40 kV
ac voltage	30 kV
pulse voltage 1.2/50µs	100 kV
divider ratio (DC) ± 1%	2500 : 1
hv-resistor	150 MΩ
hv-capacitor	50 pF
rise time	17 ns
bandwidth	20 MHz
Dimensions-:	
socket ⌀	180 mm
height	360 mm
weight	5.0 kg
cable length	5.0 m
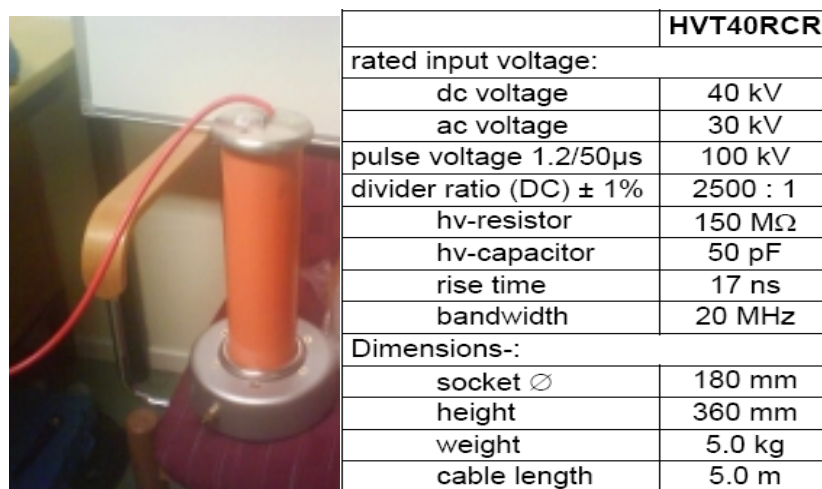
Figure 17: Voltage divider HILO Type HVT40RCR (photo left) and the parameters

Sensitivity	0.01 Volt/Ampere +1/-0%
Output resistance	50 Ohms
Maximum peak current	50000 Amperes
Maximum rms current	200 Amperes
Droop rate	0.1 %/millisecond
Useable rise time	100 nanoseconds
Current time product	2.5 Ampere-second maximum*
Low frequency 3dB cut-off	0.25 Hz (approximate)
High frequency 3dB cut-off	4 MHz (approximate)
I/f figure	12 peak Amperes/Hz
Output connector	BNC (UG-290A/U)
Operating temperature	0 to 65 ºC
Weight	23 ounces

* Maximum current-time product can be obtained by using core-reset bias as described in the *Application Notes*. 0.8 Ampere-second is typical without bias.

Figure 18: Current monitor Pearson Type D 101 (photo left) and the parameters

- **Pentium CPU** with 256 MB RAM and 40 GB harddisk
- **Built-in 3,5" floppy drive** 1,44 Mb
- **Windows** 95 or 3.11 software environment
- **easy-to-use operation concept –** select between mouse, keyboard and Swiss
- **8, 10 or 12 bit resolution,** up to 50MHz sampling rate
- **various trigger modes:** level, window (in/out), slew rate, time out and reference band
- input amplifiers with 31 hardware ranges from 100mV to 100V f.s. with **overvoltage protection, anti-aliasing filter** and offset regulation
- **modular structure** up to 32 channels with different sampling rates, resolutions and memory depths
- **on-line help function** on all important menu topics

Figure 19: Transient Recorders Type TRA 800 (photo left) and some of the specifications

3.5 Time Delay due to Measurement Devices Layout

See Figure 16 and Figure 17 in Section 3.4, the voltage dividers used for recording the voltage at breaker BRK (HILO) and transformer TX1 (NorthStar) terminals have the same bandwidth (20 MHz), hence the same time delay due to the measurement device bandwidth.

However, due to the laboratory layout, there are differences in distance between the fiber optics connecting the HILO and the NorthStar transmitters from the receivers. The illustration can be found in Figure 20.

The transmitters of the HILO voltage dividers (U_{BRK}) and the Pearson Current Transformers (I_{BRK}) are connected to the receiver via 86 m fiber optics while an extra 55 m longer fiber optics are connecting the transmitters of the NorthStar voltage dividers (U_{TX1})and the receiver. As a result, when the recordings from the NorthStar voltage dividers are compared to the HILO and the Pearson current transformers, an additional time delay due to the difference in the fiber-optic length (the 53 m) should be taken into account. In this case, the 53 m longer fiber optics will result in 0.27 μs time delay.

3.6 Control Systems

The laboratory is equipped with a sequence control system as standard being phased locked to the fundamental voltage where all sequence controlled output signals are programmed by means of a digital controller given as numerical input to the lab process central controller. The resolution of the outgoing raw signal from the sequence controller is 50μs. The total precision is dominated by output relays with 7 ms operating time before the breaker pulse output, in the order of ± 0.1 ms.
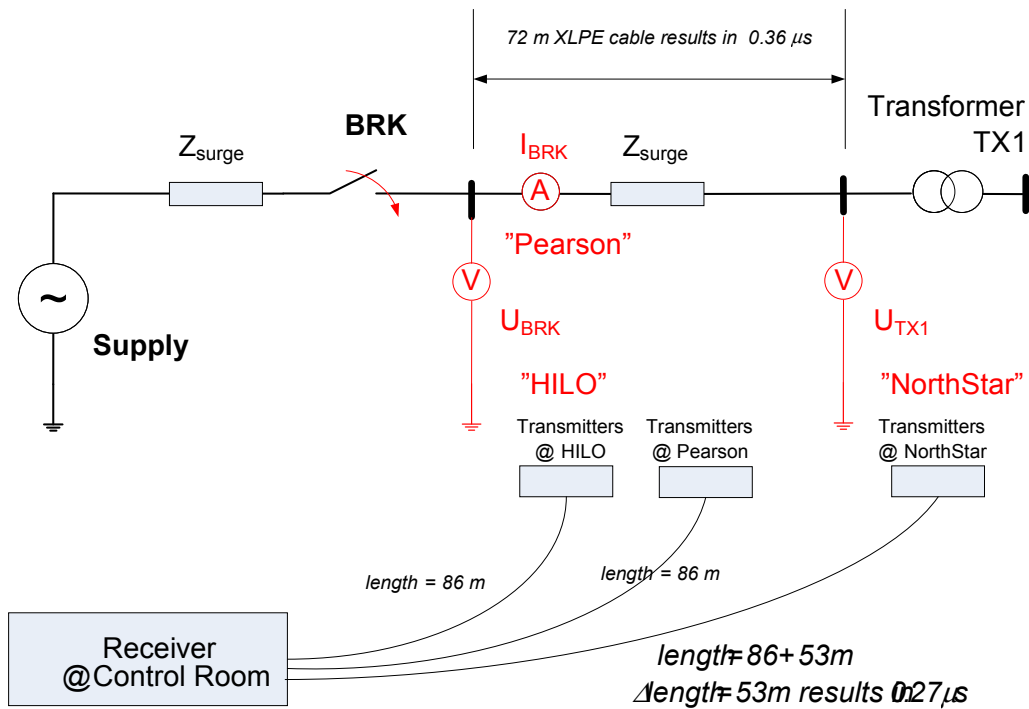
Figure 20: Illustration in the impact of measurement system to time delays on analyzing traveling wave phenomenon within the laboratory set-up

3.7 Load Type

Two load conditions are considered during the breaker switching operation in this test, namely: no-load and inductive load. When inductive load is tested, an inductive load of $X_L = 0.10 \ \Omega$ is connected at Node 1 (TX1) of the test circuit as shown in the previous schemes. The selected reactance of the load corresponds to the rated current of the transformer. The illustration of the load (inductive load) setup within the laboratory environment is shown in Figure 21.
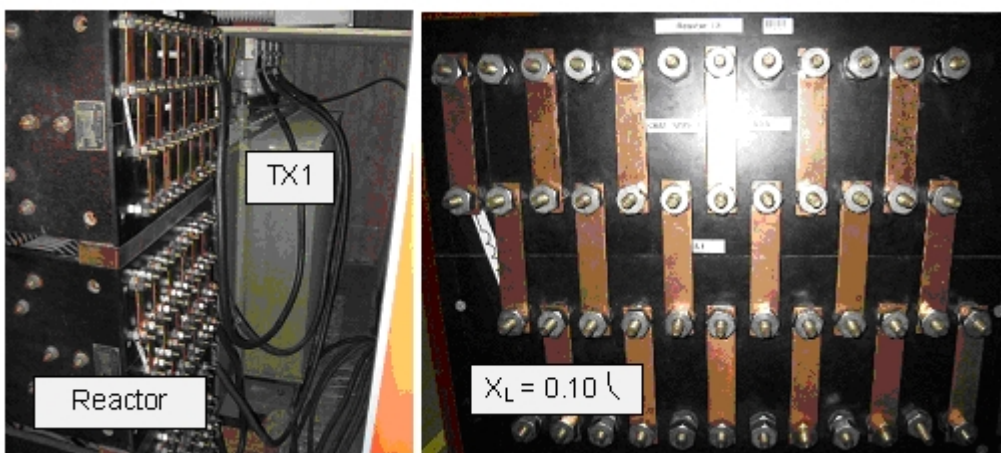
Figure 21: Inductive load setup

3.8 Test Scenarios and Cases

3.8.1 Remark on Windmill Operation

Switching operations in the Medium Voltage (MV) collection grid made under controlled conditions should be planned and performed in a programmed sequence involving minimum stress to the windmill system in all perspectives under mechanical and electrical considerations.

The MV breaker is one of several objects that can be controlled. Other controlled objects and functions can be:

- LV breakers and contactors
- Blade pitch
- Converters
- Grid fault ride through functions

Operating the MV breaker located in a windmill connection point, i.e. close to the windmill tee in a collection feeder, can be made for several reasons and in combination with control of the above. However, from an electrical point of view and with respect to the actual MV switch/breaking point, the operation is preferably made during minimum load i.e. with the windmills stopped, minimum load condition or generator disconnected.

Regardless of the reason for switch/breaker operations, the corresponding load cases defined for the MV breaker can be categorized in "no load" and "load" case. Switching under load can e.g. occur due to faults or temporary instability. "No load" cases involve the capacitive currents in an energized system. Capacitive load has to be considered in particular while operating switches and disconnectors with slow operating speed.
See section 10 Future Work.

In this study, the possibilities for opening and closing the breaker either at no load or with an inductive load connected are considered and tested (See section 3.8.3). The following concerns have been taken into account for the load conditions:

3.8.1.1 Load Case Selection

Two load conditions have been considered during the breaker switching operations, namely "no-load" and "inductive load" where "No load" refers to the case while the transformer is energized with open circuit on the low voltage side. The no load current for a power transformer is extremely low, in the order of mA, combined with capacitive charge current for all live parts and including eventual surge capacitors.

3.8.1.2 Load Current

The selected number of combinations from the total of potentially possible combinations of electrical circuit connections, components and related parameters has to be made with care in order to limit the frame of work.

Consequently it has been decided to use a constant load during all tests also in order to compare mitigation and prevention methods under equal conditions.

Studies of pre-strike and re-ignition conditions in circuit breakers with cable on both sides have shown that all load currents with both resistive and inductive dominance give rise to transients, however a mainly inductive load current provide the worse cases. In the actual experiments, a load has been selected giving a current essentially larger than the typical chopping current of a breaker and to a magnitude that corresponds to the order of equal or less than the installed power, resulting in 80 % of the installed power at the selected operating voltage point. The 80% load is based on 12 kV operating test voltage. The nominal transformer voltage is 20.5 kV

The test load was provided by a battery of low voltage air core coils configured to the reactance $X_L = 0.10\ \Omega$ @ 50 Hz connected at Node 1 (TX1) of the test circuit as shown in previous schemes. The illustration of the load (inductive load) setup within the laboratory environment is shown in Figure 21.

3.8.2 Tested Cases

The experiment has been preceded by dynamic simulations of typical off-shore windmill systems involving switching operations on the collection platform and in the nodes through out the feeders [11]. The laboratory set-up and selected cases for the study of transients and mitigations have been selected as a result of the simulations.

Furthermore, test cases are defined based on different (combinations) of surge protection devices at different locations shown earlier in Figure 12 and listed in Table 2.

Table 2 Test cases

No	Case ID	ZnO	Surge Capacitor		RC-Protection	
		Location (installation)	Location (installation)	Parameter	Location (installation)	Parameter
1	**Base Case**	**Node 2 (shunt)**				
2	C83-TX1	**Node 2 (shunt)**	**Node 2 (shunt)**	**C=130nF**		
3	C130-TX1	**Node 2 (shunt)**	**Node 2 (shunt)**	**C=83nF**		
4	**C130-BRK**	**Node 2 (shunt)**	**Node 3 (shunt)**	**C=130nF**		
5	R30C83-TX1	**Node 2 (shunt)**			**Node 2 (shunt)**	**R=30ohm C=83nF**
6	R20C83-TX1	**Node 2 (shunt)**			**Node 2 (shunt)**	**R=20ohm C=83nF**
7	R20C130-TX1	**Node 2 (shunt)**			**Node 2 (shunt)**	**R=20ohm C=130nF**
8	**R30C83-TX1-C130-TX2**	**Node 2 (shunt)**	**Node 4 (shunt)**	**C=130nF**	**Node 2 (shunt)**	**R=30ohm C=83nF**
9	**Point-on-Wave**	**Node 2 (shunt)**				

Note that the different color represents the nodes as shown in Figure 12.

3.8.3 Test Routines

Test routines are defined based on the load type (no-load or inductive load) and switching operation of breaker (opening or closing). The test routines are applied on each test case. The test routines are summarized in Table 2.

Table 3 Test Routines Summary

Load Type	No-load at Node 1		Inductive load (X_L=0.01Ω) is connected to Node 1	
Breaker Operation	**Closing**	**Opening**	**Closing**	**Opening**
Step 1	No-load is connected to Node 1		Inductive load is connected to Node 1 (X_L=0.01Ω)	
Step 2	Circuit is energized from TX2 (platform), breaker is initially opened	Circuit is energized from TX2 (platform), breaker is initially closed	Circuit is energized from TX2 (platform), breaker is initially opened	Circuit is energized from TX2 (platform), breaker is initially closed
Step 3	The voltages and currents as in Section 3.4 are recorded			
Step 4	Close breaker	Open breaker	Close breaker	Open breaker

3.8.4 Stochastic Breaker Performance

Strikes resulting from breaker operations are stochastic in nature – see Section 2.3.4. Therefore, after the instant of opening/closing the breaker contact materials resulting in the highest/steepest voltage transient is obtained from each case and test routine, 2-4 extra shots are performed within that instant time. The control equipment within this laboratory setup enables the exact and repeated shots for switching the breaker at a defined instant time.

4 Transient overvoltage Analysis Method

4.1 Transient overvoltage Indicators

As implied within the cases listed in Table 2 and the test routines presented in Table 3, there are a significant number of test cases within this experiment. To consider the stochastic behavior of the breaker, it is becoming necessary to run around 5 shots for each case. Nevertheless, in several cases, strikes which are in the order of 100s are obtained on each phase just in a single test. Figure 22, e.g. shows a typicall tov. that is experienced by the transformer TX1 which occurred when the breaker is opening with an inductive load connected at the LV side. Thus, to analyze all tov. individually e.g. by visual inspections would then be cumbersome and ineffective.
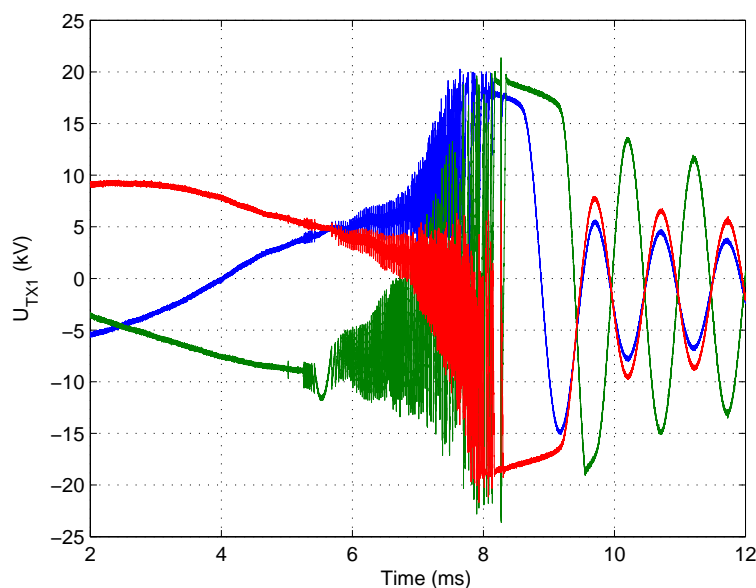
Figure 22: The worst multiple re-ignitions occurred at transformer TX1 terminals when breaker is opening with an inductive load connected

Therefore in this experiment, an algorithm is developed for the determination of transient indicators from the measurement results. tov. from every individual test result is then identified and quantified.

There are three main indicators identified and quantified from each test and each strike, namely:

1. Number of strikes (#strikes).

2. Step change magnitude of voltage during strikes (ΔU).

3. Steepness of voltage during strikes $\dfrac{dU}{dt}$ or $\dfrac{\Delta U}{\Delta t}$.

The identification of the number of strikes is performed by counting the number of voltage changes whose magnitude is above a certain magnitude (e.g. 0.5 U_{peak}). Another boundary like a steepness limit can be also applied, e.g. strikes within ΔU and Δt windows where the $\dfrac{\Delta U}{\Delta t}$ is above a certain value (e.g. 5 kV/µs).

Every strike with both magnitude and steepness higher than the predefined values is recorded.

4.2 The Algorithm

The algorithms of the tov. quantification method can be explained as follow.

4.2.1 Filtering

Post-processing filtering is crucial for defining a strike especially to define the starting and ending edges. This is illustrated in Figure 23.
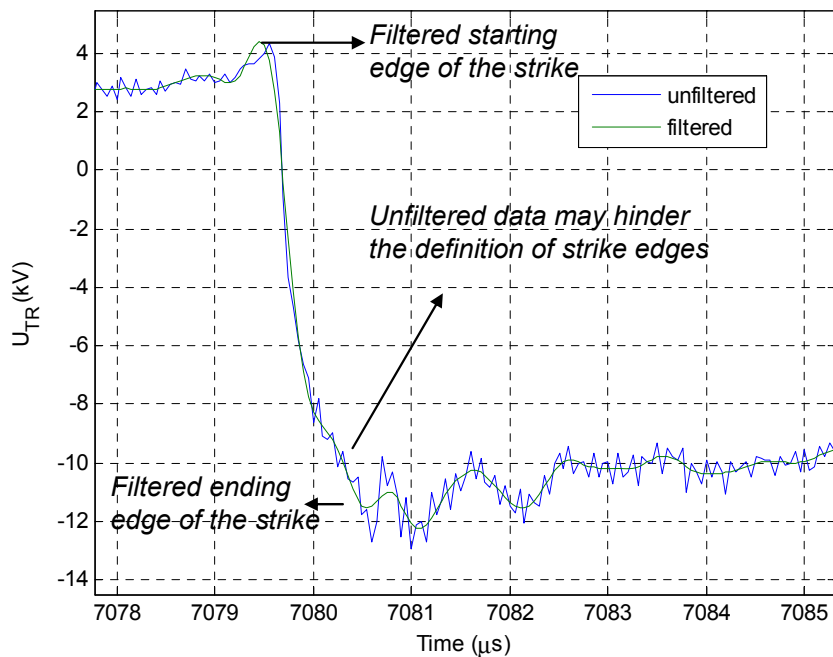
Figure 23: Illustration of the starting and ending edges of a strike

4.2.2 Strike Max-Min Identification

Once the starting and ending edges of a strike are defined, identification is performed on all maxima and minima within the measurement results. Thus, every maximum will be between two minima, vice versa, except for ones in the edges of the test result window. This process is illustrated in Figure 24.
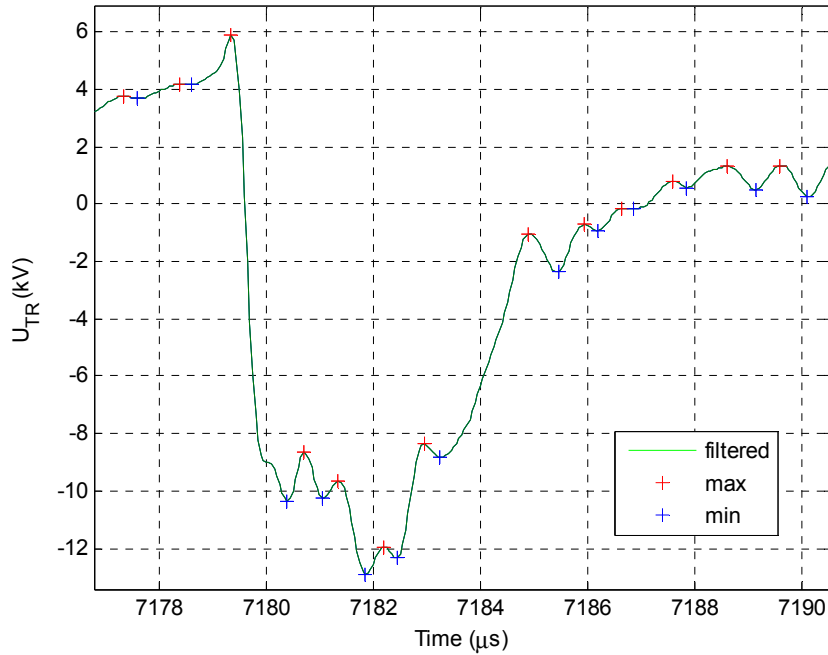
Figure 24: Illustration of defining maxima and minima points within test results

4.2.3 Strike Magnitude Definition and Quantification

Every two adjacent maximum and minimum point is compared. The voltage deviation from the two adjacent maximum and minimum point is calculated as well as the voltage-deviation-divided-by-the-time-difference between the two points ($\left| \dfrac{U_{max} - U_{min}}{t_{max} - t_{min}} \right|$). A minimum level of strike magnitude (i.e. ΔU_{limit}) and a minimum level of voltage-deviation-divided-by-the-time-difference (i.e. $\left| \dfrac{U_{max} - U_{min}}{t_{max} - t_{min}} \right|_{limit}$) are then defined. When both levels are surpassed by a strike, the strike is recorded and the magnitude is recorded. Figure 25 illustrates this process.
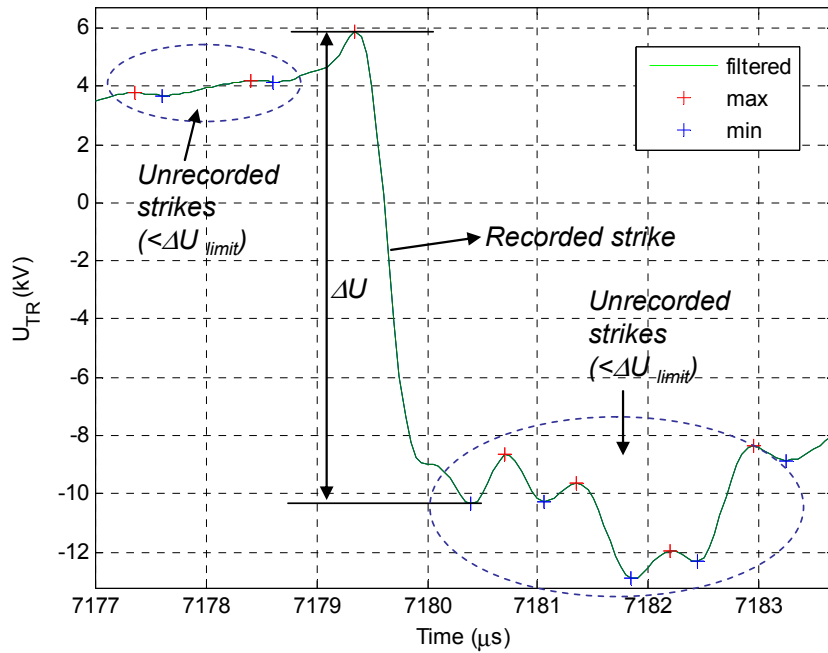
Figure 25: Illustration of strike magnitude definition and quantification

4.2.4 Strike-Steepness Definition and Quantification

The definition and quantification of strike-steepness are done in several ways, all presented in this report.

1. $\max\left(\dfrac{dU}{dt}\right)$ is derived from the filtered signal (see Figure 26 – upper graph, the green lines and text).

2. $\max\left(\dfrac{dU}{dt}\right)$ is derived from the unfiltered signal (see Figure 26 – upper graph, the blue lines and text).

3. $\left(\dfrac{dU}{dt}\right)_{10\%-90\%}$ is derived from the 10% and 90% values of the voltage magnitude obtained from the filtered voltage (see Figure 26 – upper graph, the green lines and text).

4. $\left(\dfrac{dU}{dt}\right)_{10\%-90\%}$ is derived from the 10% and 90% values of the voltage magnitude obtained from the unfiltered voltage (see Figure 26 – upper graph, the blue lines and text).
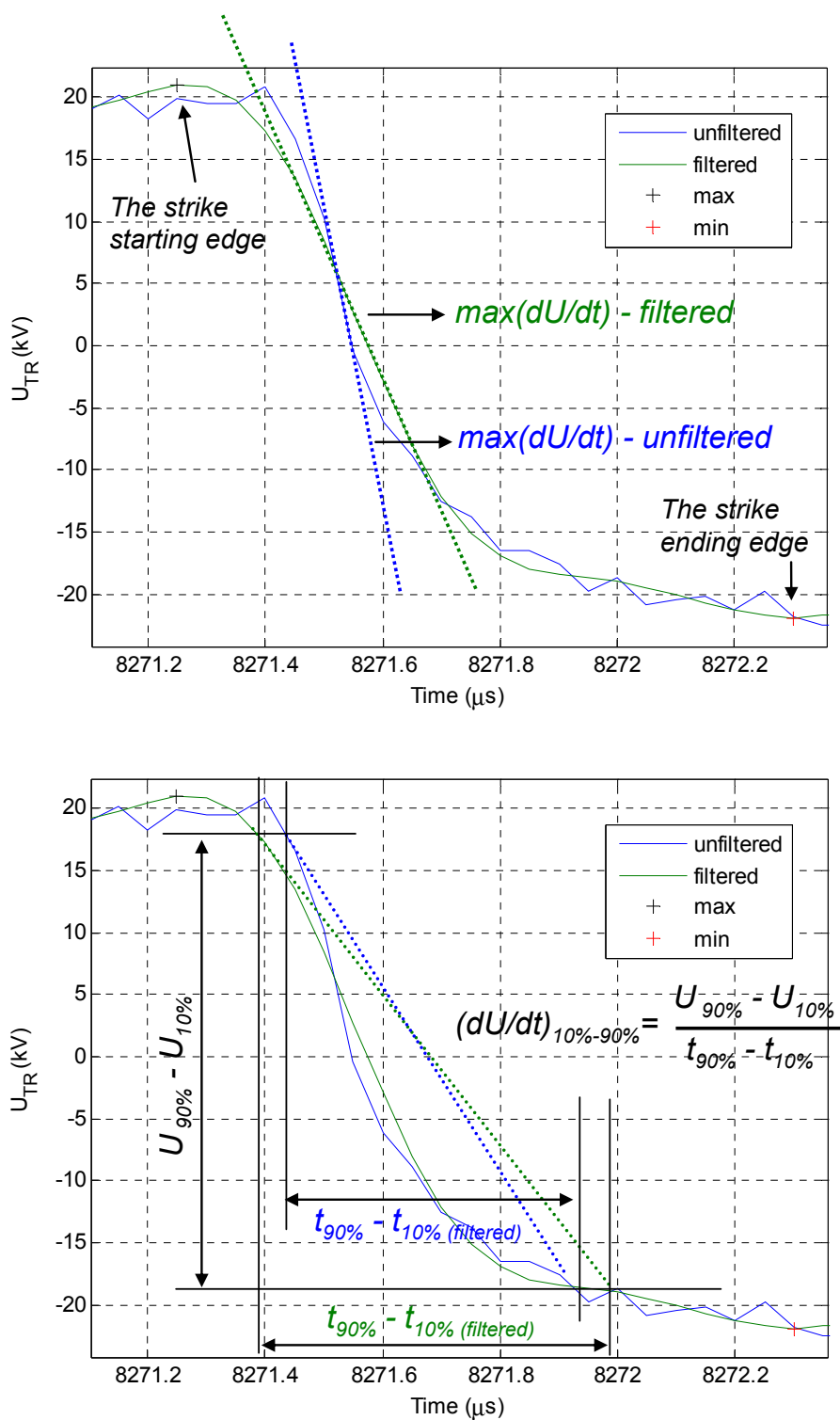
Figure 26: Illustrations of strike steepness definition and quantification

4.3 Scattered Plot Diagram

The indicators of the recorded strikes can be plotted as scattered plot diagram for illustrating the number of strikes as well as their indicators (magnitude and steepness). Figure 27 shows an example of a scattered plot diagram illustrating the recorded strikes, their magnitudes ΔU and the $\max\left(\dfrac{dU}{dt}\right)$ (filtered and unfiltered). These scattered plot diagrams are obtained from applying the tov. quantification method to the measured voltage at the terminal (the phase b) of the transformer TX1 when the breaker is opening with an inductive load connected (the green curve in Figure 44).

A great flexibility exists regarding the displaying of the results in scattered plot diagrams further on. For example, strikes in only one phase of the measurement voltage (e.g. the phase with worst strike) can be illustrated but showing all different indicators such as the $\max\left(\dfrac{dU}{dt}\right)$ from the filtered and unfiltered voltage signals, as well as the $\left(\dfrac{dU}{dt}\right)_{10\%-90\%}$ from the filtered and unfiltered signals as (which is illustrated in Figure 28). Alternatively, an indicator can be chosen (e.g. $\max\left(\dfrac{dU}{dt}\right)$ from filtered voltage signal), then the tov. indicators of all three-phases are displayed. This is illustrated in Figure 29.

For additional information, the time plot diagram around the time with the maximum strike can also be plotted for further analysis (the quantification method records the time where the maximum strike occurs). For example, the time plot diagram around the maximum strike whose indicators are shown in Figure 28 was actually displayed in Figure 26.
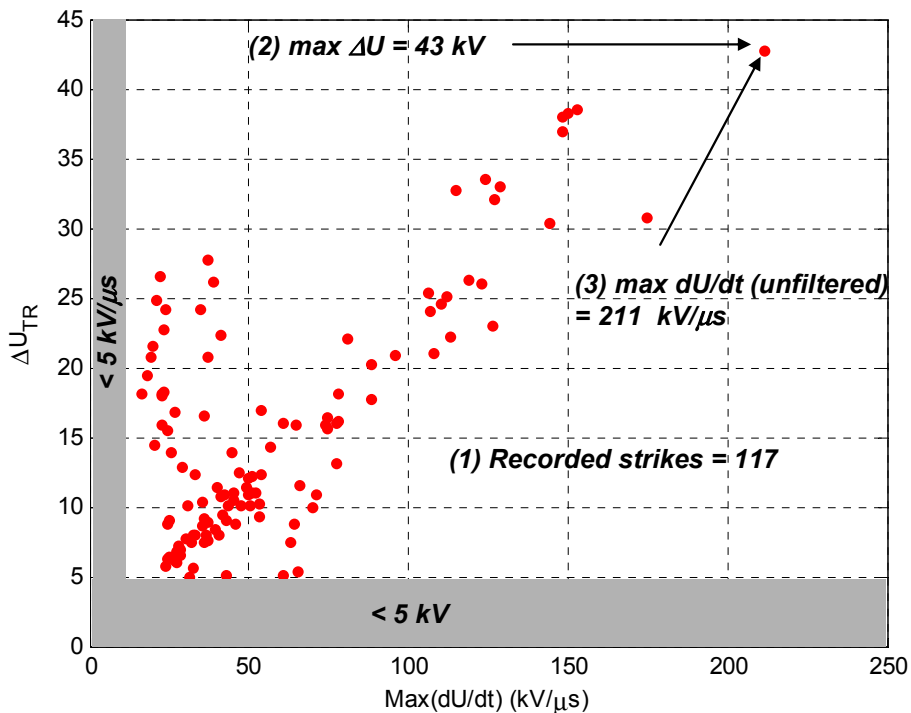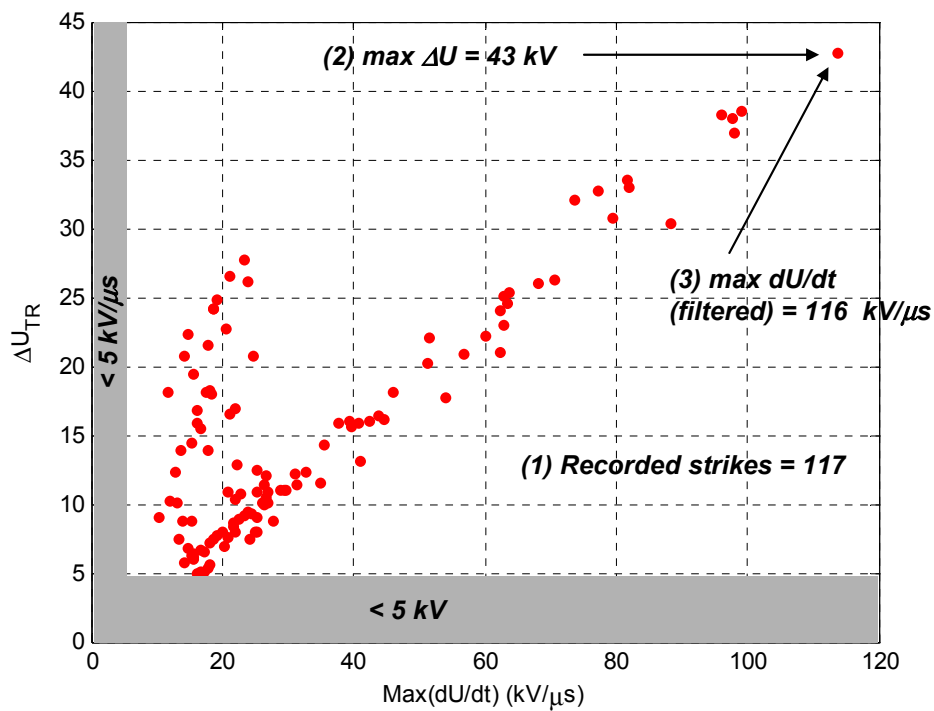
Figure 27: Examples of scattered plot diagrams illustrating the recorded strikes with limits at minimum magnitude and steepness have been used (filtered – upper graph and unfiltered – lower graph)
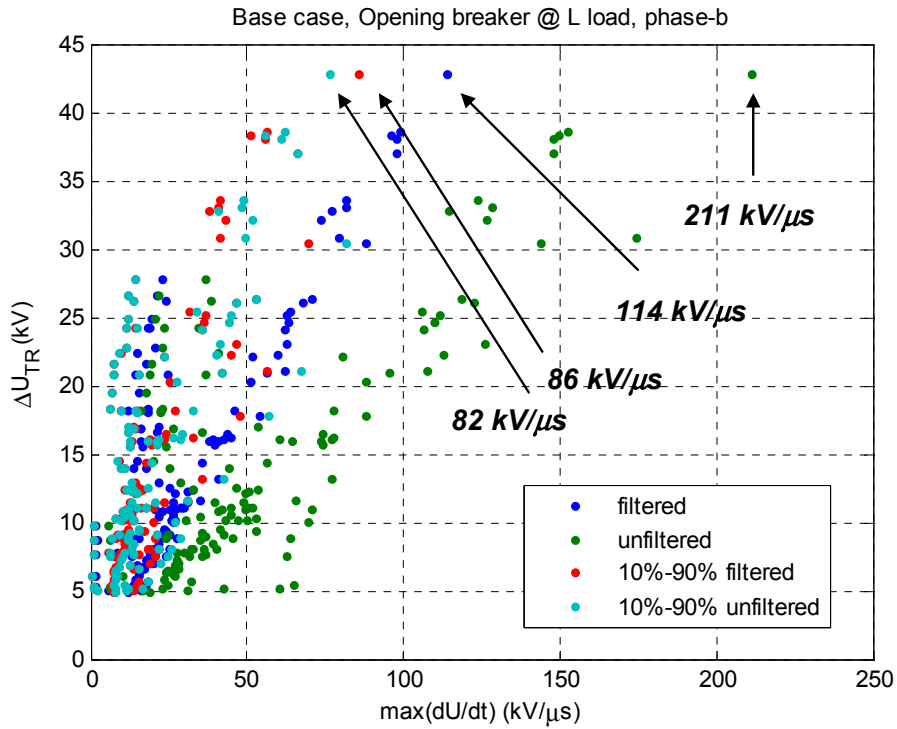
Figure 28: Illustration of displaying all strike indicators in one phase
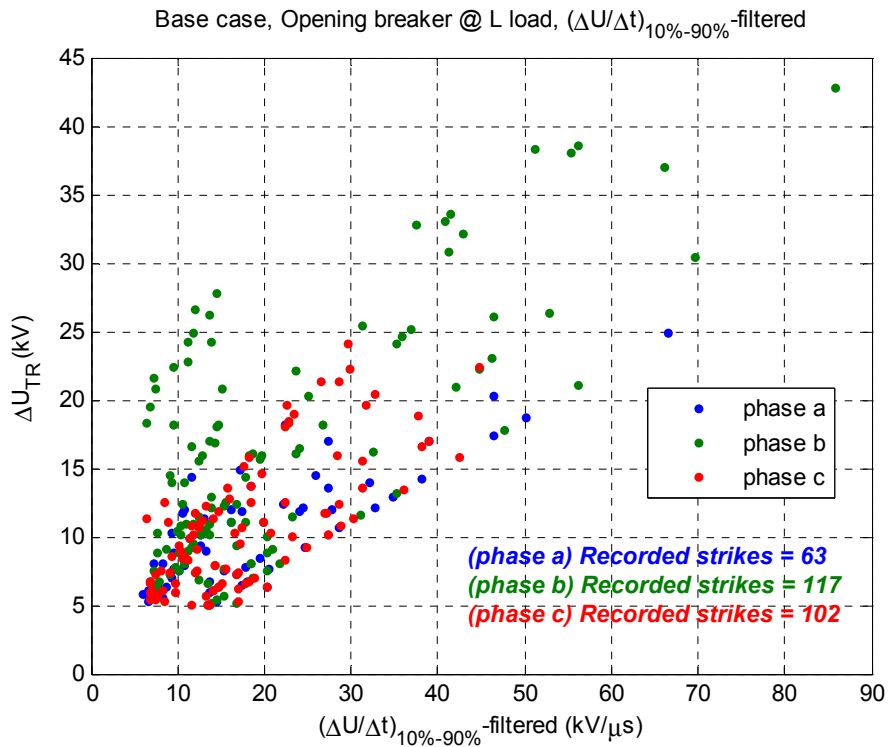

Figure 29: Illustration of displaying one strike indicators in all three phases

4.4 Table of Transient Quantified Indicators

For each test case, a table of quantified tov. indicators can be made. An example is shown in Table 4 when the breaker opening with an inductive load connected was performed on the base case. As expected, the indicators of $\left(\dfrac{dU}{dt}\right)_{10\%-90\%}$ are lower in values compared to the indicators of $\max\left(\dfrac{dU}{dt}\right)$ of both the filtered and unfiltered measured voltages (see Figure 26).

Table 4 An example of tabling the transient quantified indicators

Case	# strikes ($\Delta U > 5$ kV and within $\dfrac{\Delta U}{\Delta t} > $)	max ΔU	$\max\left(\dfrac{dU}{dt}\right)$		$\left(\dfrac{\Delta U}{\Delta t}\right)_{10\%-90\%}$	
			(filtered)	(un-filtered)	(filtered)	(un-filtered)
Opening breaker with inductive load connected at base case	117 (phase b)	43 kV	114 kV/µs	211 kV/µs	86 kV/µs	82 KV/µs

4.5 Remark on Indicator for transient overvoltage Steepness

From this point forward, three tov. indicators are used to quantify a strike. The number of strikes is used to quantify the repetitiveness. The strike magnitude is quantified by the maximum voltage step. The steepness of the strike is quantified based on the $\left(\dfrac{\Delta U}{\Delta t}\right)_{10\%-90\%}$ value of the filtered data. The other indicators for quantifying the strike steepness (as in Table 4) are however recorded and presented in the end of this report as Enclosure C, Section 14.

5 Base Case (ZNO Only) Results and Analysis

5.1 Laboratory Circuit of Case ID: Base Case

The base case is defined as the case with surge arresters (ZnO) installed at the terminal of transformer TX1 without any other surge protection device installed (see Table 2). The laboratory setup in the base case is shown in Figure 30.

No	Case ID	ZnO	Surge Capacitor		RC-Protection	
		Location (installation)	Location (installation)	Parameter	Location (installation)	Parameter
1	Base Case	Node 2 (shunt)				
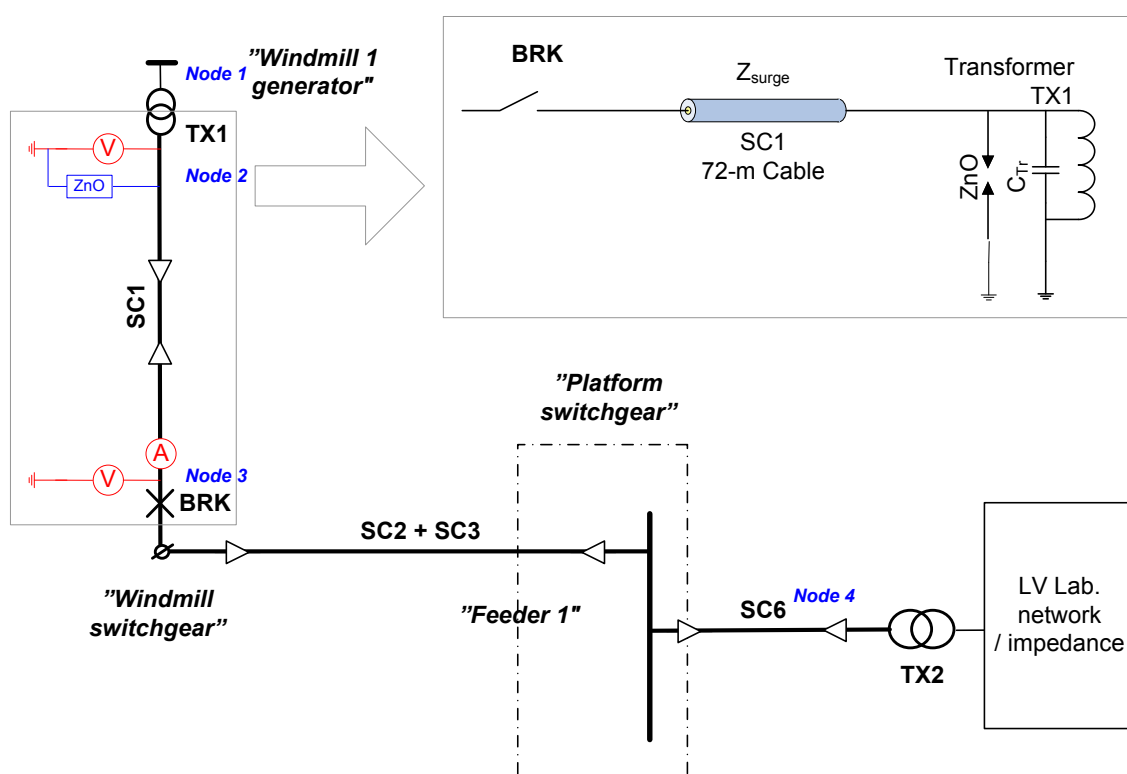
Figure 30: Laboratory setup and circuit for Case ID Base Case – only surge arresters shunted at the terminals of transformer TX1

43

5.2 Results of the Test Routines

5.2.1 Closing Breaker at No Load

In this case, the breaker is closed when no load is connected to transformer TX1. Six shots have been taken. One typical example of voltages and currents measured from the three measurement devices and channels (see Figure 14) is selected and shown in Figure 31. The voltages measured at the terminals of transformer TX1 is shown in the top graph, the voltages measured at the terminals of the breaker shown in the middle graph and the measured current flowing through the breaker is shown in the bottom graph. Note that the title on the top graph ("WW20080430.007.total") is taken from the index of the particular shot. In some shots the phenomena of inrush current when the transformer TX1 is first energized are obtained. One typical result is shown in Figure 32.
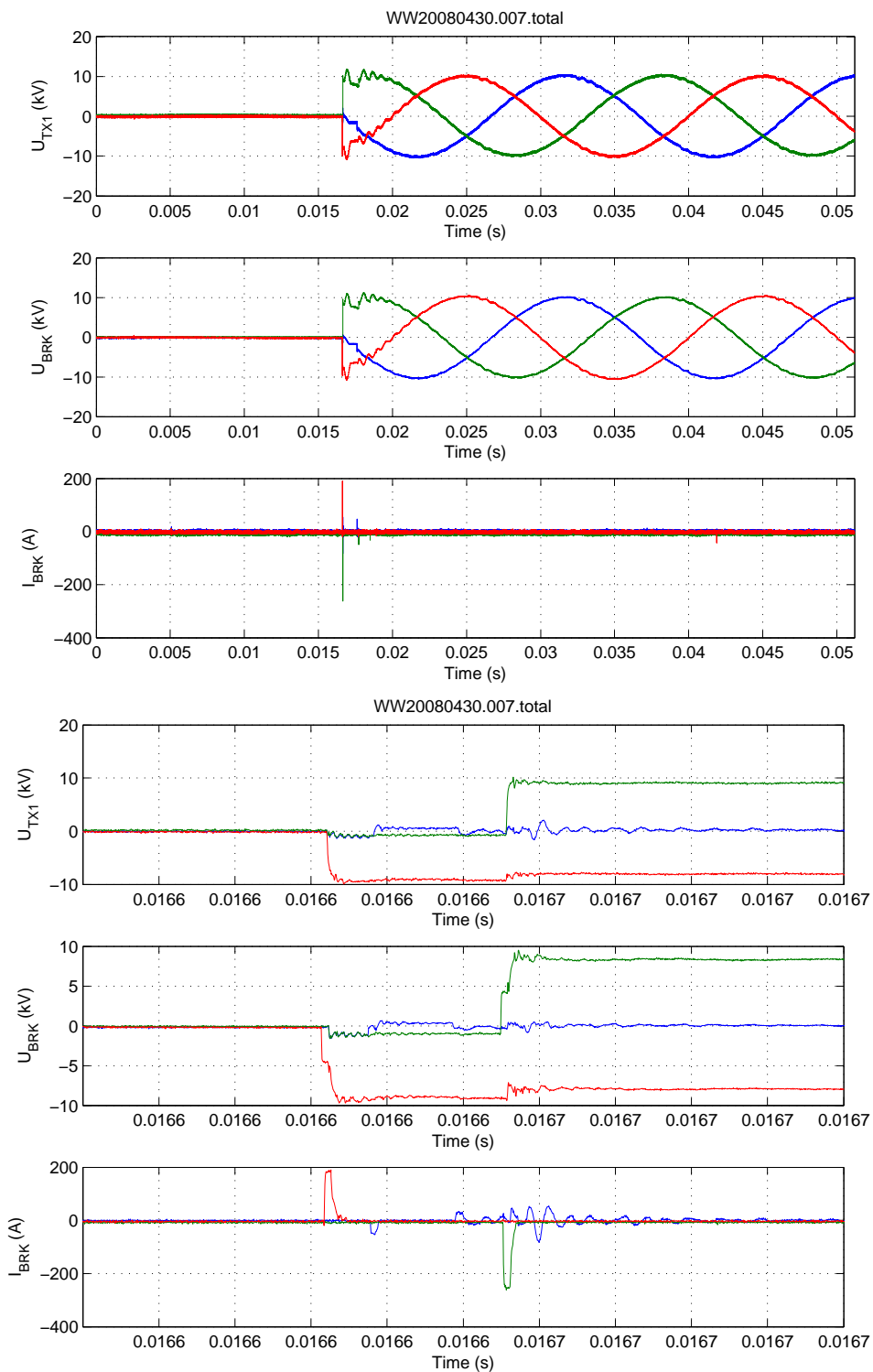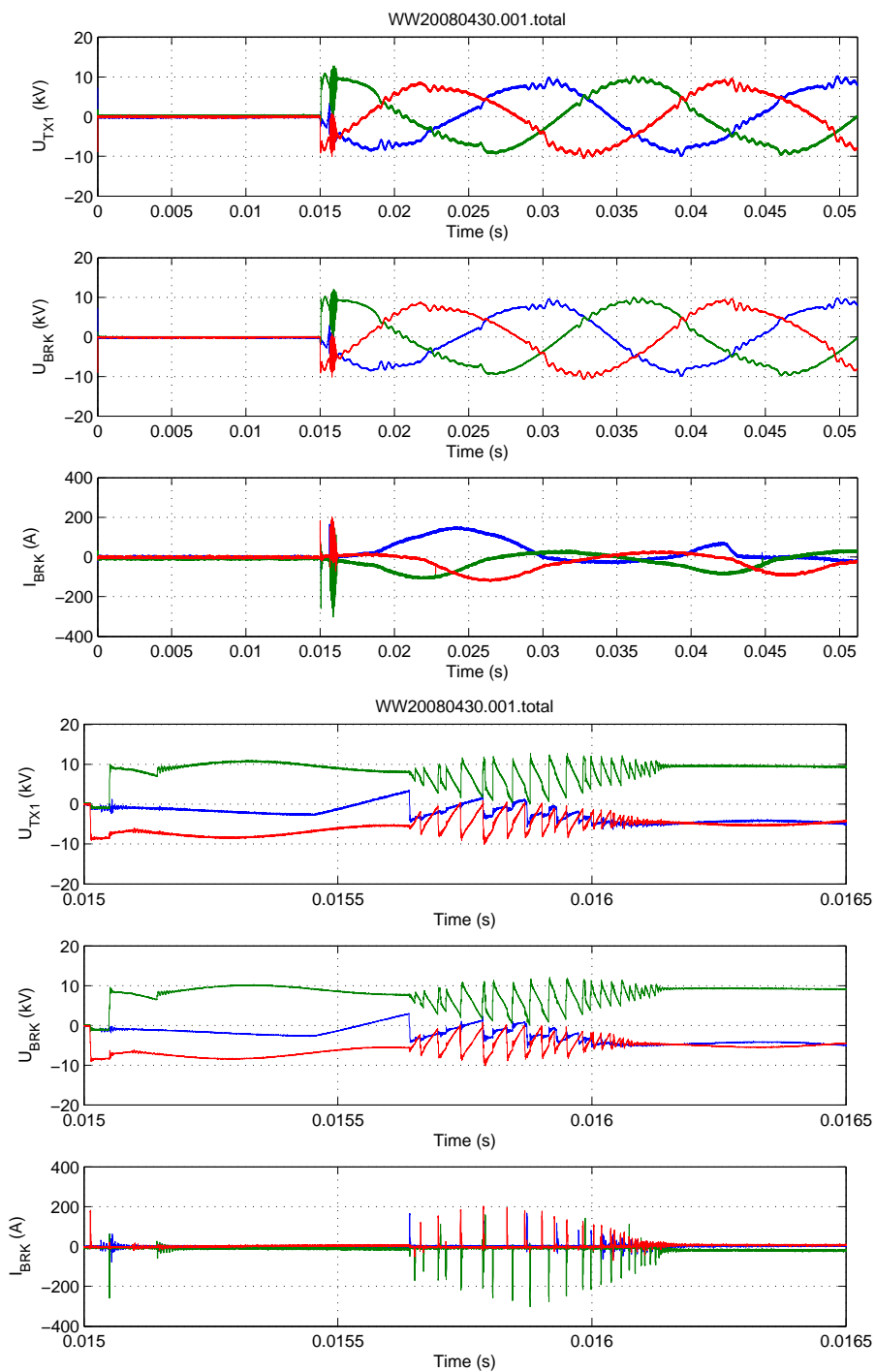
Figure 31: Measurement data from the Case ID Base Case: Closing breaker at no load (the lower graph is zoomed within 100 µs window)
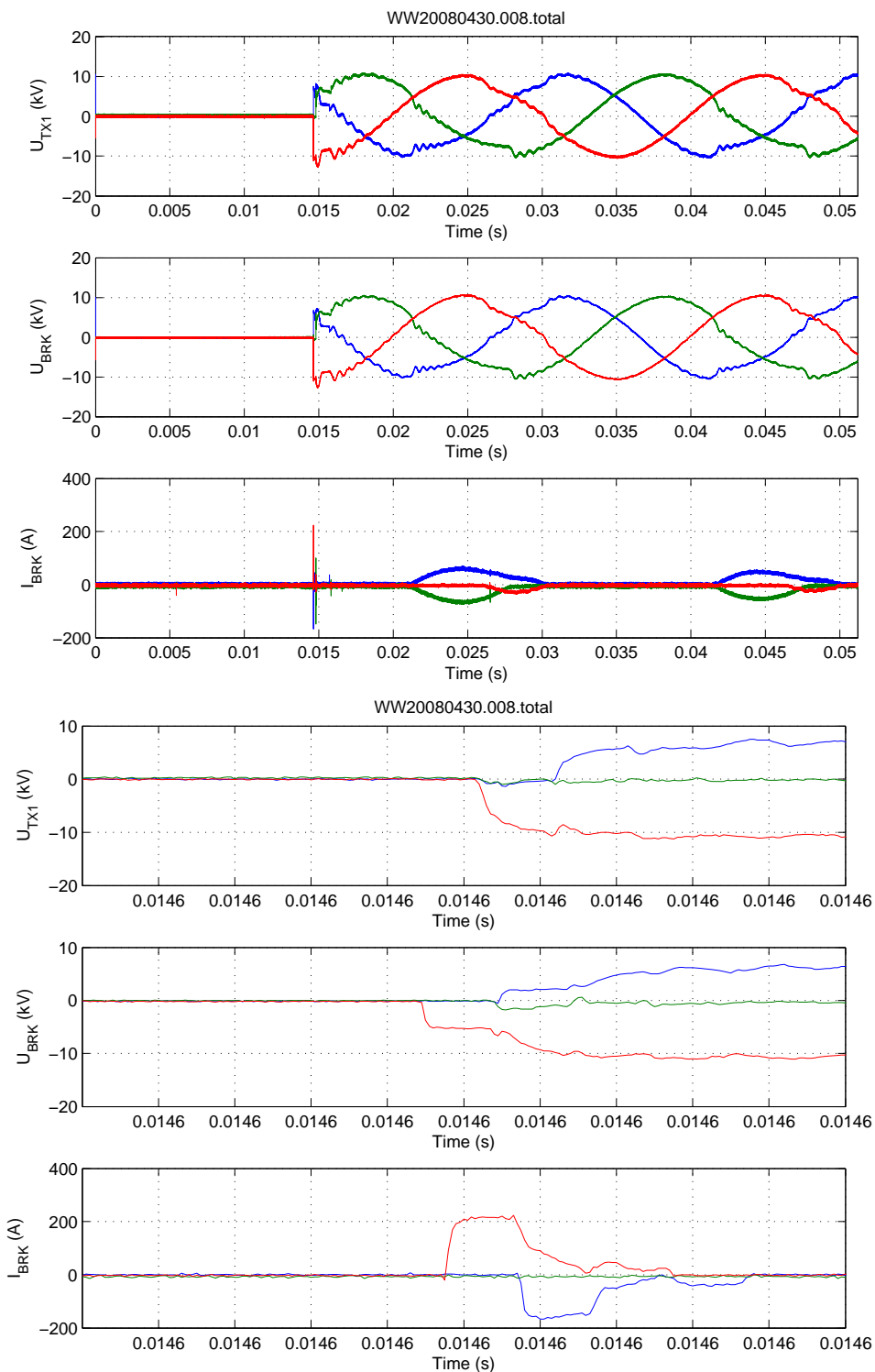
Figure 32: Measurement data from the Case ID Base Case: Closing breaker at no load with inrush currents (the lower graph is zoomed within 100 μs window)

5.2.2 Opening Breaker at No Load

In this case, the breaker is opened when no-load is connected to transformer TX1. Several shots have been taken. A typical result is shown in Figure 33.
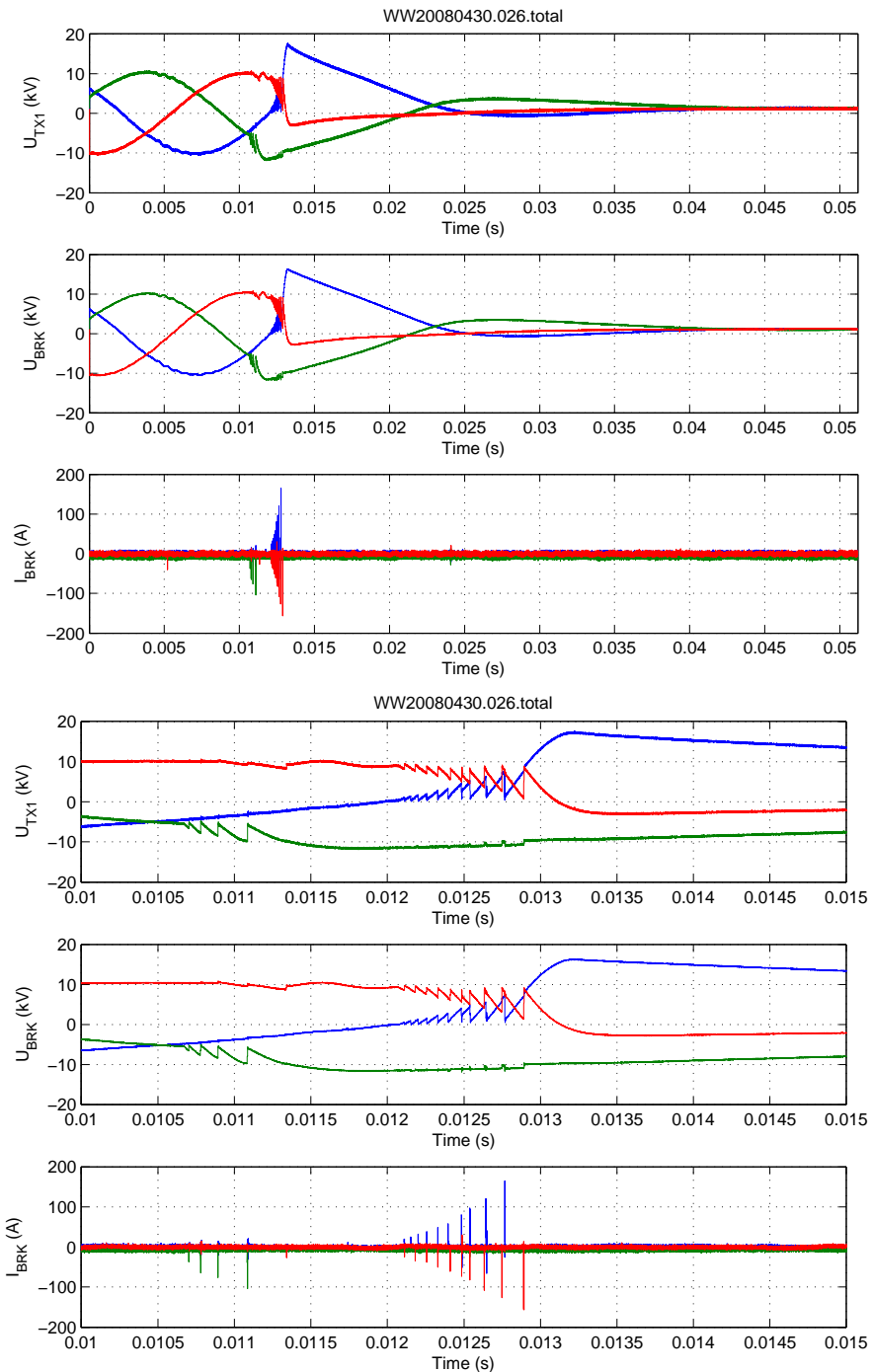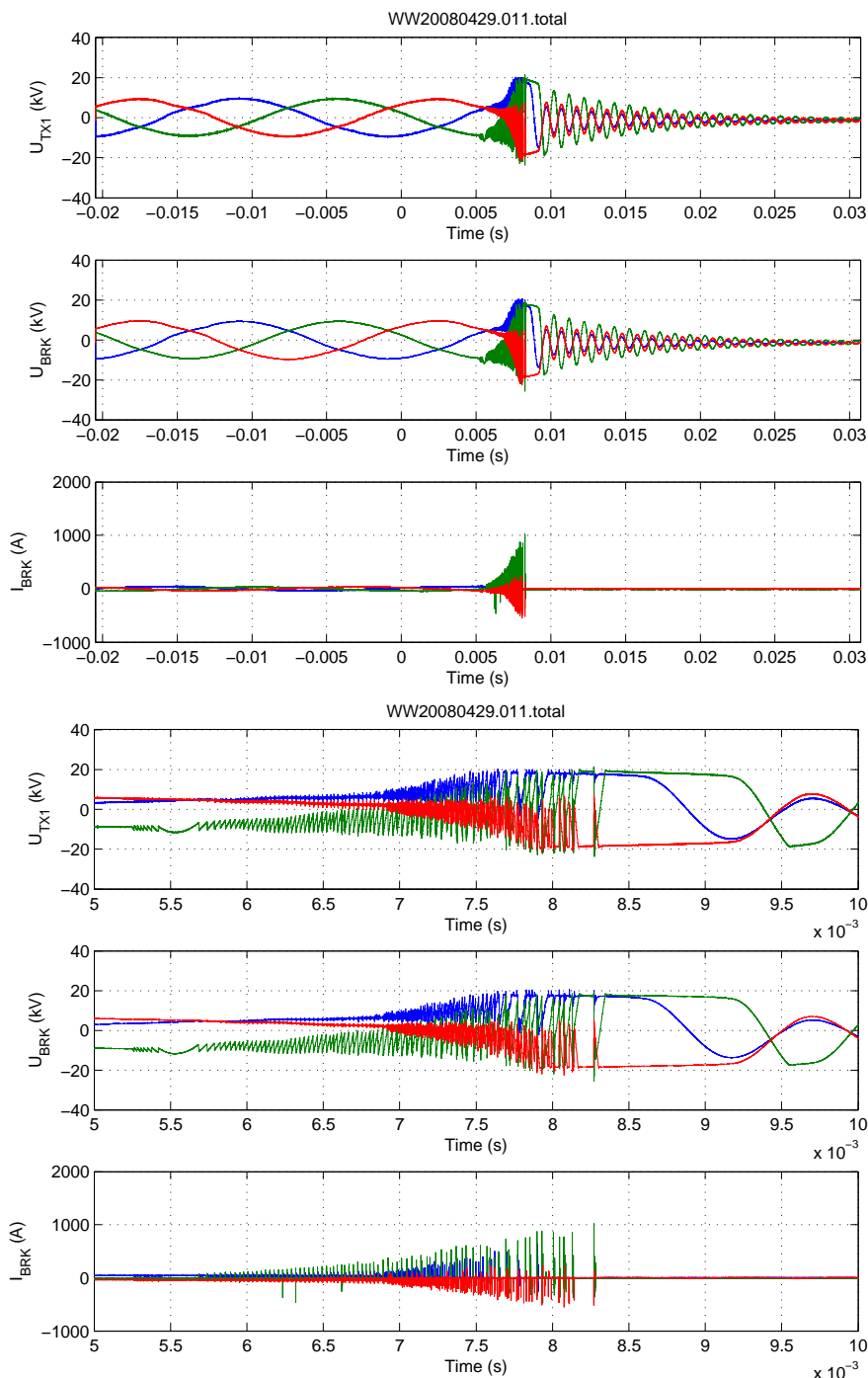

Figure 33: Measurement data from the Case ID Base Case: Opening breaker at no load (the lower graph is zoomed within 1 ms window)

5.2.3 Closing Breaker with Inductive-Load

In this case, the breaker is closed when the inductive load is connected to transformer TX1. Several shots have been taken. A typical result is shown in Figure 34.

Figure 34: Measurement data from the Case ID Base Case: Closing breaker with inductive load (the lower graph is zoomed within 1.5 ms window)

5.2.4 Opening Breaker with Inductive Load

In this case, the breaker is opened when the inductive load is connected to transformer TX1. Several shots have been taken. A typical result is shown in Figure 35.

Figure 35: Measurement data from the Case ID Base Case: Opening breaker with inductive load (the lower graph is zoomed within 5 ms window)

5.3 Verification of the Rise Time

The time constant τ for the voltage across a load like a transformer when it is hit by a step voltage propagating along a cable is:

$$\tau = Z_{surge}C_{load} \qquad (1)$$

where Z_{surge} is the surge impedance of the cable and C_{load} is the capacitance of the load (see Figure 36).
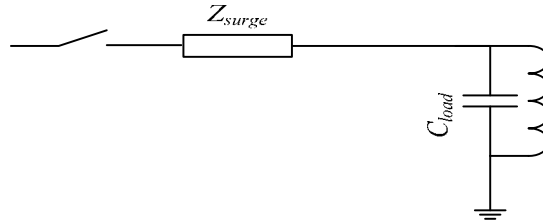
Figure 36: Simplified model for the electrical circuit when tov. pass across a transformer connected to a cable

In the base case, the time constant can be calculated by taking the value of the cable surge impedance Z_{surge} equal to 24.8 Ω and the value of load (in this case transformer TX1) capacitance equal to 8.5 nF. Using (1), the resulted time constant τ is 210 ns. This τ can be further converted into the rise time t_{rise} using

$$t_{rise} = 2.2\tau \quad (2).$$

t_{rise} is found to be 0.462 μs.

The voltage response across the transformer TX1 can be plotted using the mathematical equation for switching on an RC-circuit (C is not pre-charged):

$$U_{TX1} = U_{max}\left(1 - e^{-\frac{t}{Z_{surge}C_{load}}}\right) \qquad (3)$$

with $U_{max} = \dfrac{\sqrt{2}}{\sqrt{3}}U_n$ and U_n = 12 kV. Verification of the laboratory result can be done by comparing the calculated voltage step to measurement. For this purpose, the step voltage calculated using (3) is compared to measurement results obtain from closing breaker at no-load (see Section 5.2.1). Closing the breaker at no load represents the provocation of a step voltage on the transformer. One typical measured voltage-step (from one phase) obtained from the case of closing the breaker at no-load is compared to the calculated one and the comparison is shown in Figure 37. As it can be seen in Figure 37, the calculation produces satisfactory result with the result from the laboratory measurement. The steepness of the tov. is very well matched. The t_{rise} obtained from the measurement is 0.478 μs which matches the calculated value satisfactorily.
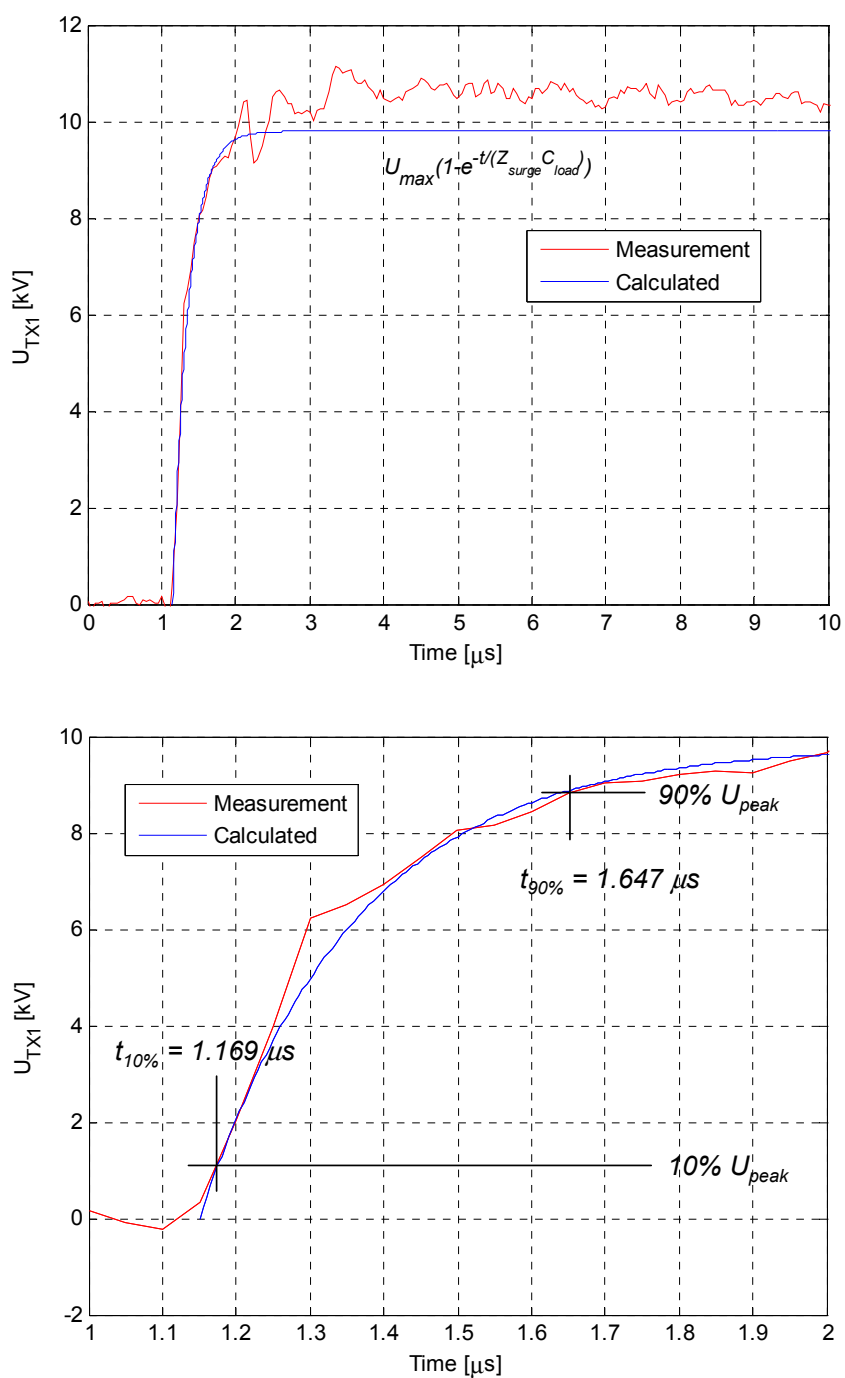
Figure 37: The voltage response across transformer TX1 – when breaker is closing with no-load installed at the transformer – as resulted from calculation (blue lines) compared to the measurement result (red lines). The lower graph is zoomed within 2-µs window

Two different aspects are implied here:

- The measurement result can be verified with a satisfactory match towards the theoretical calculations.

- The case of closing the breaker at no load is practical to be used for analyzing the rise time of the tov. occurred during breaker switching. It represents a provocation of a step voltage across the transformer TX1 and therefore the verification to the theoretical calculation is straightforward.

5.4 Voltage Step Magnitude

Due to the circuit configuration (see Figure 38), with the surge impedance (Z_{surge}) of the cable before and after the breaker equal, the maximum voltage step at the breaker terminal when the breaker is switched on will be half of the supply peak voltage (U_{peak}). The cables with the same surge impedance (Z_{surge}) act like a voltage divider. Thus, the voltage step recorded at the breaker terminal (U_{BRK}) should be half of the supply peak voltage (U_{peak}) and this is verified by the measurement result as shown in Figure 39.
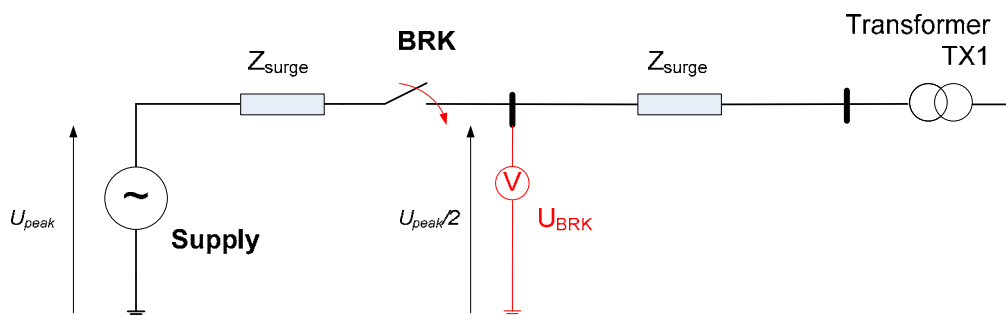
Figure 38: Circuit diagram for explaining the determination of the maximum voltage steps recorded at breaker terminal
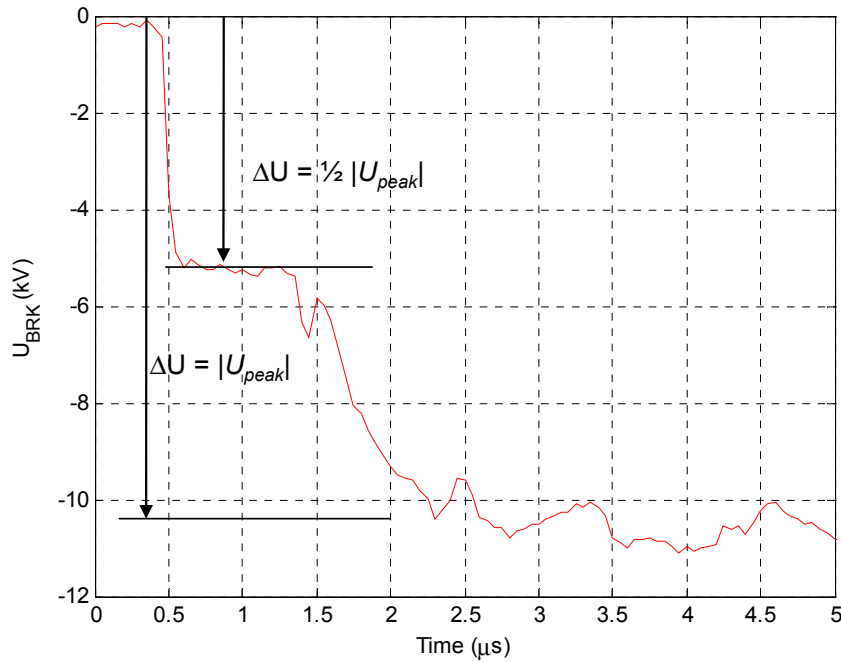
Figure 39: Measurement results showing the maximum voltage steps recorded at breaker terminal phase-c (when breaker is closing at no load)

5.5 Traveling Waves

The surge propagation speed for an XLPE cable is 200 m/µs. The distance between the breaker and the transformer TX1 is 72 m (see Figure 4). Therefore a time delay, t_{delay}, of 0.36 µs will occur from the recording of the voltage between the breaker and transformer TX1 due to this 72 m cable distance between them. Moreover, taking into account the time delay which is equal to 0.27 µs introduced by an extra 53 m fiber optic on the recording at transformer TX1 (see Section 3.5), a 0.63 µs time delay can be theoretically expected between the recordings of U_{BRK} and U_{TX1}. Figure 40 shows the time delay between the recordings of voltage at the breaker, U_{BRK} (upper graph) and transformer TX1, U_{TX1} (lower graph) terminals which is equal to 0.7 µs. Thus, the measurement results match satisfactorily with the calculation.
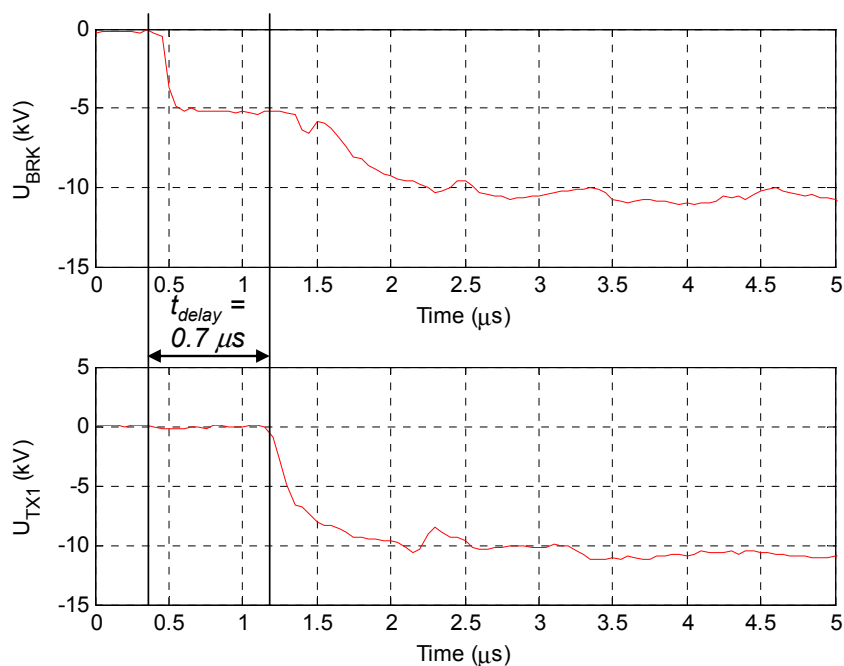
Figure 40: Time delay between the recordings of voltage at breaker (upper graph) and transformer TX1 (lower graph) terminal phase c (when the breaker is closing at no load)

5.6 Wave Reflections

When the maximum voltage step recorded at the terminal of transformer TX1 (U_{TX1}) is observed, wave reflection phenomenon should be considered. This phenomenon is shown in Figure 41 and can be explained by considering traveling waves initiated by energizing an open-circuited line [12]. In this case, the currents traveling toward the transformer TX1 (no load) will be reflected with the same magnitude but opposite in polarity, hence becoming zero. In this situation the magnetic energy associated with the current disappears when the current is brought to zero and it reappears as electric energy, which manifests itself in the doubling of the voltage (2 x ½ $\left|U_{peak}\right|$)

coming in from the direction of the breaker (see Figure 42). Note that the current transformers are installed at the breaker (see Figure 30) so that a time delay equal to 0.63 μs is expected. The measurement results show the time delay of 0.7 μs between the current-going-down-to-zero recorded at the breaker and the doubling of voltage at the transformer TX1 terminal (see Figure 41). Thus, the measurement results from the cable system laboratory are verifying the traveling wave phenomenon.
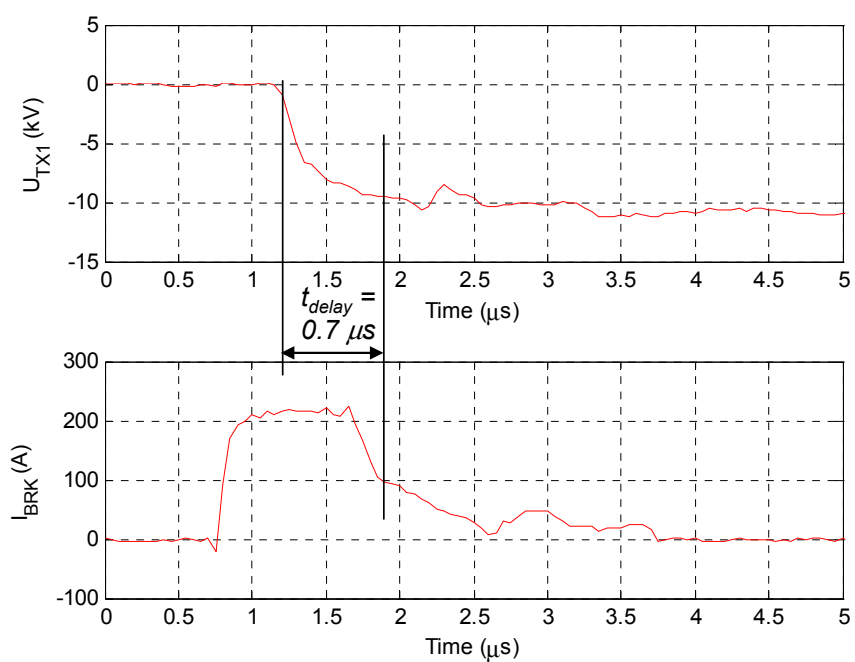
Figure 41: Reflection-wave phenomenon at transformer TX1 terminal phase c when breaker is closing at no load
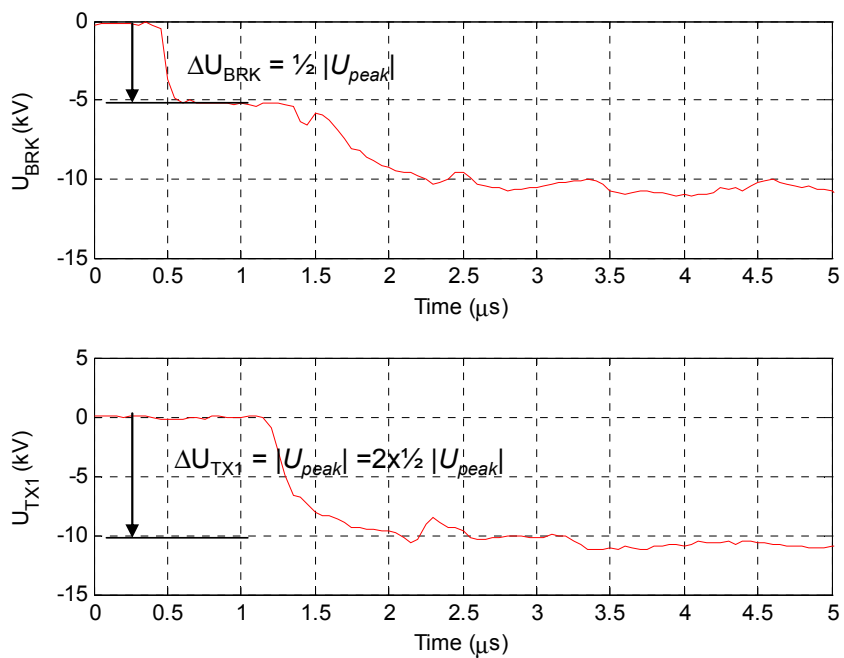

Figure 42: Voltage doubling at transformer TX1 terminal phase c due to wave reflection

Another wave reflection phenomenon can be observed on the voltage response recorded at the breaker terminals. The voltage that travels to the transformer TX1 is doubled and reflected back to the breaker. When this reflected wave arriving back at the breaker and is compared (in time) to the initial voltage step (at the breaker), there should also be a time delay of 0.63 µs (due to the 72 m cable distant and the 55 m longer fiber optics – see Section 5.5). This is verified in the measurement results shown in Figure 43.
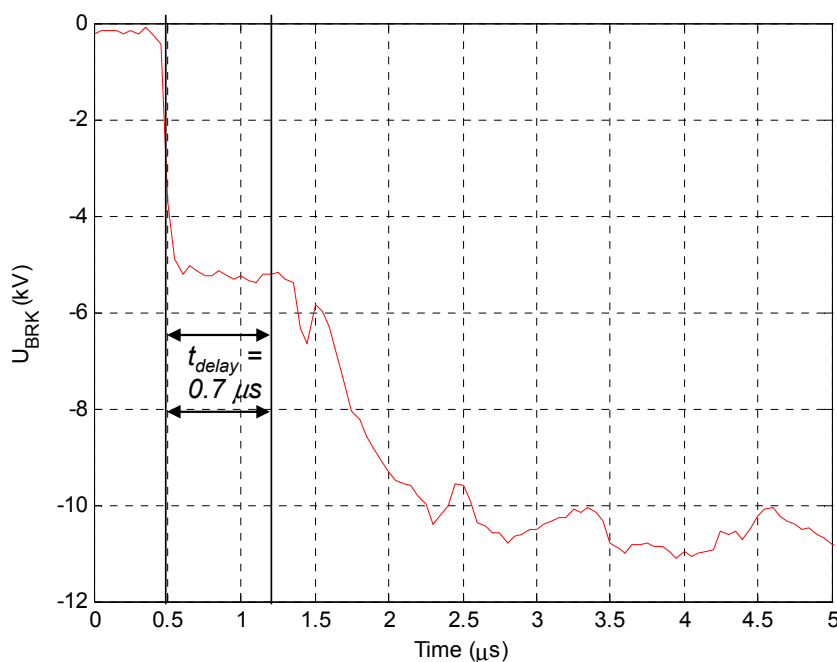
Figure 43: Reflection wave phenomenon at breaker terminal phase c (in case of closing the breaker at no load)

5.7 Repetitive Pre-Strikes and Re-Ignitions

Using the approach described in Section 2.3.4, where the operation (opening/closing) of the breaker is performed in such a way that the worst case is resulted, repetitive pre-strikes and re-ignitions can be generally observed in the base case from all test routines. As can be seen in Figure 31 to Figure 35, repetitive pre-strikes and re-ignitions are observed in the base case from closing and opening the breaker at no-load as well as closing and opening the breaker with inductive load connected at the LV side of the transformer TX1. The number of strikes occurring in each breaker switching can be many (in case of closing and opening breaker at no load) up to tens and hundreds (in case of closing and opening breaker with inductive load connected).

As expected, the worst tov. experienced by the transformer TX1 occurred when the breaker is opening with an inductive load connected at the LV side of the transformer and the opening moment is at its closest to the chopping current level. In this situation, the breaker can immediately chop the current,

however the separation of the breaker contacts are still in the initial (small) distance. In this case, the voltage across the contacts can easily surpass the dielectric recovery, hence multiple re-ignitions overvoltages can easily occur. A typical measurement result with this kind of worst multiple re-ignitions occurred at transformer TX1 terminals when the breaker is opening with the inductive load being connected, is shown in Figure 44.
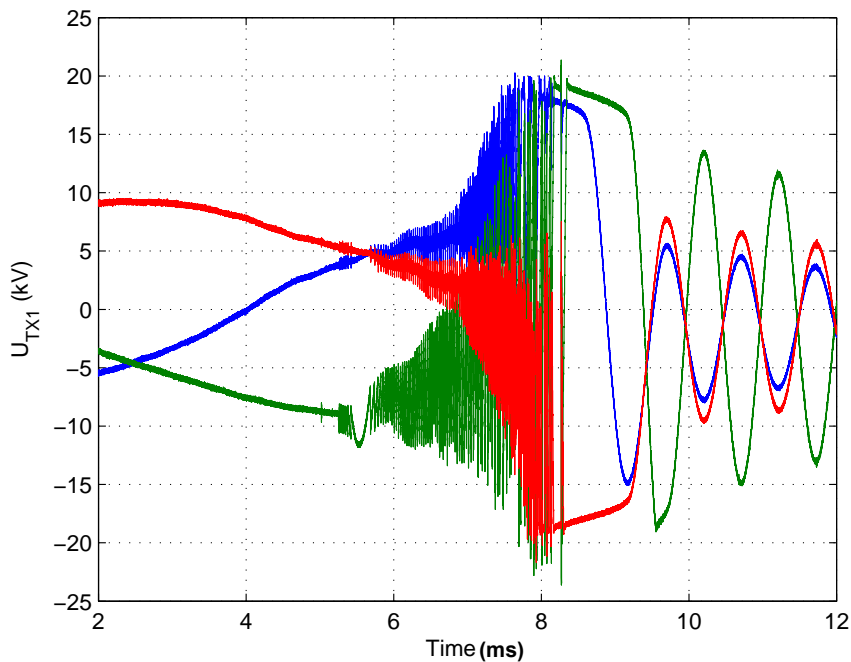

Figure 44: The worst multiple re-ignitions occurred at transformer TX1 terminals when the breaker is opening with an inductive load being connected

5.8 Transient Overvoltage Quantifications from Measurement Results (U_{TX1})

Transient overvoltage quantifications from the measurement results using the quantification method developed in Section 4 can be used for "finger printing" each measurement result and showing it as the a scattered plot diagram like in Figure 27 as well as obtaining the maximum values and presenting them in a table format as in Table 4. Figure 45 to Figure 52 show the use of the quantification method for "finger printing" the measurement results of the base case. Table 5 and Figure 53 summarize the maximum values obtained from them.

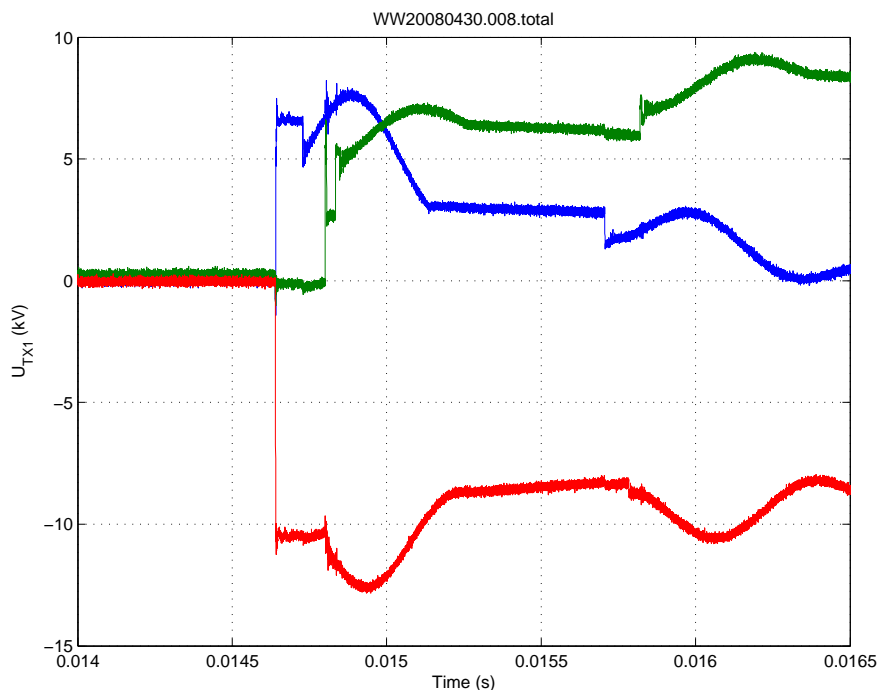## 5.8.1 Closing Breaker at No Load (Base Case)

Figure 45: Measured voltage at the transformer TX1 terminals
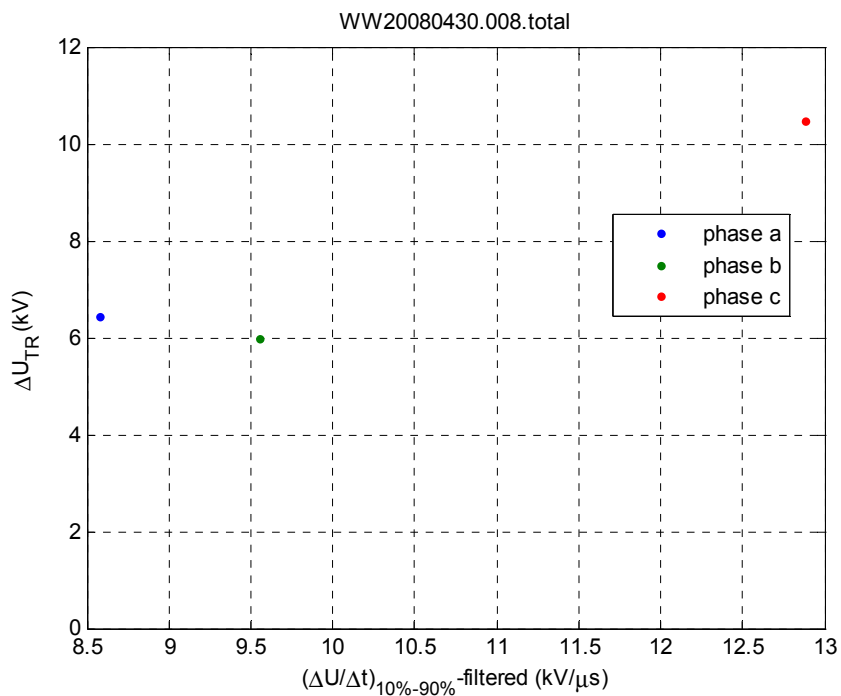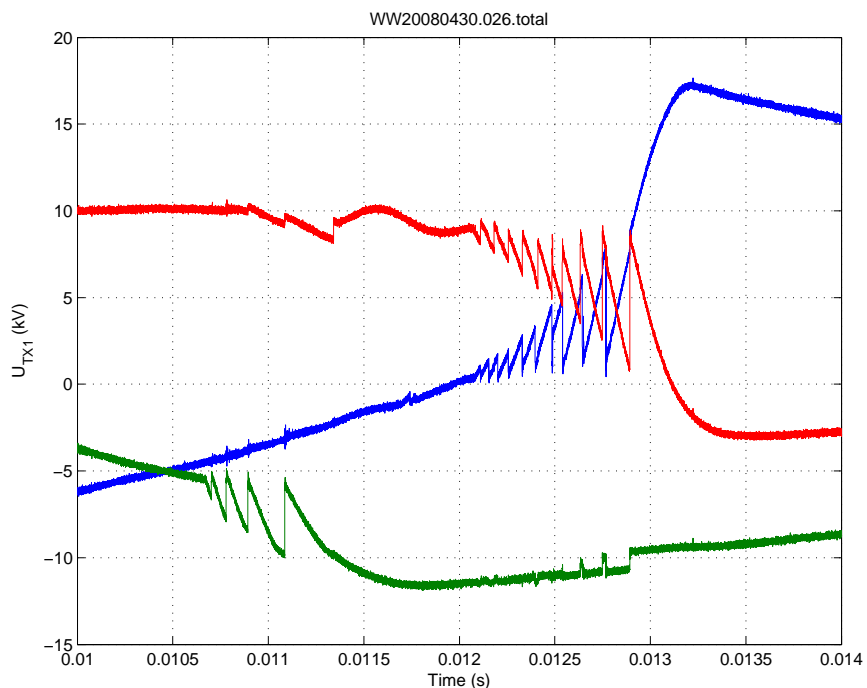

Figure 46: Quantifying strikes of the measured voltage at the transformer TX1 terminals of Figure 45

5.8.2 Opening Breaker at No Load (Base Case)

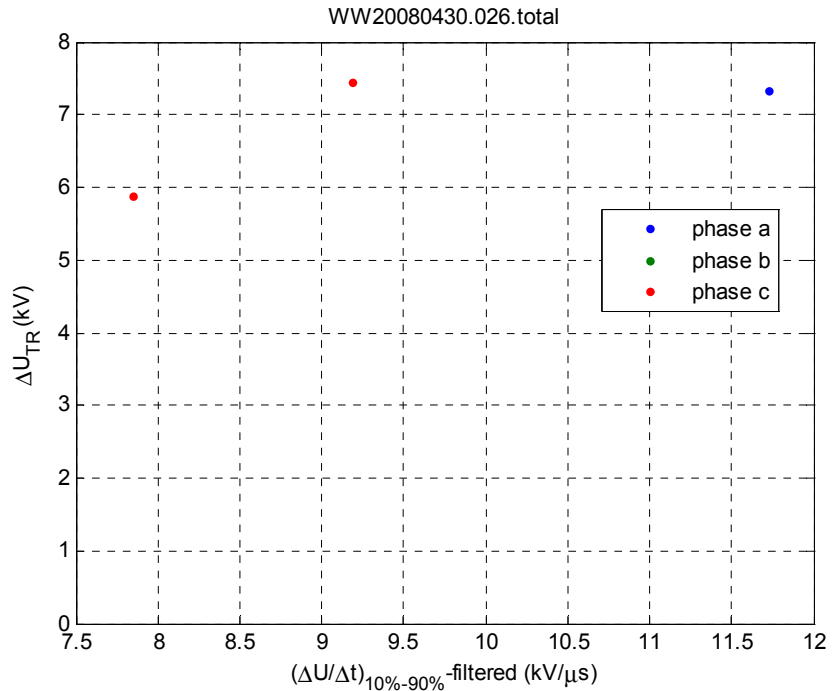*Figure 47: Measured voltage at the transformer TX1 terminals*

Figure 48: Quantifying strikes of the measured voltage at the transformer TX1 terminals of Figure 47

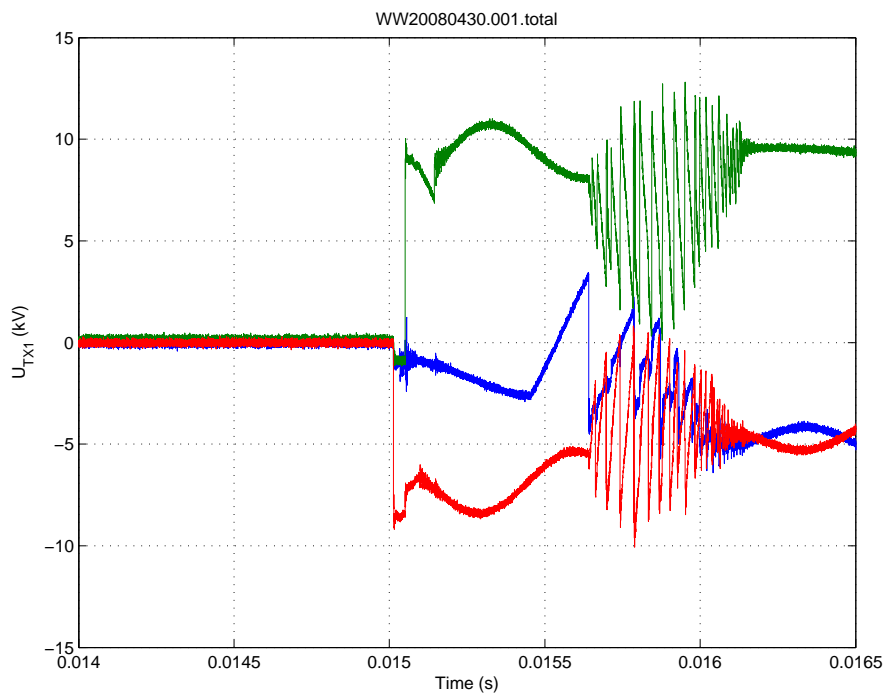### 5.8.3 Closing Breaker with an Inductive Load Connected (Base Case)

Figure 49: Measured voltage at the transformer TX1 terminals
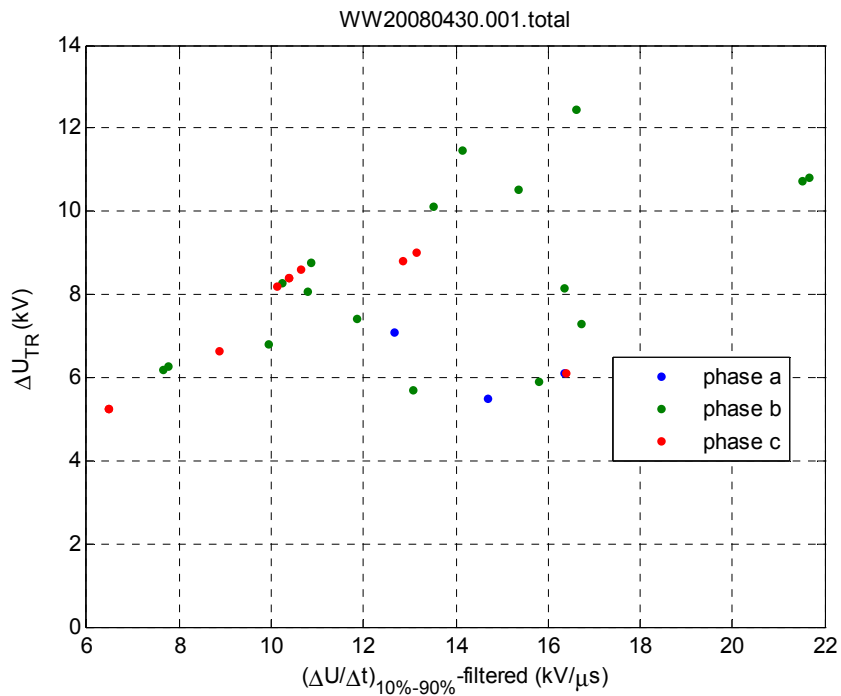

Figure 50: Quantifying strikes of the measured voltage at the transformer TX1 terminals of Figure 49

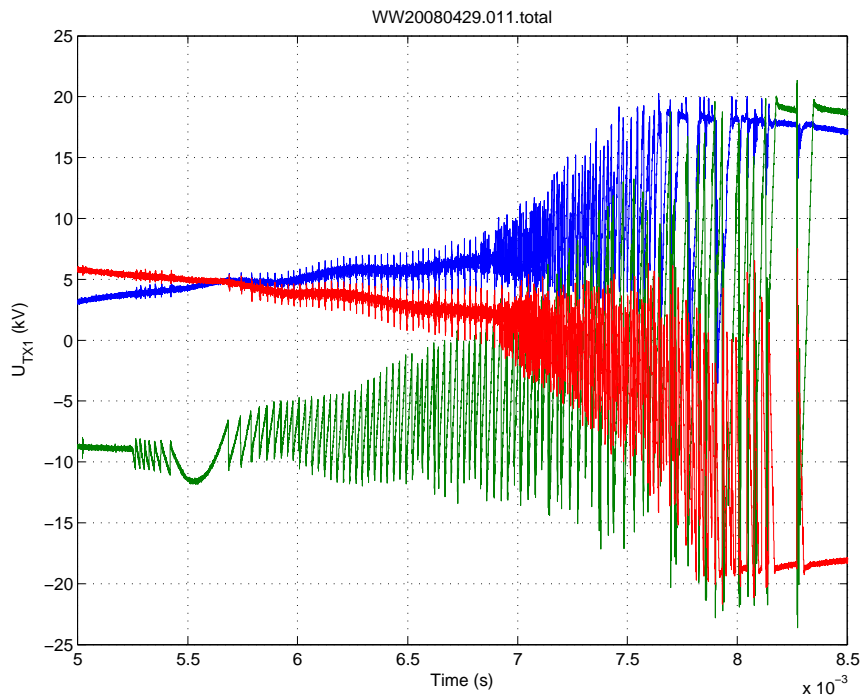## 5.8.4 Opening Breaker with an Inductive Load Connected (Base Case)

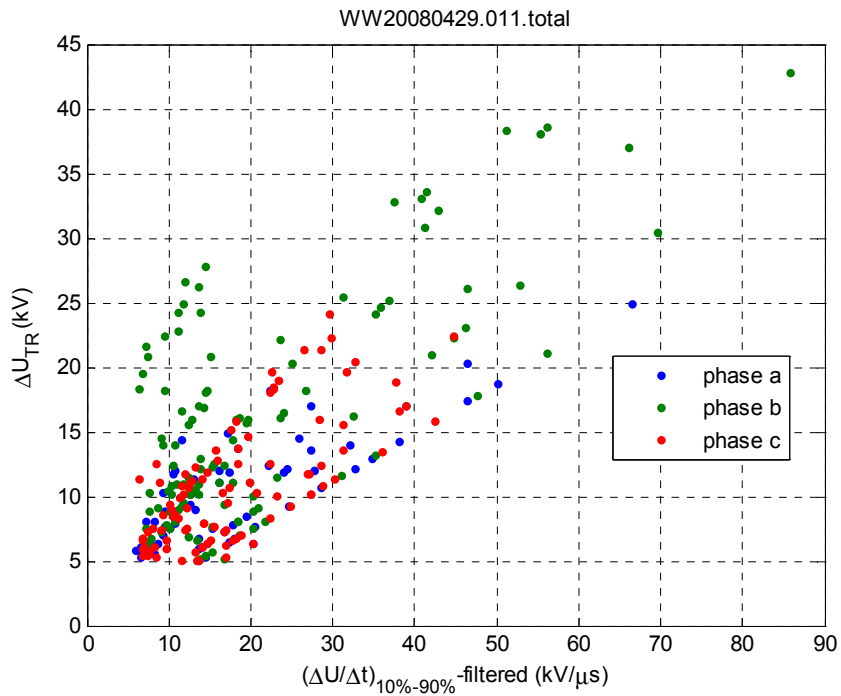*Figure 51: Measured voltage at the transformer TX1 terminals*

Figure 52: Quantifying strikes of the measured voltage at the transformer TX1 terminals of Figure 51

Table 5 Summary of strikes indicators from the base case on all test routines

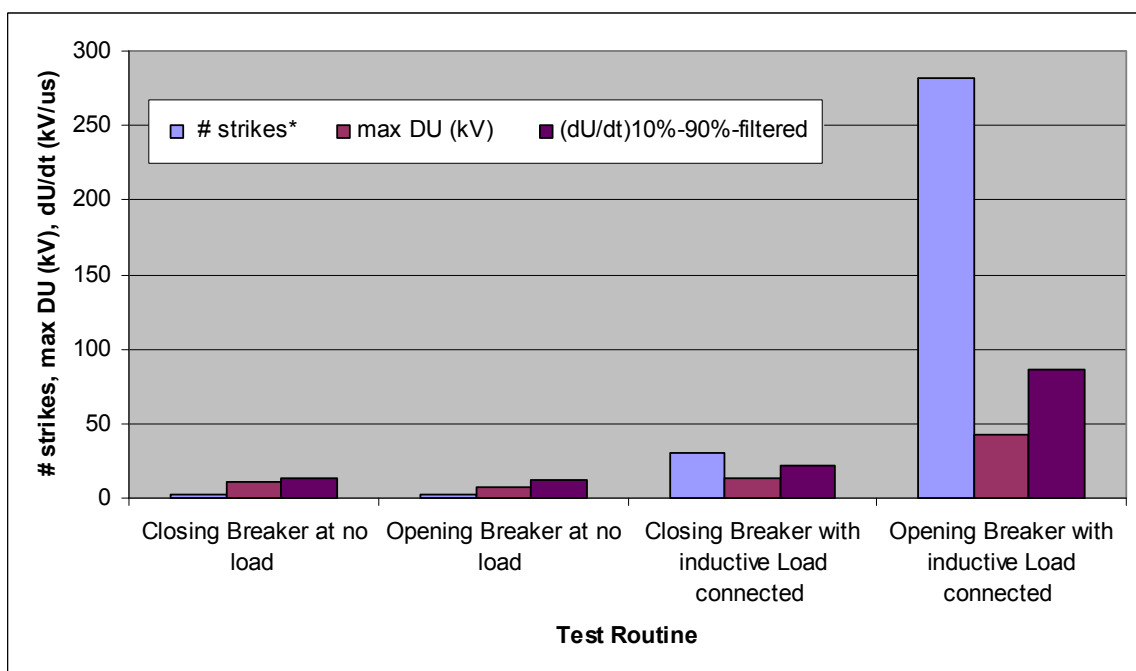| Case	# strikes (ΔU > 5 kV and within $\dfrac{\Delta U}{\Delta t}$ > 5 kV/µs, phase a-b-c)	max ΔU (kV)	$\left(\dfrac{dU}{dt}\right)_{10\%-90\%}$ filtered (kV/µs)
Closing Breaker at no load	3	10.5	13
Opening Breaker at no load	3	7.5	12
Closing Breaker with inductive Load connected	30	13	22
Opening Breaker with inductive Load connected	282	43	86

Figure 53: Summary of strikes indicators from the base case on all test routines

5.9 Results from Statistical Data Collections

As presented earlier in Section 3.8.4, breaker operation will be stochastic in terms of closing and opening time. In this experiment, several shots (3-5) are performed within one instant of breaker switching (opening/closing) time for the purpose of investigating/recording the stochastic performance of the breaker operation.

Two examples of the statistical data collections are presented in this section, namely: the breaker closing at no load and the breaker opening with an inductive load connected, both within the base case. These examples are presented with the measurements results shown in Figure 54 and Figure 57, as well as the strikes quantifications in Figure 55 and Figure 58.,The summary of the strike quantifications are shown in Table 6-and-Figure 56 and Table 7-and-Figure 59, in the next Sections 5.9.1 and 5.9.2. Note that the control equipment within this laboratory setup enables the exact and repeated shots for switching the breaker at a defined instant time.'

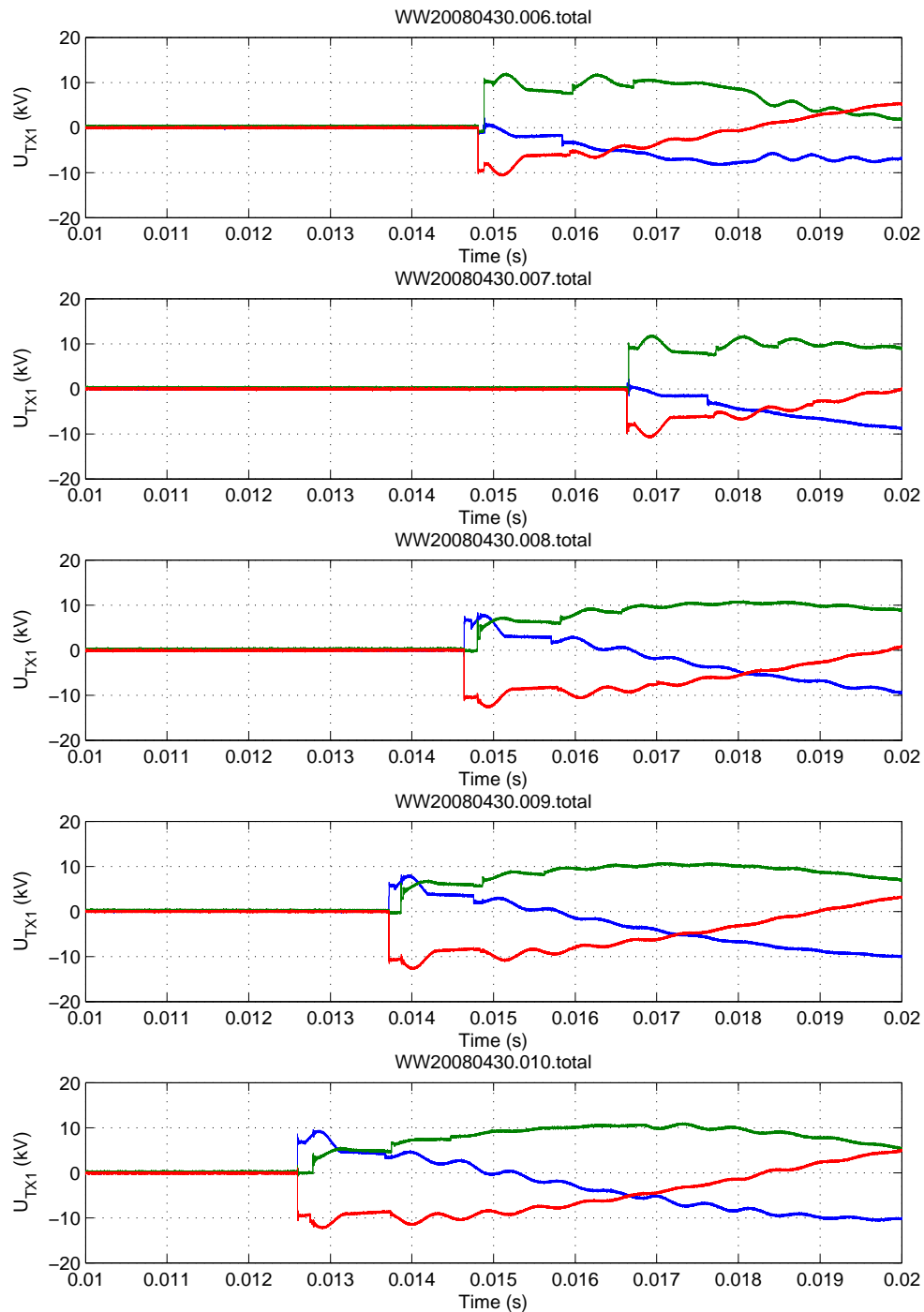## 5.9.1 Base Case: Closing Breaker at No Load

Figure 54: Voltage measured at the transformer TX1 terminals in the Base Case: Closing breaker at no load for statistical data collection

Figure 55: Quantifying strikes of the measured voltage at the transformer TX1 terminals in Figure 54 (color: blue = phase-a, green = phase-b, red = phase-c; marker: pluses = 'WW20080430.006', circles = 'WW20080430.007', crosses = 'WW20080430.008', squares = 'WW20080430.009', triangles = 'WW20080430.010')

Table 6 Base Case: Closing breaker at no load – statistical data collection

Case (shot #)	# strikes (ΔU > 5 kV and within $\dfrac{\Delta U}{\Delta t}$ > 5 kV/µs, phase a-b-c)	max ΔU (kV)	$\left(\dfrac{dU}{dt}\right)_{10\%-90\%}$ filtered (kV/µs)
0430.006	2	10.5	15
0430.007	2	11	19
0430.008	3	10.5	13
0430.009	3	10.5	14
0430.010	2	11	30

Figure 56: Base Case: Closing breaker at no load – statistical data collection

5.9.2 Base Case: Opening Breaker with an Inductive Load Connected
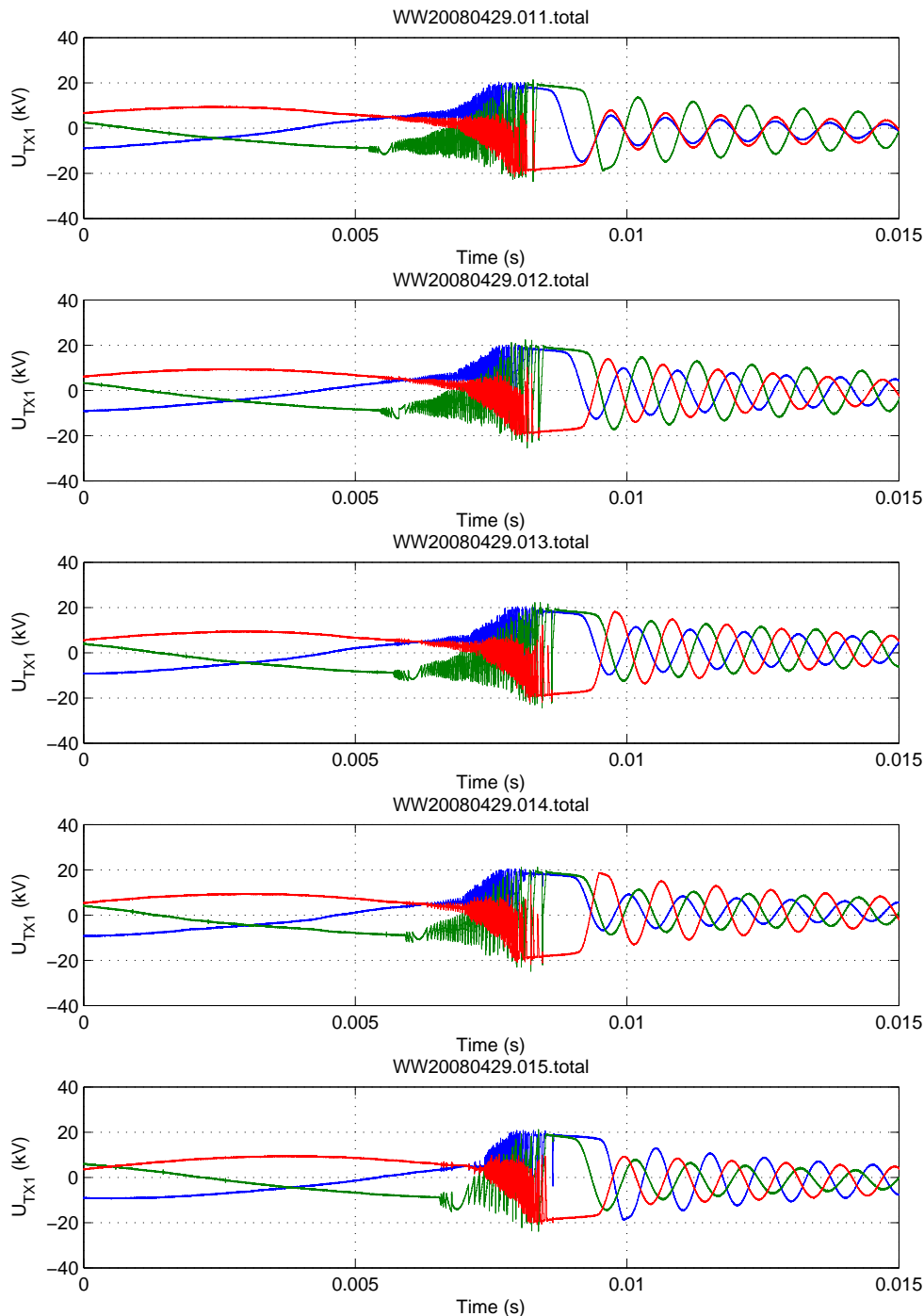
Figure 57: Voltage measured at the transformer TX1 terminals in the Base Case: Opening breaker with an inductive load connected for statistical data collection
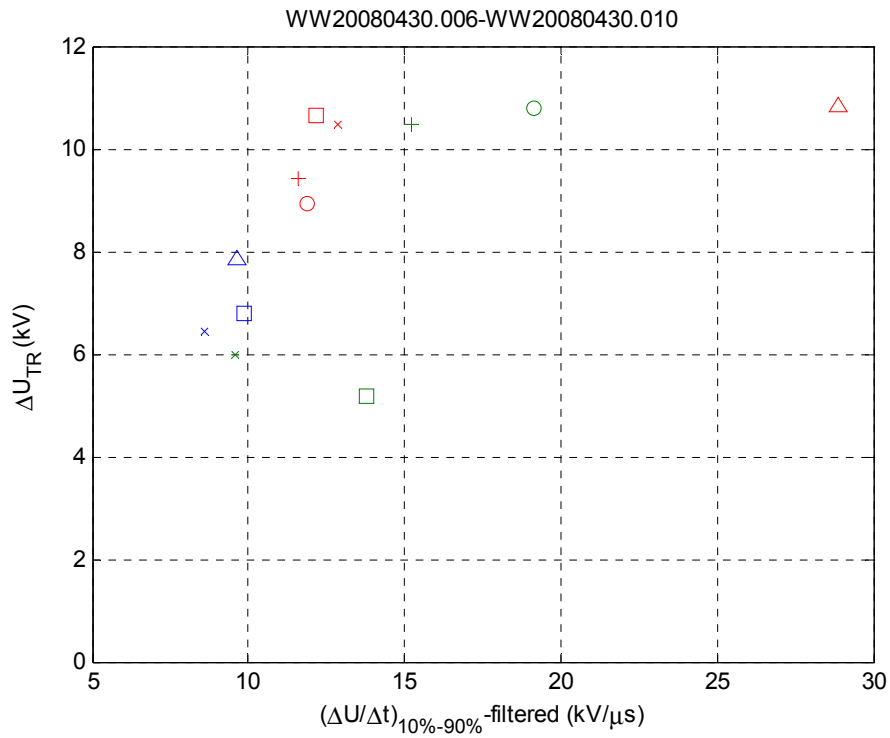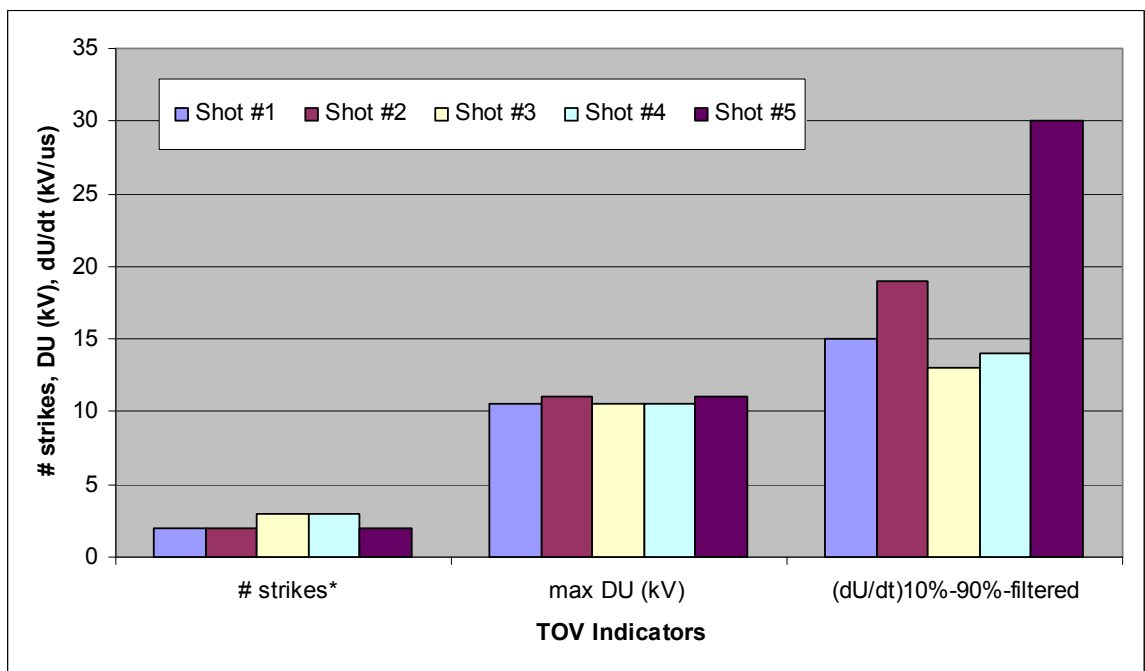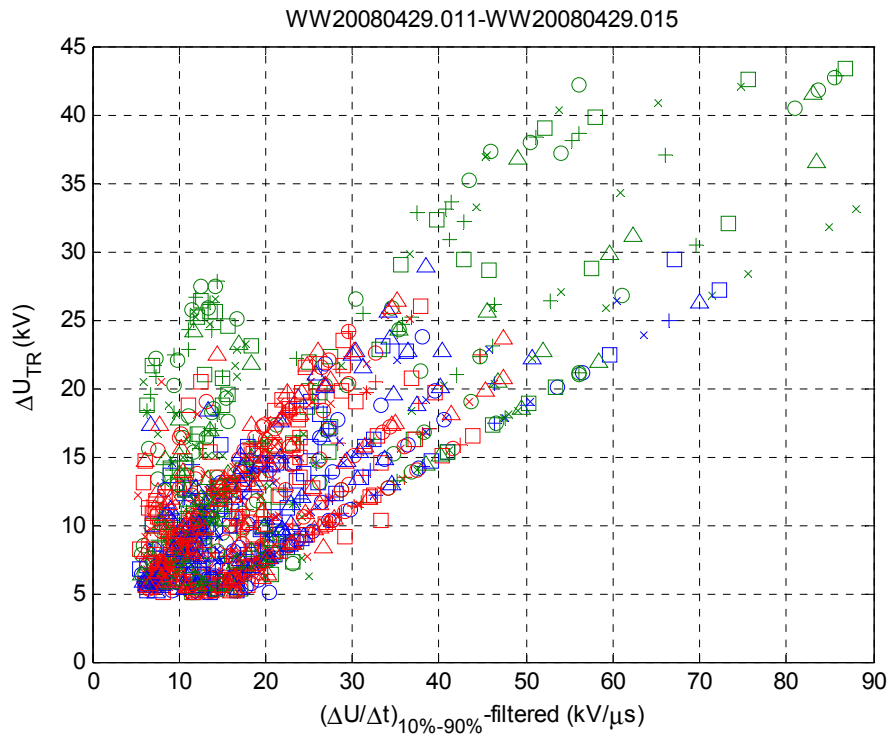
Figure 58: Quantifying strikes of the measured voltage at the transformer TX1 terminals in Figure 57(color: blue = phase-a, green = phase-b, red = phase-c; marker: pluses = 'WW20080429.011', circles = 'WW20080429.012', crosses = 'WW20080429.013', squares = 'WW20080429.014', triangles = 'WW20080429.015')

Table 7 Base Case: Opening breaker with an inductive load connected – statistical data collection

Case (shot #)	# strikes (ΔU > 5 kV and within $\dfrac{\Delta U}{\Delta t}$ > 5 kV/µs, phase a-b-c)	max ΔU (kV)	$\left(\dfrac{dU}{dt}\right)_{10\%-90\%}$ filtered (kV/µs)
0429.011	282	43	86
0429.012	264	43	85.5
0429.013	323	42	88
0429.014	274	43	87
0429.015	230	41.5	82.5

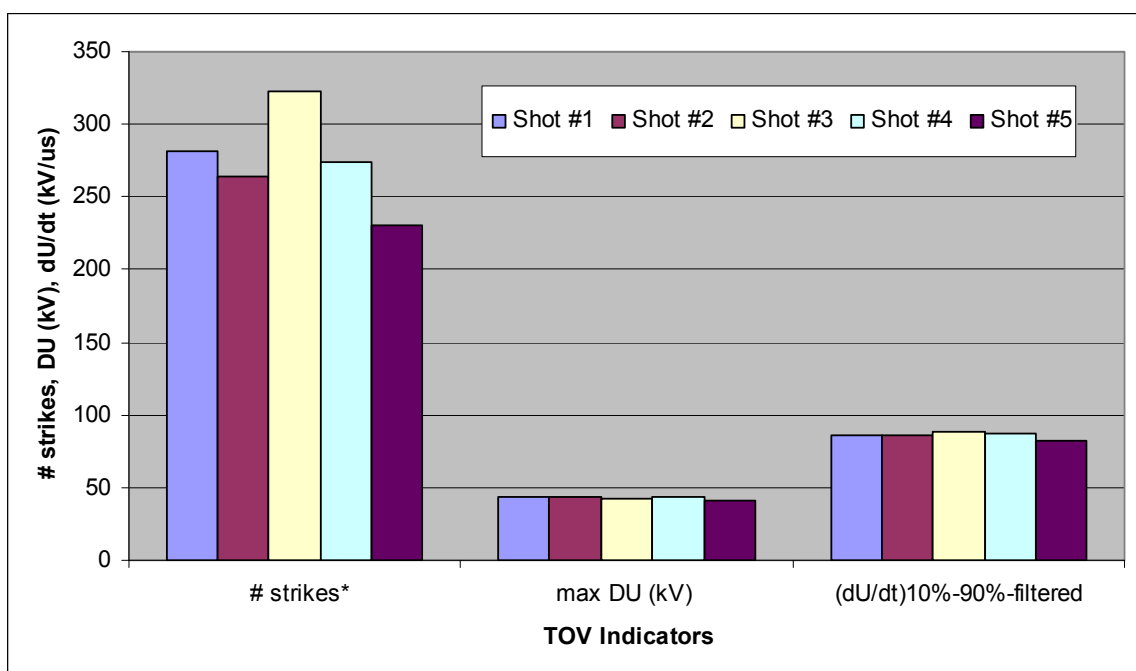Figure 59: Base Case: Opening breaker with an inductive load connected – statistical data collection

69

6 Experiment and Verifications of Transient Overvoltage Mitigation Methods

6.1 Surge Capacitors

6.1.1 Impact of Surge Capacitors on Fast Transient Overvoltages

In the previous Section 5.3 the voltage across a load like a transformer when it is hit by a step voltage propagating is described as (1) where the time constant of the voltage τ is proportional to the Z_{surge} (the surge impedance of the cable) and C_{load} (the capacitance of the load).

Surge capacitor can be used to decrease the rate-of-rise (steepness) of the recovery voltage. For this purpose, a surge capacitor is connected in <u>shunt</u> to the circuit (see Figure 60). The total capacitance in (1) will be increased, so that the time constant, τ_2, that is the time constant after surge capacitors are installed, then becomes:

$$\tau_2 = Z_{surge}\left(C_{load} + C_{surge-cap}\right) \qquad (4).$$

For example, when a surge capacitor with a capacitance value of 10 times higher than the load capacitance is installed, roughly 10 times longer time constant can be expected (compared to the original case without any surge capacitor installed).
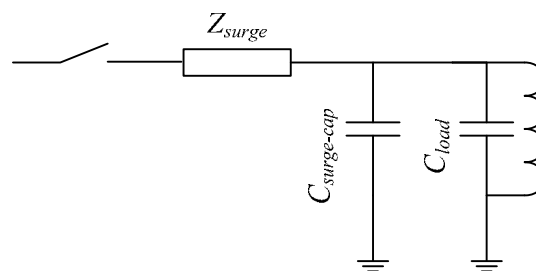
Figure 60 Simplified model for the electrical circuit when tov. pass across a transformer connected to a cable and surge capacitors are installed

Within the laboratory experiment, two different capacitance values of surge capacitors are tested, namely: 83 nF and 130 nF. These two capacitance values correspond to the time constants which are equal to 5.0 μs and 7.56 μs, respectively. These values are roughly 10 times and 20 times higher than the base case (without any surge capacitor installed) where the time constant is equal to 0.46 μs (see Section 5.3).

Figure 61 shows the calculated expected voltage response across transformer TX1, based on (4) and (2) for the base case with no capacitor and for the cases with 83 nF and 130 nF surge capacitors installed at the transformer terminals.
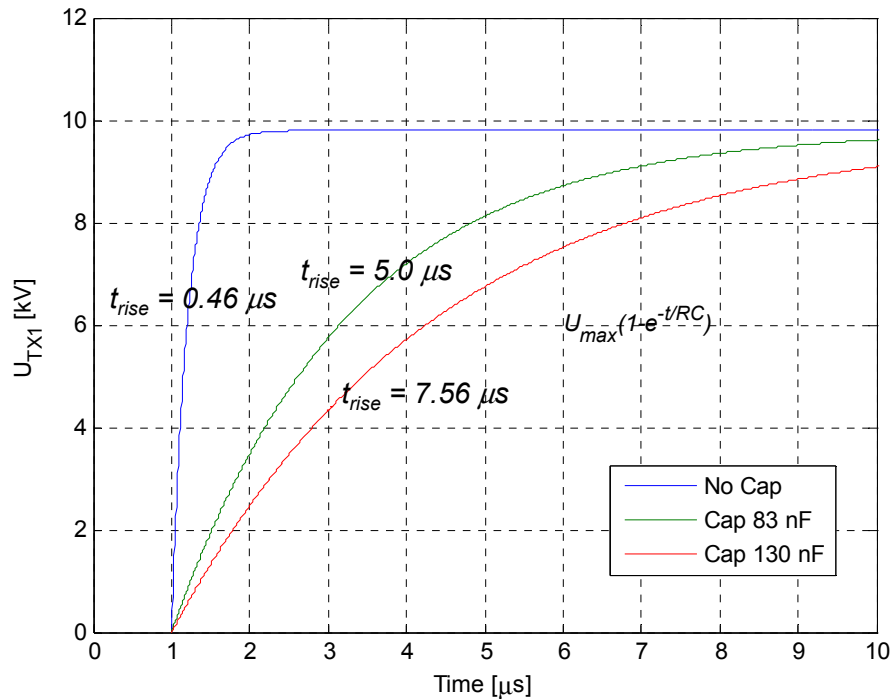
Figure 61: Voltage responses across transformer TX1 when the case with surge capacitors installed at the transformer terminals is compared to the base case

6.1.2 Verification of the Surge Capacitor Impact on Fast tov.

The impact of the surge capacitors are verified by comparing the measurement with the hand calculation results.

Case number 2 and 3 listed in Table 2 are corresponding to the case of installing surge capacitors as protection devices for tov. mitigations at the transformer TX1 terminals. In case number 2, 83-nF surge capacitors are installed and in case number 3, 130-nF surge capacitors are installed. The laboratory circuits for these two cases are shown in Figure 62.

72

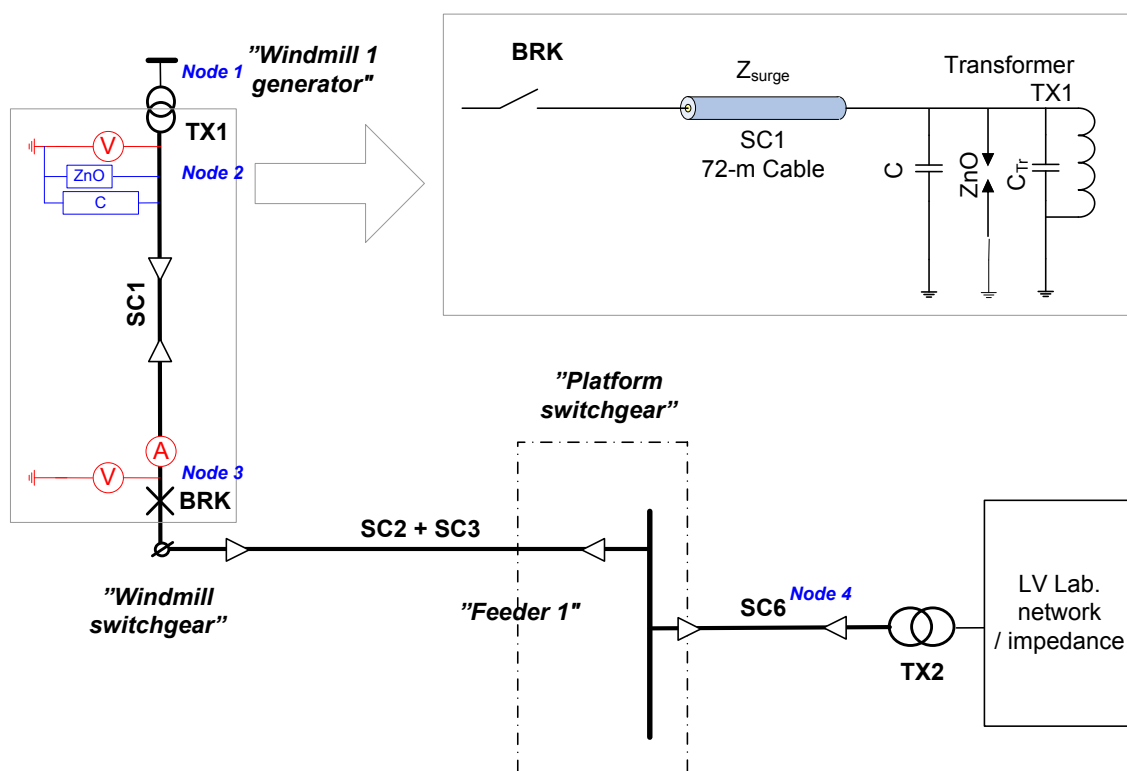| No	Case ID	ZnO	Surge Capacitor		RC-Protection	
		Location (installation)	Location (installation)	Parameter	Location (installation)	Parameter
2	C83-TX1	Node 2 (shunt)	Node 2 (shunt)	C=130nF		
3	C130-TX1	Node 2 (shunt)	Node 2 (shunt)	C=83nF		

Figure 62: Laboratory setup and circuit for Case ID: C83-TX1 and C130-TX1 – respectively, in addition to the surge arresters, surge capacitors with capacitance equal to 83 nF and 130 nF each are shunted at the terminals of the transformer TX1 (node 2)

Figure 63 shows the measurement results of installing surge capacitors at the terminals of transformer TX1 (solid lines) compared to the results derived from the theoretical calculations using (1) to (4). The measurement results are obtained from the operation of closing the breaker at no load. Patterns can be observed that the reductions of rise time shown in the calculation results are followed by the results from measurement. However, the experimental results still show very high derivative in the very beginning of the step transient. This is due to the stray inductance of the connection to the surge capacitor. This phenomenon is shown in detail in Enclosure B in Section 13.
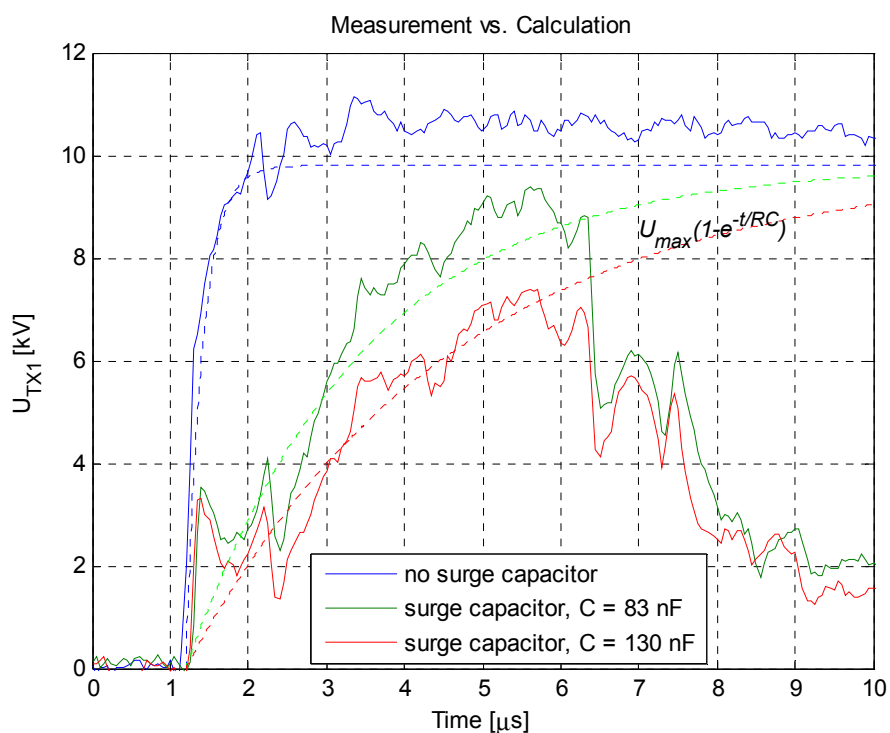

Figure 63: Measurement results of installing surge capacitors at the terminals of transformer TX1 (solid lines) compared to the results derived from calculations using (1) to (4) (dotted lines)

6.1.3 Surge Capacitors at Breaker Terminals

A case where surge capacitors are installed at the breaker terminal is tested, widh the laboratory circuit composed as shown in Figure 64.

No	Case ID	ZnO	Surge Capacitor		RC-Protection	
		Location (installation)	Location (installation)	Parameter	Location (installation)	Parameter
4	C130-BRK	Node 2 (shunt)	Node 3 (shunt)	C=130nF		
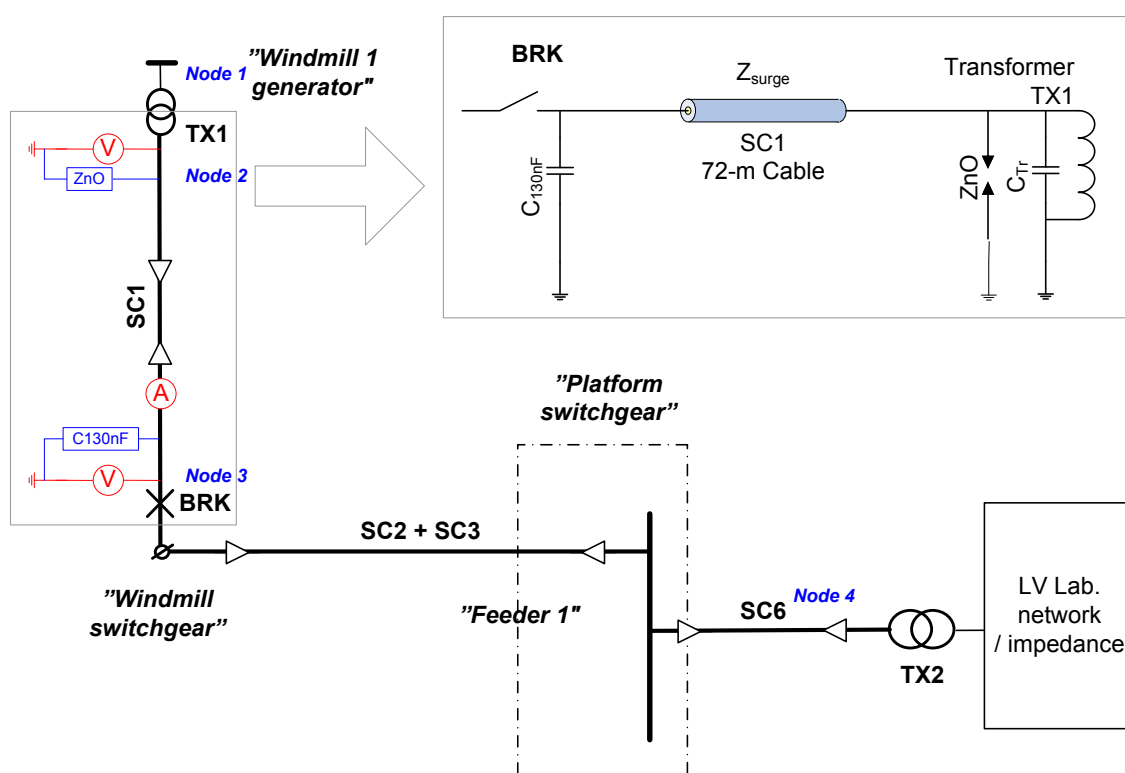
Figure 64: Laboratory setup and circuit for Case ID: C130-BRK – in addition to the surge arresters shunted at the terminals of Transformer TX1, surge capacitors with capacitance equal to 130 nF each are shunted at the terminals of the breaker BRK (towards TX1, node 3)

The measurement results of the circuits when the surge capacitors (C=130 nF) are installed at the transformer TX1 terminals (see Figure 62) and when the surge capacitors are installed at the breaker BRK terminals (see Figure 64) are displayed and compared in Figure 65 and generally, similar voltage responses at the transformer TX1 terminals are obtained (the breaker is closing at no load).
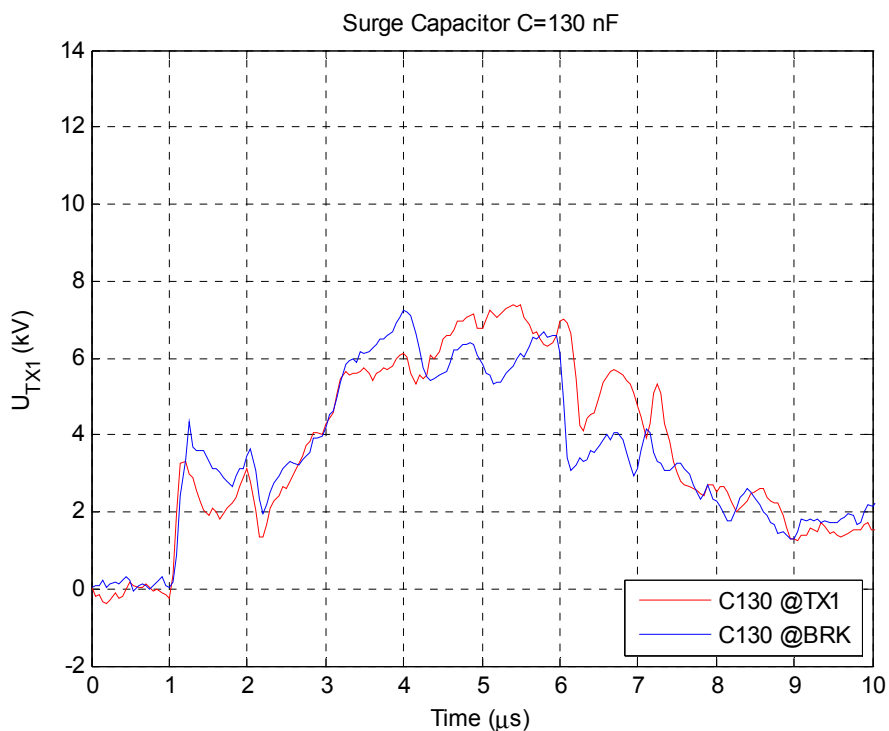
*Figure 65: Generally similar voltage responses at the transformer TX1
terminal are obtained (breaker is closing at no load) when the surge
capacitors (C=130 nF) are installed at the transformer TX1 terminals (see
Figure 62) and when the surge capacitors are installed at the breaker BRK
terminals (see Figure 64)*

6.1.4 Impact on Transient Overvoltage Repetitiveness

6.1.4.1 Typical measurement results from breaker opening with an inductive load connected

As in the base case, the worst transient voltages are obtained in cases when
the breaker is opening with an inductive load connected. The typical results
with tov. repetitiveness obtained from the measurement when surge
capacitors are installed and the breaker is opening with an inductive load
connected are therefore highlighted in Figure 66 to Figure 68.
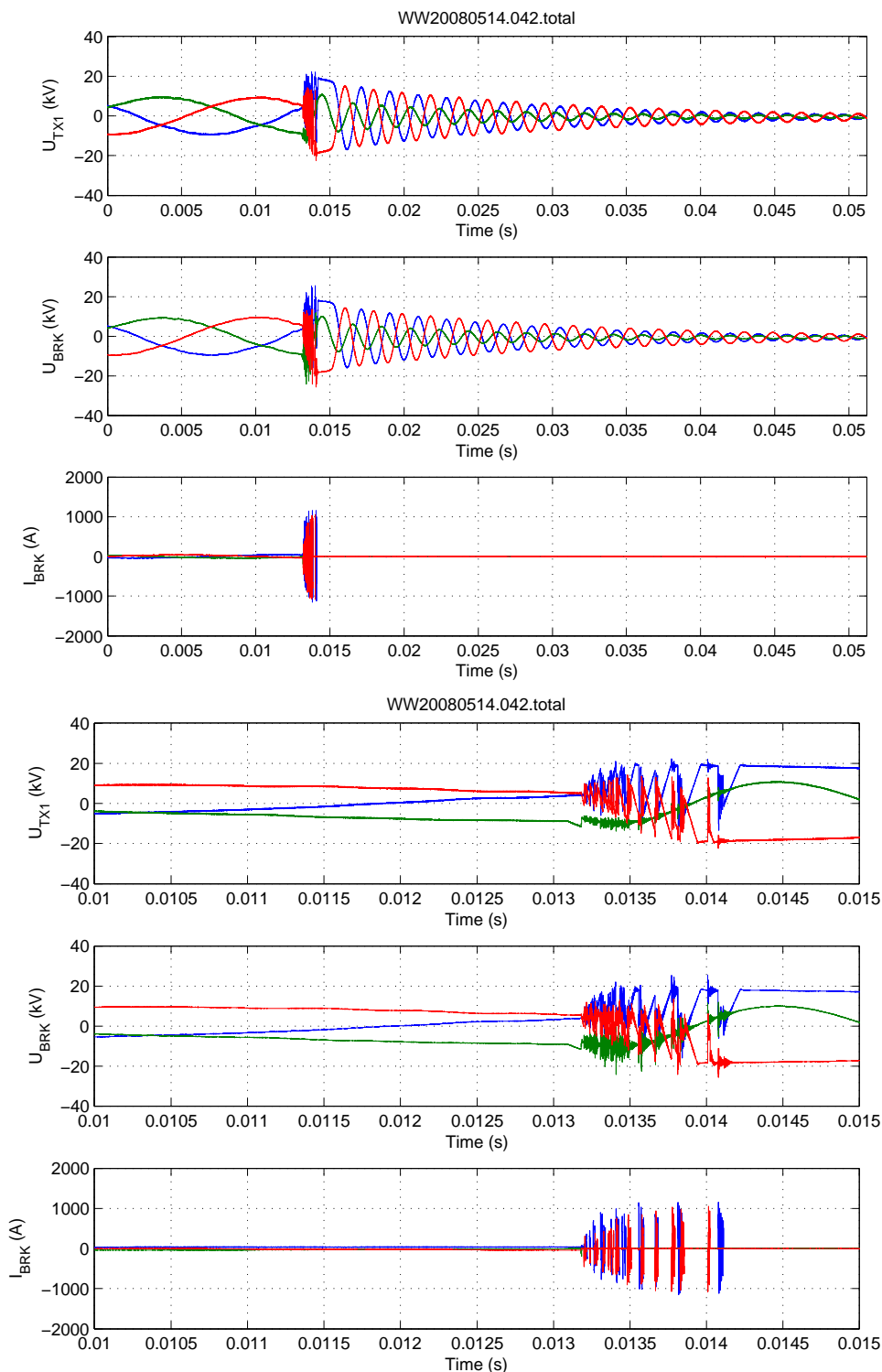
Figure 66: Measurement data from the Case ID C83-TX1: Opening breaker with an inductive load connected (at transformer TX1 terminals)
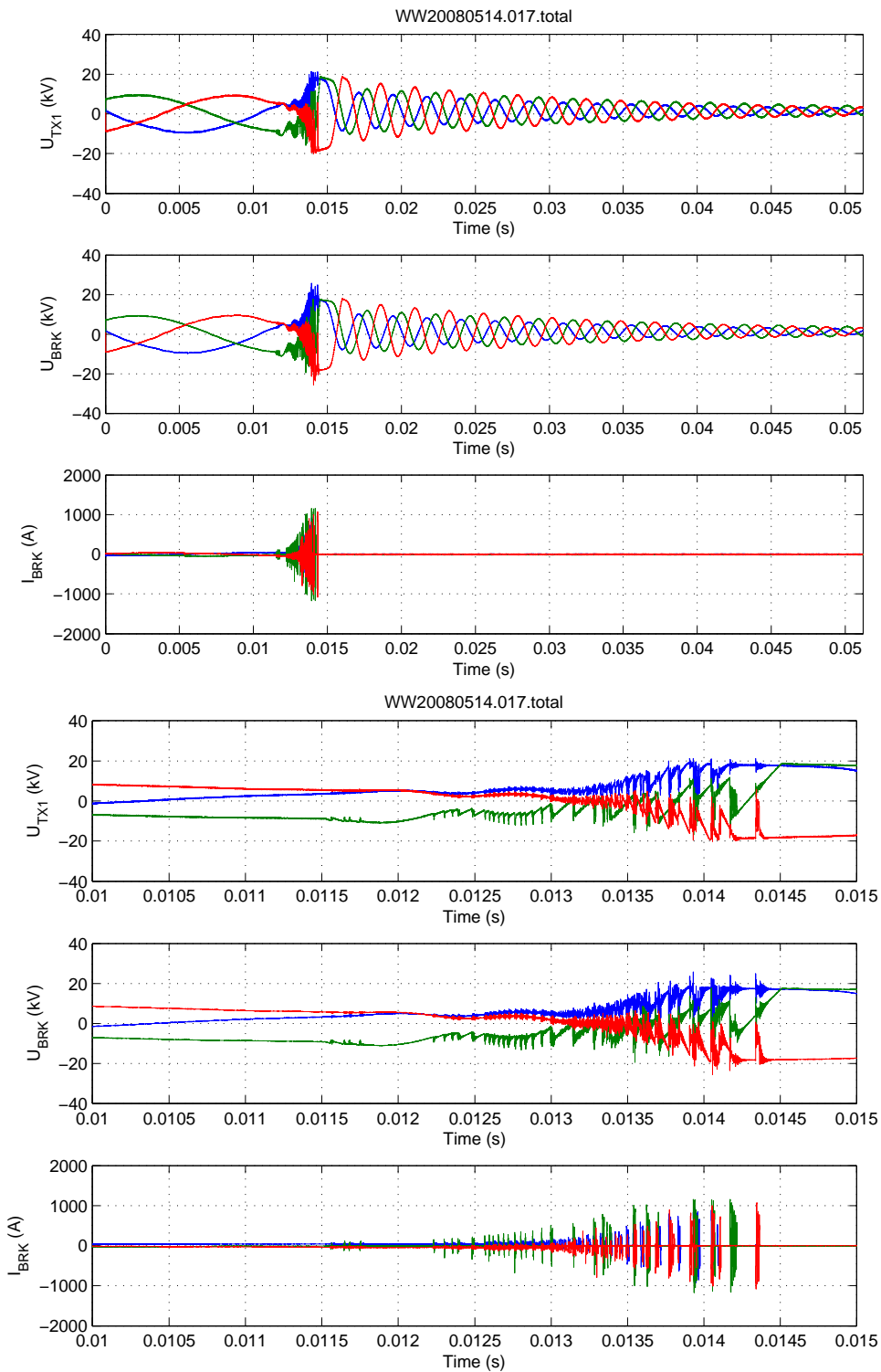
Figure 67: Measurement data from the Case ID C130-TX1: Opening breaker with an inductive load connected
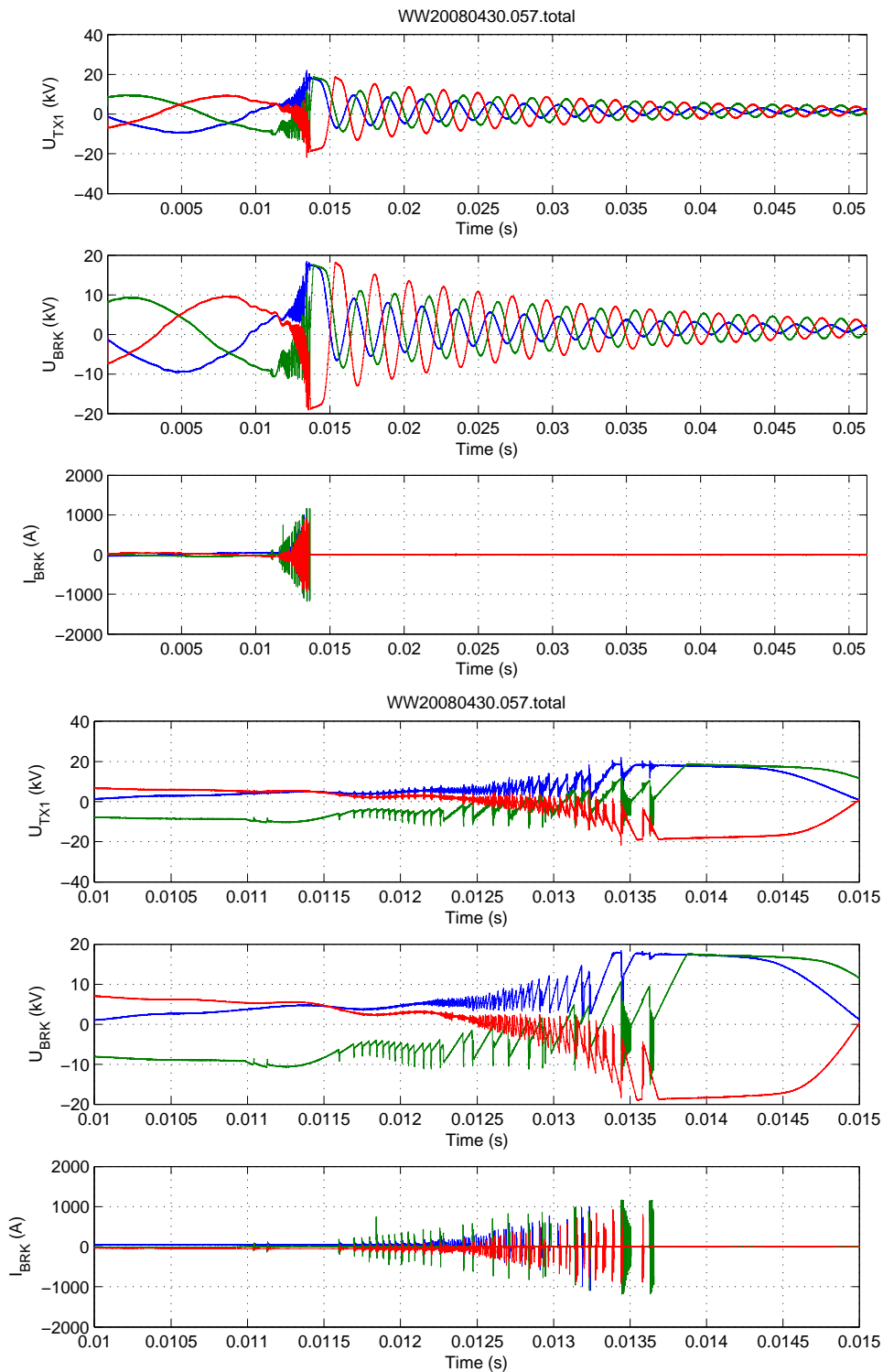
Figure 68: Measurement data from the Case ID C130-BRK: Opening breaker with an inductive load connected

6.1.4.2 Strike Quantifications

The strikes highlighted in Figure 66 to Figure 68 can be quantified further as respectively shown in Figure 69 to Figure 71.
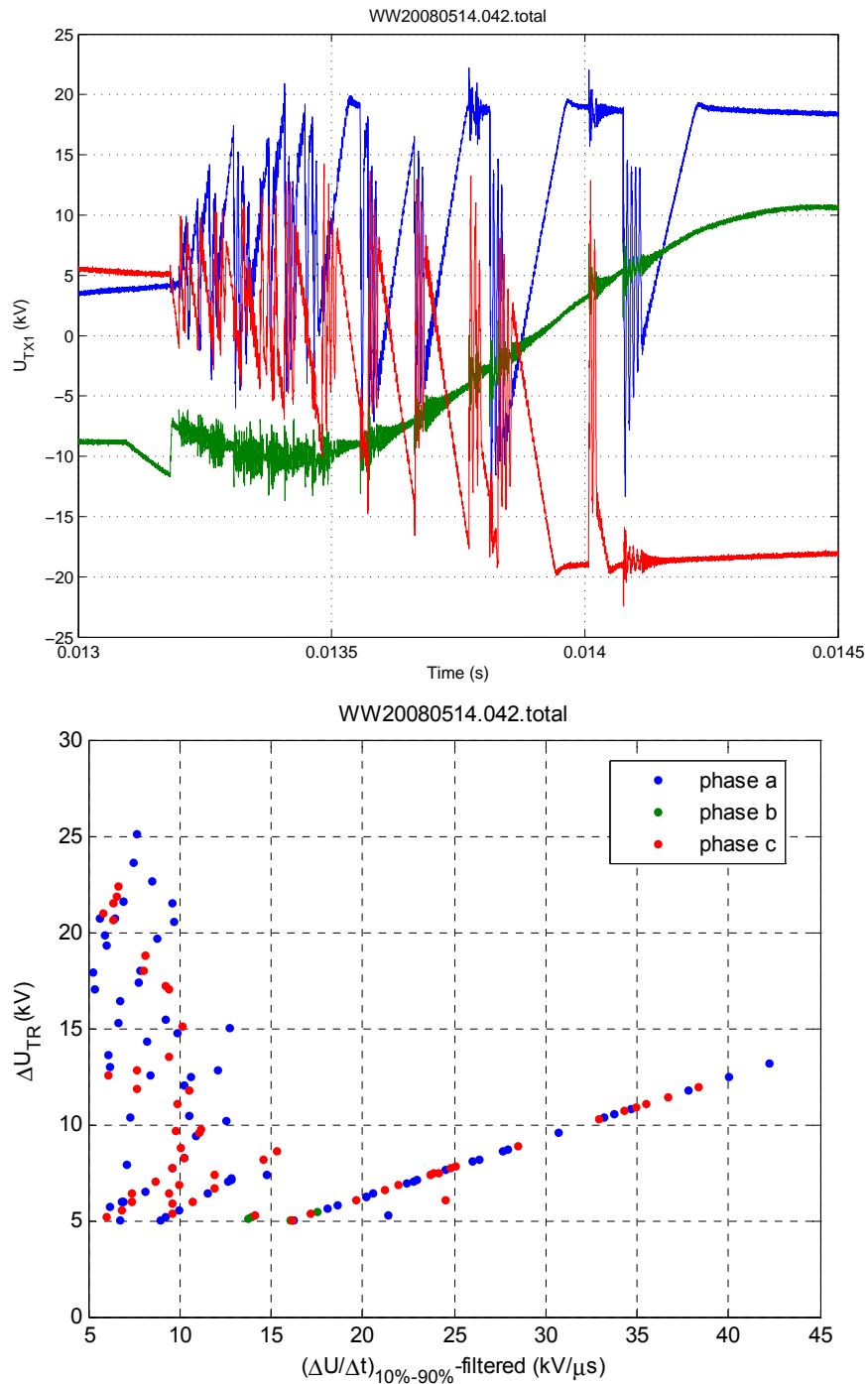
Figure 69: Voltage at transformer terminal TX1 (upper graph) and the corresponding quantification of the strikes (lower graph)
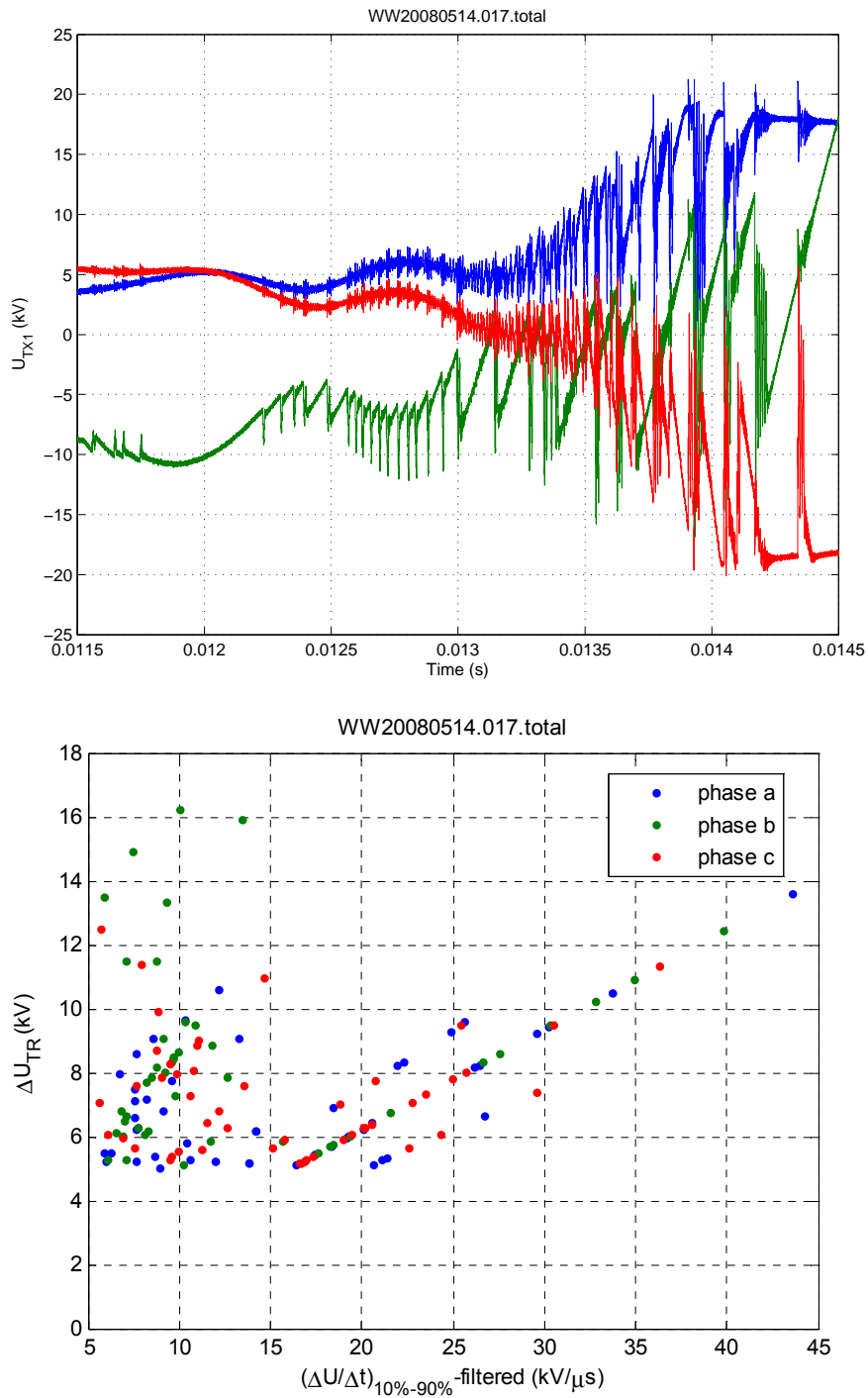
Figure 70: Voltage at transformer terminal TX1 (upper graph) and the corresponding quantification of the strikes (lower graph)
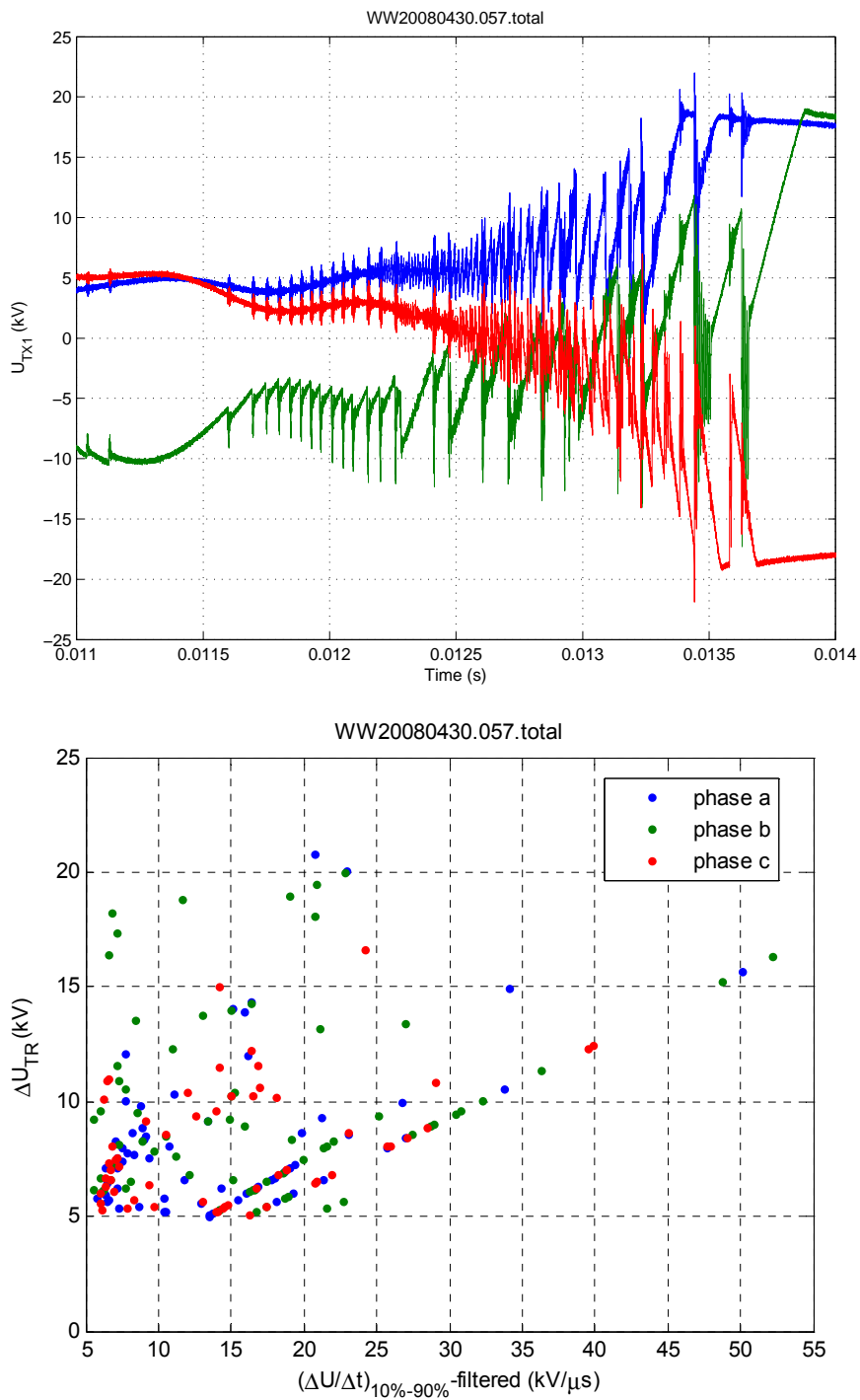
Figure 71: Voltage at transformer terminal TX1 (upper graph) and the corresponding quantification of the strikes (lower graph)

6.1.4.3 Summary of Strikes Quantifications

Table 8 Summary of Strikes Quantifications on cases with Surge Protections: at breaker opening with an inductive load connected (worst cases)

Case ID	# strikes (ΔU > 5 kV and within $\dfrac{\Delta U}{\Delta t}$ > 5 kV/µs, phase a-b-c)	max ΔU (kV)	$\left(\dfrac{dU}{dt}\right)_{10\%-90\%}$ filtered (kV/µs)
C83-TX1	129	25	42
C130-TX1	145	16.5	44
C130-BRK	190	21	52

6.2 RC-Protection

6.2.1 RC-Protection Impact

When an RC-Protection is shunted in front of the protected transformer (see Figure 72), during the fast transient, the capacitor part will be seen as a short circuit and therefore the voltage is only seeing the resistor. A general termination of a line is applied in this case. When a traveling wave reaches such a termination in the case of Figure 72 the reflection a and refraction b coefficients can be computed using:

$$a = \frac{R_{protection} - Z_{surge}}{R_{protection} + Z_{surge}} \quad \text{(5) and}$$

$$b = \frac{2R_{protection}}{R_{protection} + Z_{surge}} \quad \text{(6).}$$
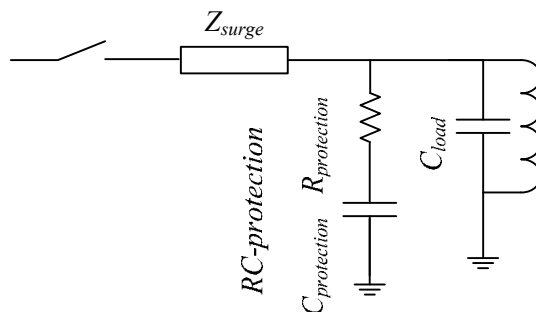
Figure 72: Simplified model for the electrical circuit when tov. pass across a transformer connected to a cable and RC-protection is installed

Seeing (6) and (7), a special case of interest will be supposing the $R_{protection}$ is numerically equal to the Z_{surge}. In this case, the incident wave will be completely absorbed. There is no reflected wave, as the reflection coefficient a will be zero. This is basically the main idea of implementing RC-protection.

Within the laboratory experiment the surge impedance of the cable Z_{surge} is equal to 24.8 Ω (see Section 3.2), and therefore the calculated expected voltage response across transformer TX1, when the value of $R_{protection}$ is equal to 25 Ω will be as shown in Figure 73.
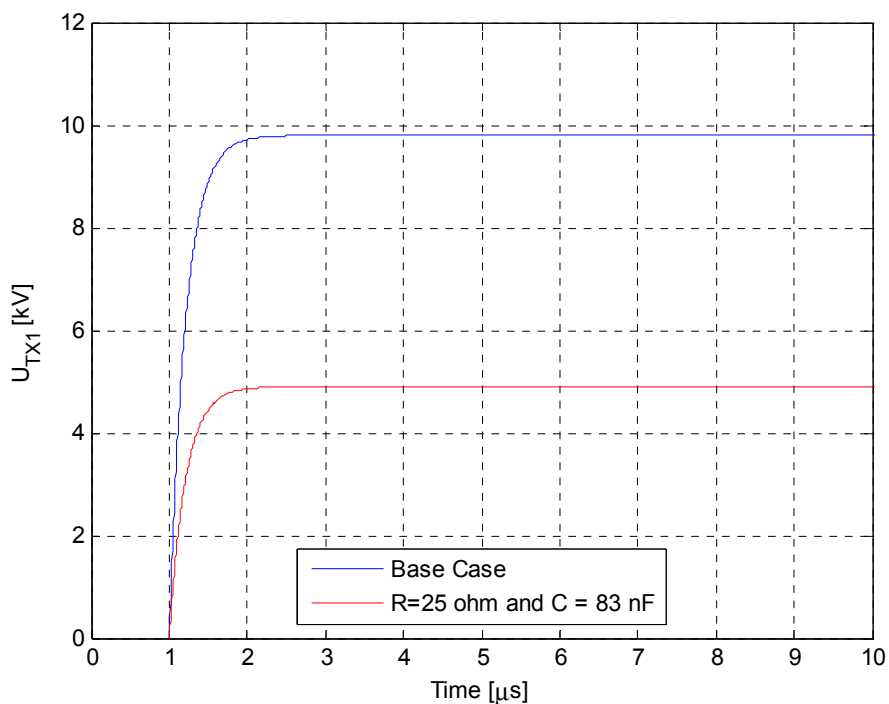
Figure 73: Calculated Expected voltage response across transformer TX1 with RC-protection installed at the transformer TX1 terminal when the value of $R_{protection}$ is equal to 25 Ω (breaker is closing at no load)

6.2.2 Verification

The impact of the RC-protection implementation is verified by comparing calculations and measurements.

Case number 5 listed in Table 2 corresponds to the case of installing RC-protections at the transformer TX1 terminals with the values of $R_{protection}$ and $C_{protection}$ respectively equal to 30 Ω and 83 nF. The laboratory circuit for this case is shown in Figure 74.

No	Case ID	ZnO	Surge Capacitor		RC-Protection	
		Location (installation)	Location (installation)	Parameter	Location (installation)	Parameter
5	R30C83-TX1	Node 2 (shunt)			Node 2 (shunt)	R=30ohm C=83nF
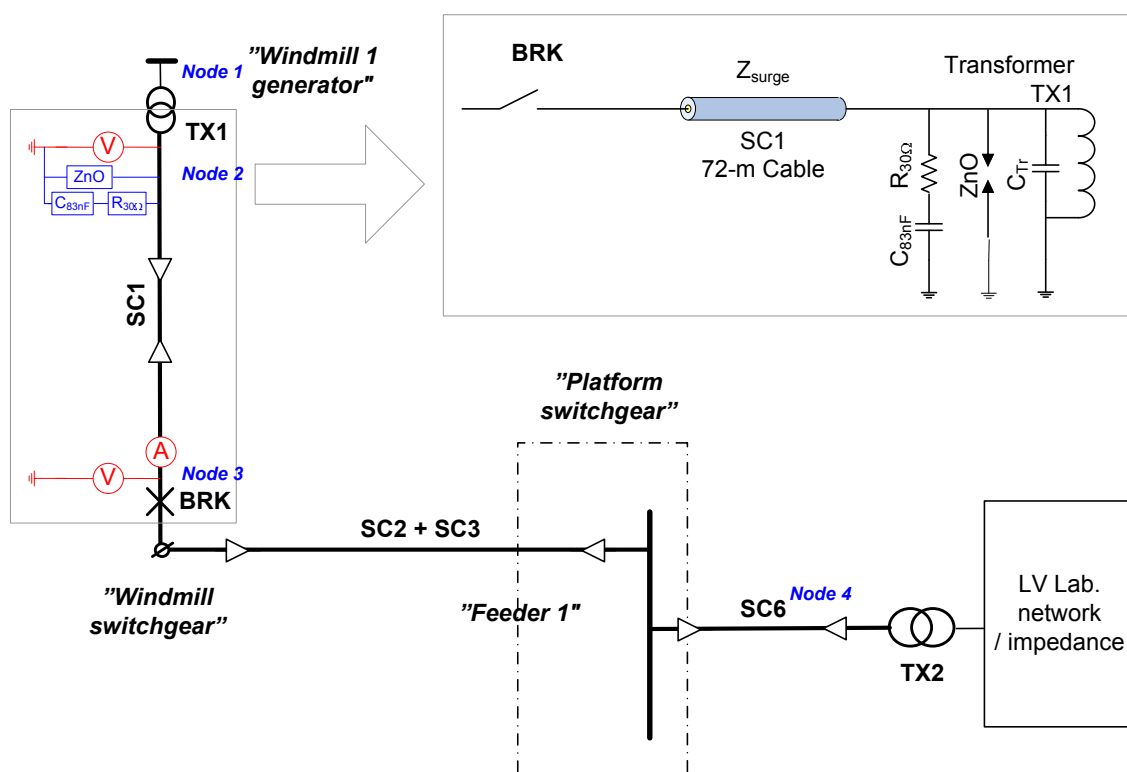
Figure 74: Laboratory setup and circuit for Case ID: R30C83-TX1 – in addition to the surge arresters, resistors in series with surge capacitors with resistance and capacitance equals to 30 Ω and 83 nF each are shunted at the terminals of Transformer TX1 (node 2)
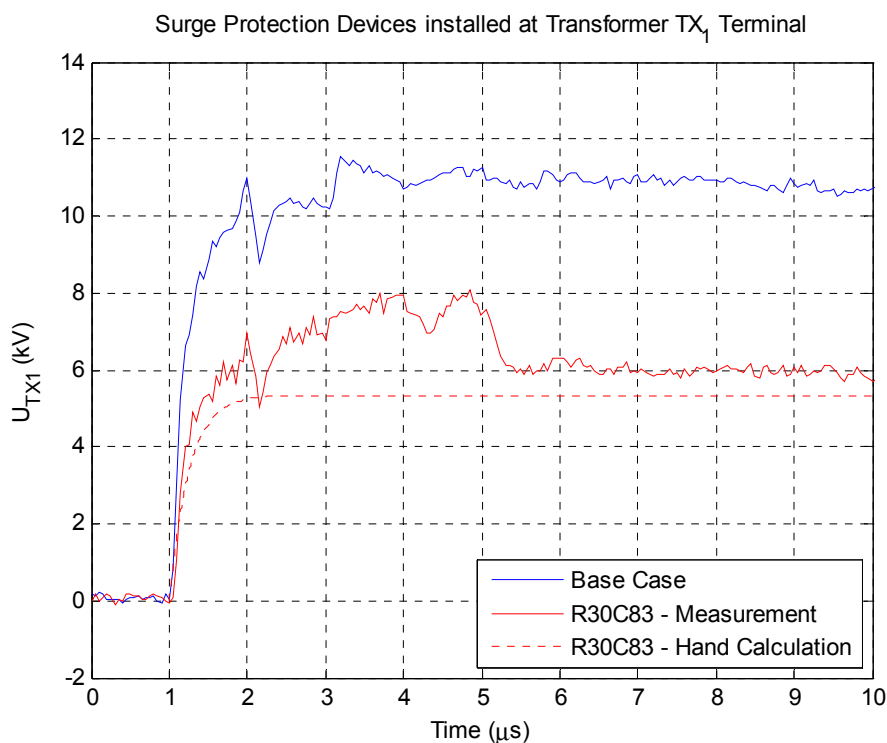
Figure 75: Measurement results of installing RC protections at the terminals of transformer TX1 (solid lines) compared to the results derived from hand calculations (dotted lines)

6.2.3 Impact on Transient Overvoltage Repetition

6.2.3.1 Typical Measurement Results

As in the base case, the worst transient voltages are generally obtained in cases when the breaker is opening with an inductive load connected. In the case with an RC-protection installed, the typical results with tov. repetitiveness are measured on the case number 5, 6, 7 and 8 listed in Table 2 when the breaker is opening with an inductive load connected will be highlighted. In case number 8, a combination of RC-protection at the transformer TX1 terminals and surge capacitors at the transformer TX2 terminals is tested.

The laboratory circuit for case number 5 was presented in Figure 74, and the typical results with tov. repetitiveness obtained from the measurement when the breaker is opening with an inductive load connected is shown in Figure 76.

Furthermore, for the cases number 6, 7 and 8, the laboratory circuits and typical results with tov. repetitiveness obtained from the measurement when the breaker is opening with inductive load connected, is shown in Figure 77 to Figure 81. The typical measurement result with the tov. repetitiveness is following the laboratory circuit for each case.
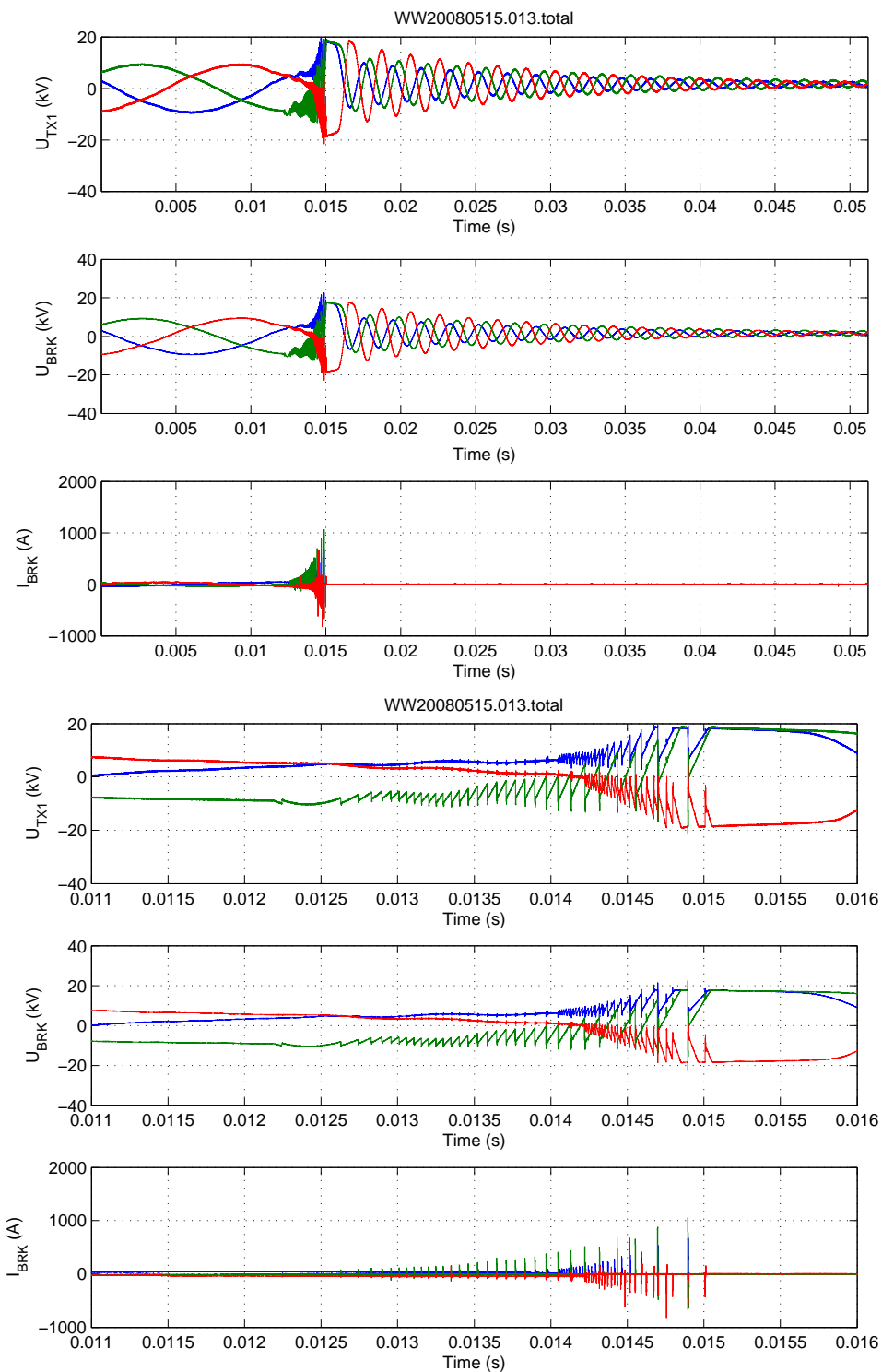
Figure 76: Measurement data from the Case ID R30C83-TX1: Opening breaker with an inductive load connected

6.2.3.2 Case ID: R20C83-TX1 and R20C130-TX1

No	Case ID	ZnO	Surge Capacitor		RC-Protection	
		Location (installation)	Location (installation)	Parameter	Location (installation)	Parameter
6	R20C83-TX1	Node 2 (shunt)			Node 2 (shunt)	R=20ohm C=83nF
7	R20C130-TX1	Node 2 (shunt)			Node 2 (shunt)	R=20ohm C=130nF
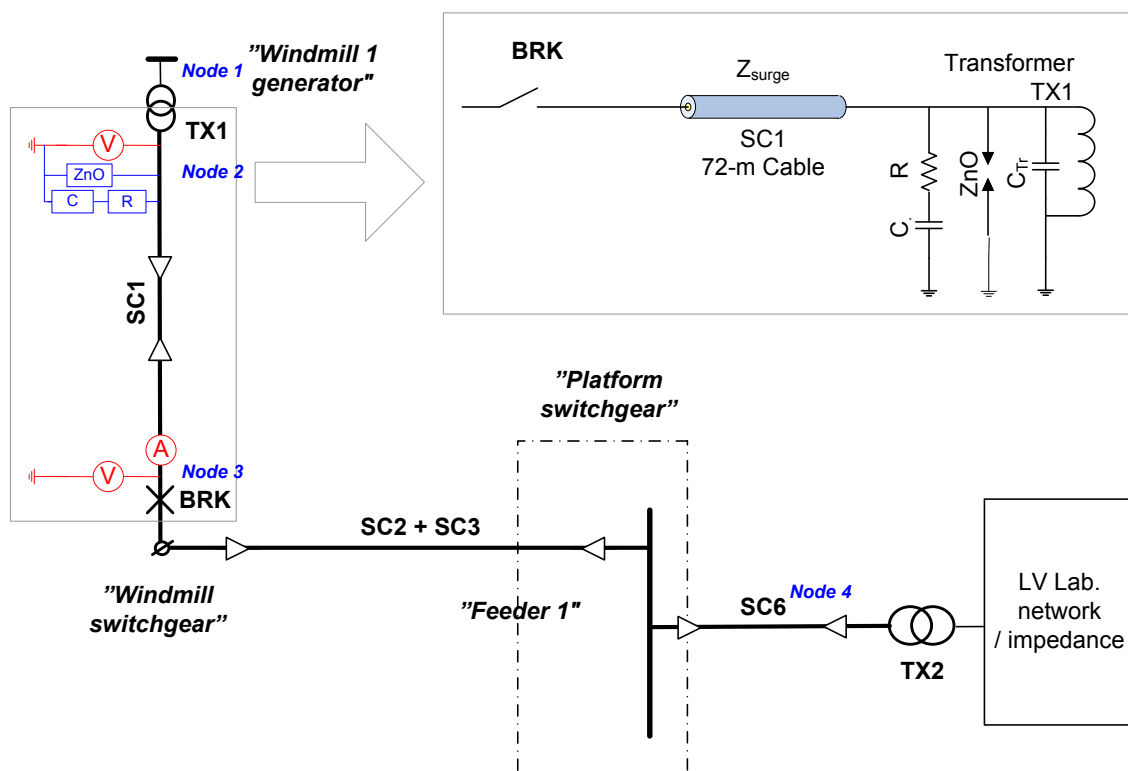
Figure 77: Laboratory setup and circuit for Case ID: R20C83-TX1 – in addition to the surge arresters, resistors in series with surge capacitors with resistances and capacitances equal to 20 Ω and 83 nF each are shunted at the terminals of transformer TX1
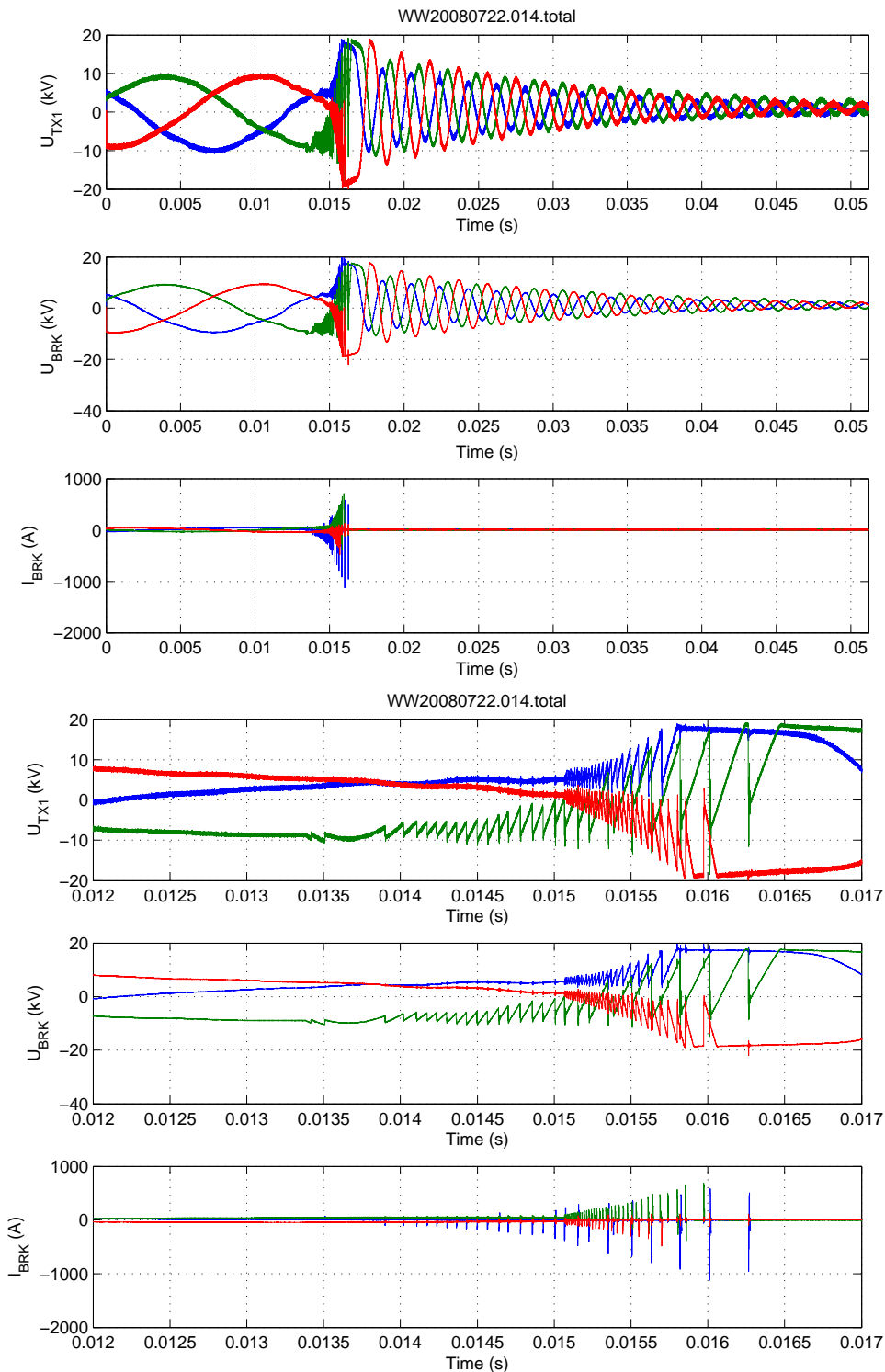
Figure 78: Measurement data from the Case ID R20C83-TX1: Opening breaker with an inductive load connected
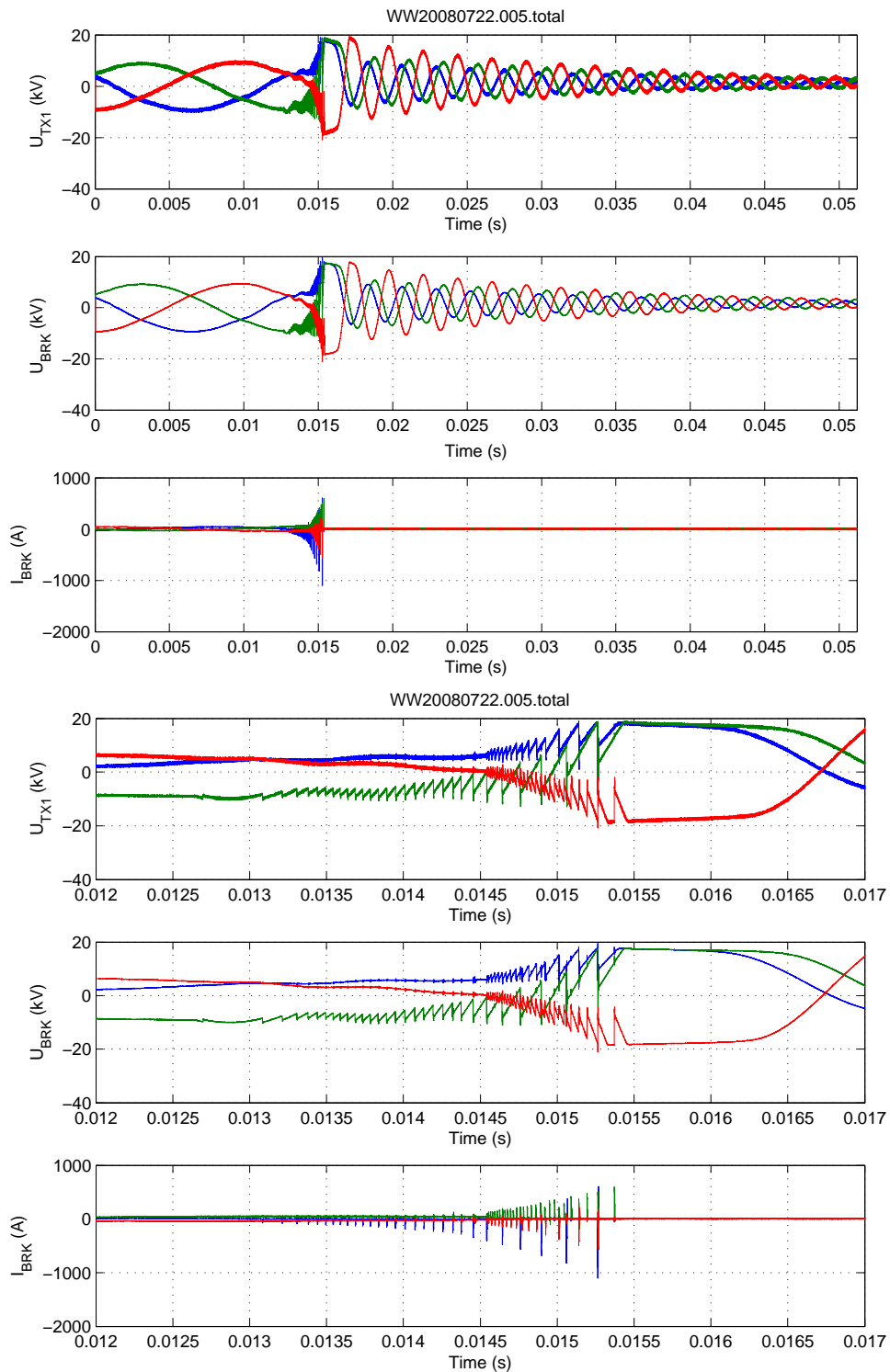
Figure 79: Measurement data from the Case ID R20C130-TX1: Opening the breaker with an inductive load connected

6.2.3.3 Case ID: R30C83-TX1-C130-TX2

No	Case ID	ZnO	Surge Capacitor		RC-Protection	
		Location (installation)	Location (installation)	Parameter	Location (installation)	Parameter
8	R30C83-TX1-C130-TX2	Node 2 (shunt)	Node 4 (shunt)	C=130nF	Node 2 (shunt)	R=30ohm C=83nF
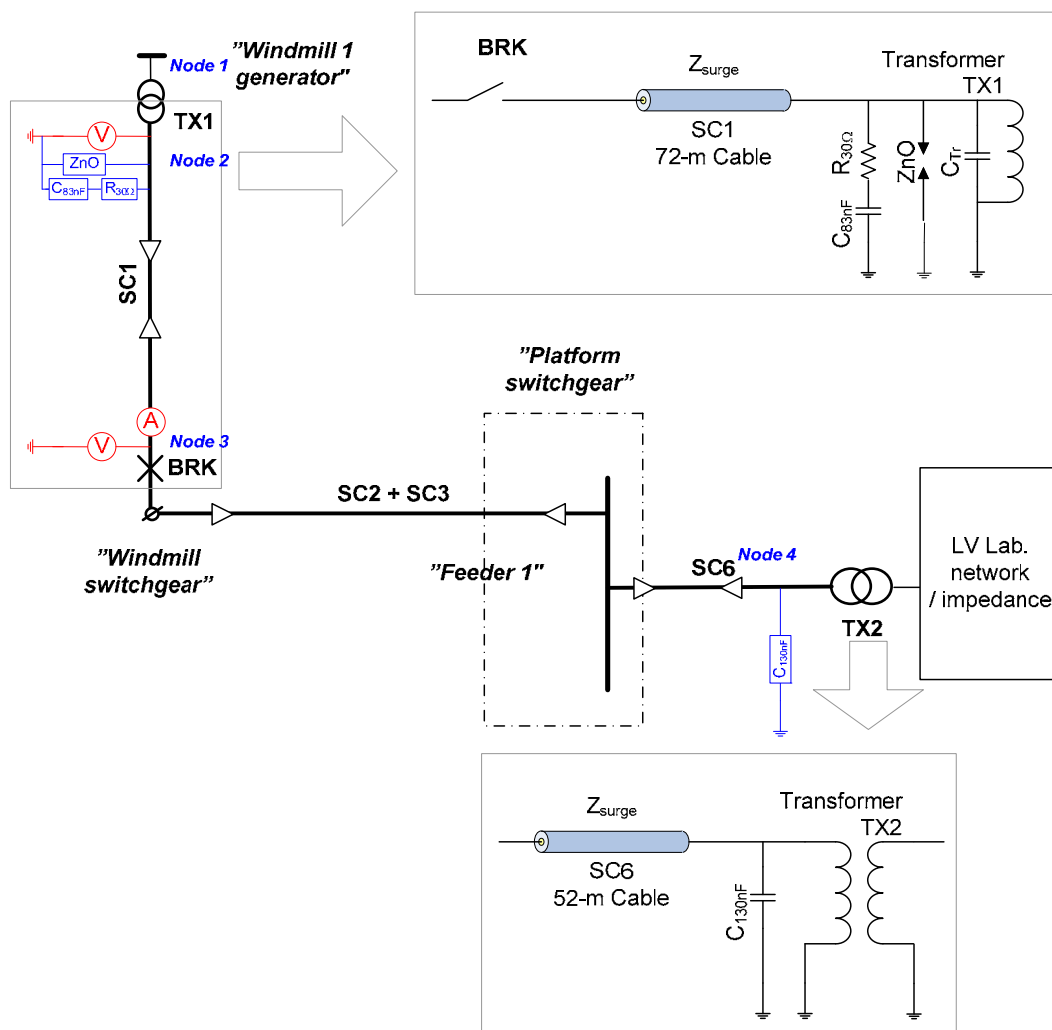
Figure 80: Laboratory setup and circuit for Case ID: R30C83-TX1-C130-TX2– in addition to the surge arresters, resistors in series with surge capacitors with resistances and capacitances equal to 30 Ω and 83 nF each, are shunted at the terminals of Transformer TX1 (node 2).

Moreover, surge capacitors with capacitance equals to 130 nF each are shunted at the terminals of transformer TX2 (node 4)
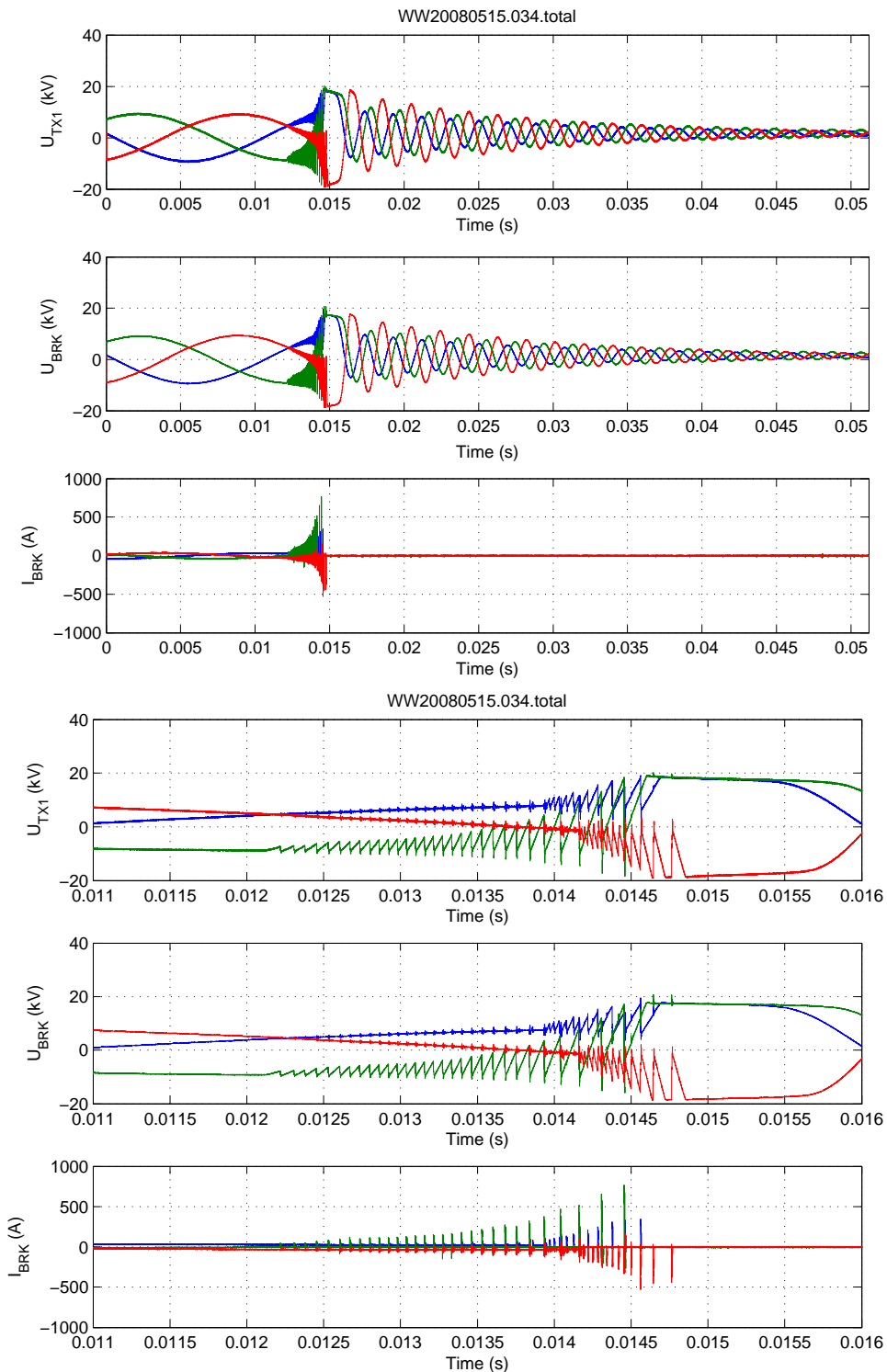
Figure 81: Measurement data from the Case ID R30C83-TX1-C130-TX2: Opening the breaker with an inductive load connected

6.2.3.4 Strike Quantifications

The tov. indicators of the strikes highlighted in Figure 76, Figure 78, Figure 79 and Figure 81 can be quantified as shown in Figure 82, Figure 83, Figure 84 and Figure 85.
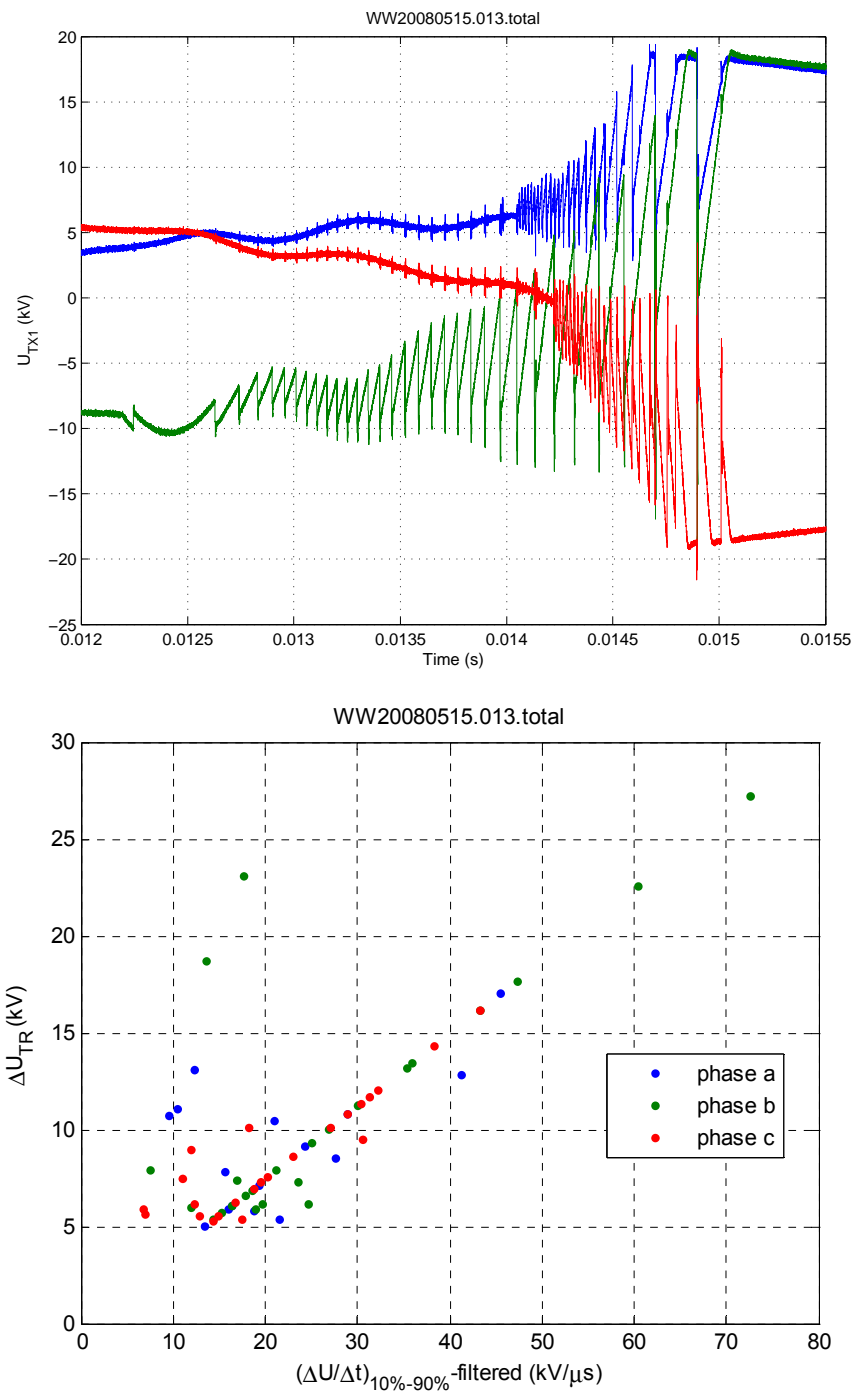
Figure 82: Voltage at transformer terminal TX1 (upper graph) and the corresponding quantification of the strikes (lower graph)
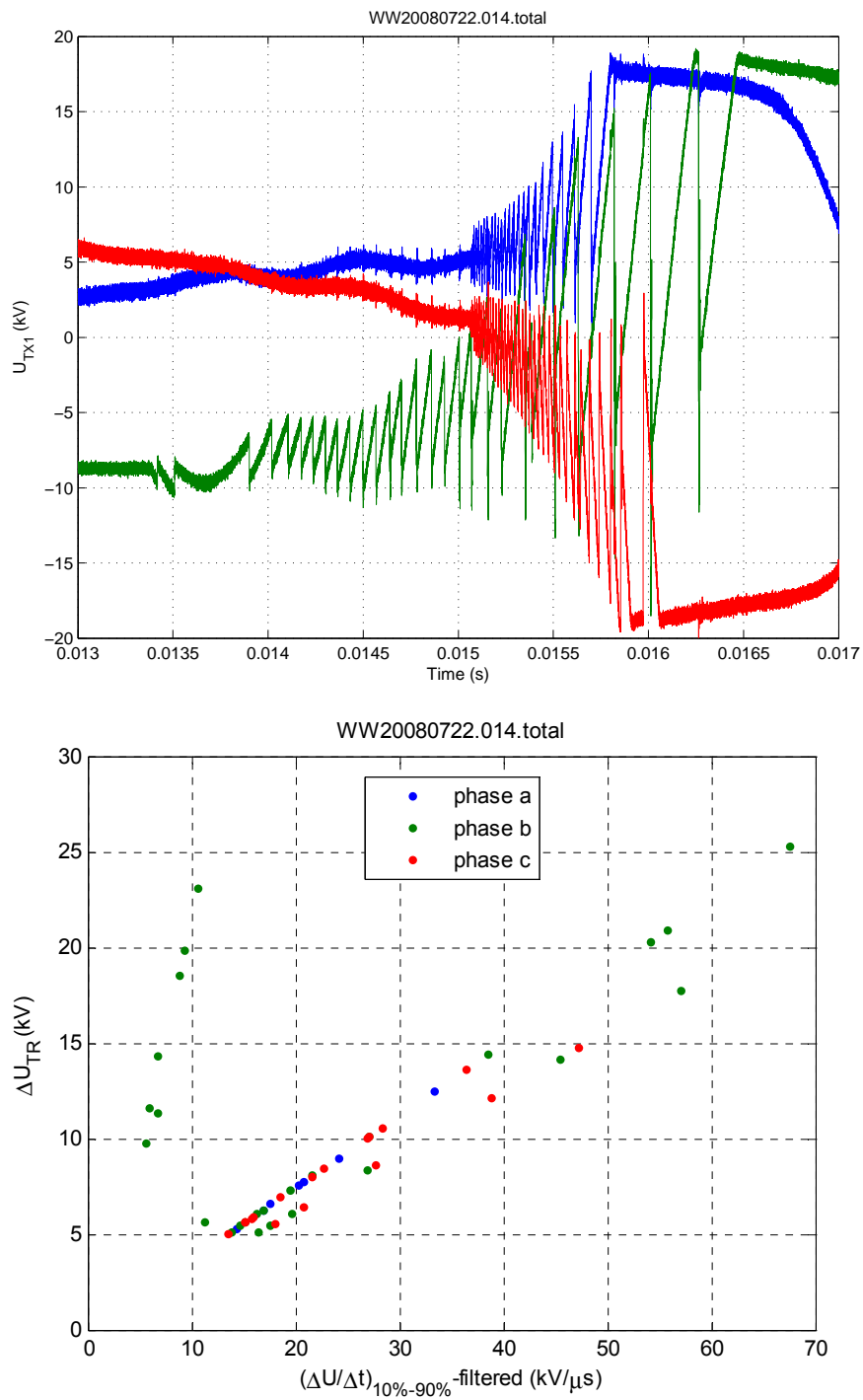
Figure 83: Voltage at transformer terminal TX1 (upper graph) and the corresponding quantification of the strikes (lower graph)
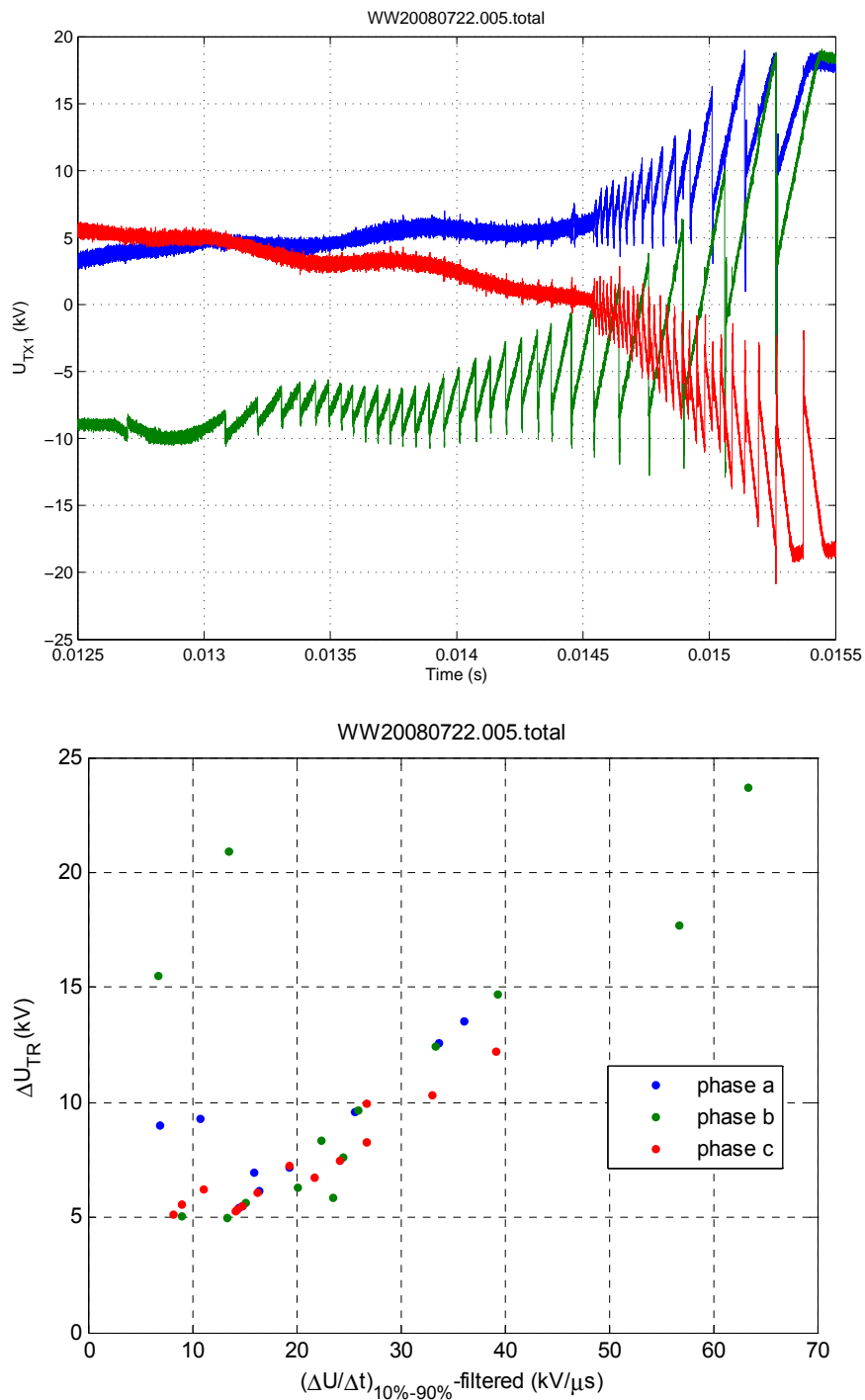
Figure 84: Voltage at transformer terminal TX1 (upper graph) and the corresponding quantification of the strikes (lower graph)
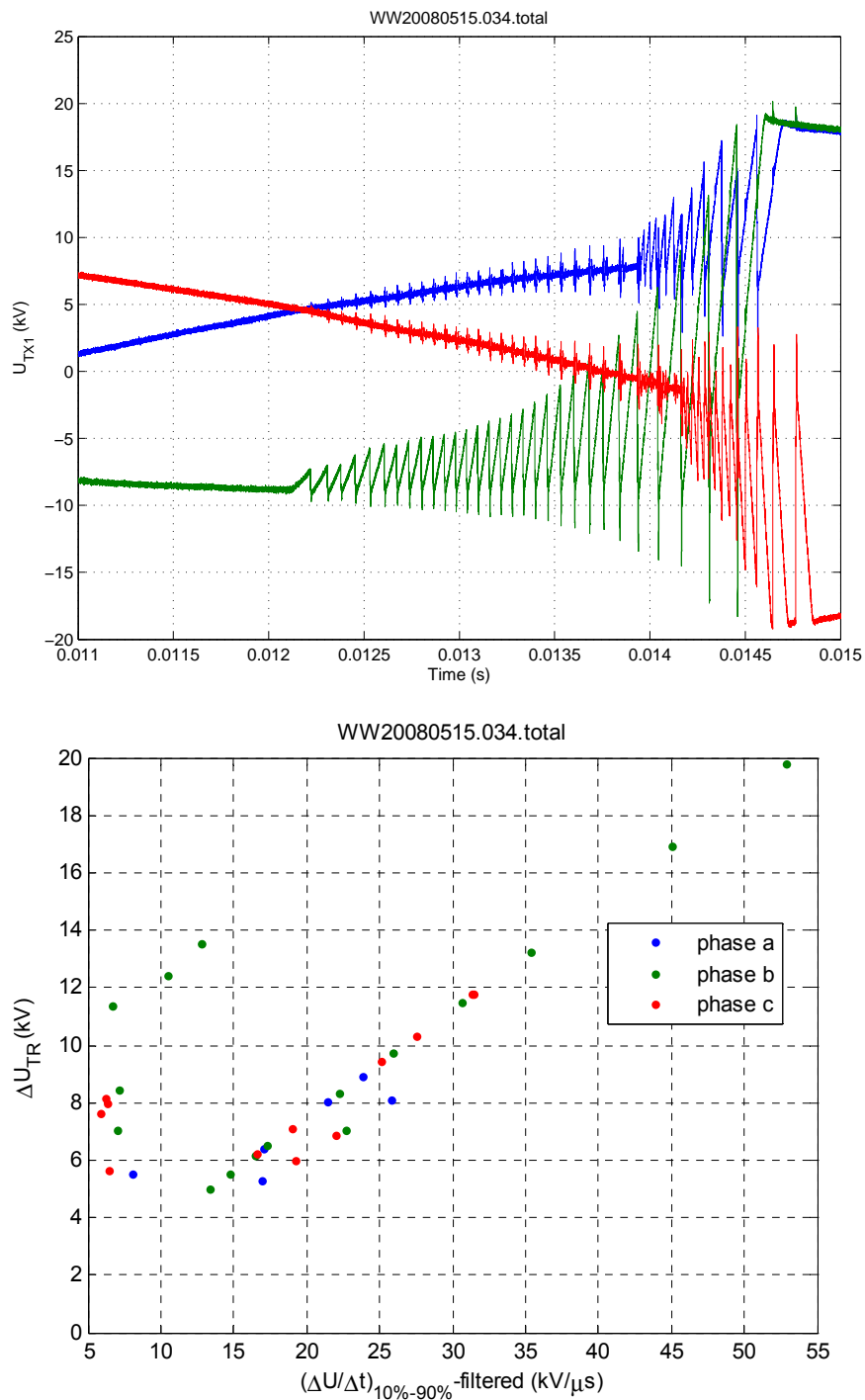
Figure 85: Voltage at transformer terminal TX1 (upper graph) and the corresponding quantification of the strikes (lower graph)

6.2.3.5 Summary of Strikes Quantifications

Table 9 Summary of Strikes Quantifications on cases with RC-Protections: at breaker opening with an inductive load connected (worst cases)

Case ID	# strikes (ΔU > 5 kV and within $\dfrac{\Delta U}{\Delta t}$ > 5 kV/μs, phase a-b-c)	max ΔU (kV)	$\left(\dfrac{dU}{dt}\right)_{10\%-90\%}$ filtered (kV/μs)
R30C83-TX1	63	27	72.5
R20C83-TX1	50	25	67
R20C130-TX1	38	24	63
R30C83-TX1-C130-TX2	34	20	53

6.3 Circuit Parameter Influence versus Stochastic Behaviors

There are two aspects for evaluating the performances of surge protection devices against tov., namely:

1. The influence of the circuit parameters.
2. The stochastic/random behavior of the breaker.

6.3.1 The influence of the circuit parameters

The influence of the circuit parameters has been verified in Section 5.3 (voltage transient behavior in circuit with surge arresters), Section 6.1 (voltage transient behavior in circuit with surge capacitors) and Section 6.2.2 (voltage transient behavior in circuit with RC-protections). In those Sections, measurement results from provoking a step voltage to the system, by the closing of the breaker at no load, match the calculations satisfactorily. The formula for the calculations is derived based on the circuit parameters.

It can be summarized that surge capacitors and RC-protection slow down the system as compared to the base case where only surge arresters are installed. Both surge capacitors and RC-protections increase the circuit time constants hence reduce the steepness of the tov. In the case with surge capacitors, less tov. steepness will be obtained when surge capacitors with higher capacitances are installed. In both surge capacitors and RC-protection cases, the value of the capacitance of the capacitors must also be significantly higher than the cable capacitance.

When these surge protection devices are used within cases where the breaker is opening, a transformer being connected to an inductive load (the worst case where we would expect the most multiple pre-strikes and re-ignitions), based on their influence to the circuit parameters, it should be expected that:

1. With surge capacitors and RC-protections, there would be fewer multiple strikes as compared to the base case (with ZnO only). The reason is because surge capacitors slow down the system and thus it takes longer time before the voltages escalate until they hit the withstand voltage of the breaker that create re-ignitions. Furthermore, fewer strikes could be expected when surge capacitors with higher capacitance are installed.

2. With surge capacitors and RC-protections, the voltage steepness would also be reduced since the time constant of the system is higher.

3. With RC-protections however the multiple re-ignitions would not be prevented. The reason is that in the turbine transformer with high impedance, the 50-Hz current is low, so that the superimposed high-frequency current with the 50-Hz current would not prevent zero crossings of the high-frequency current. The situation would be different in the case of an industrial motor with high 50-Hz current. In this industrial motor case with RC-protections and with the rightly tuned resistance value, the high-frequency current superimposed to the 50-Hz current would not result in zero crossings of the high-frequency current thus multiple re-ignitions would not occur.

Table 10 shows the summary of the strikes quantification of the typical measurement results (obtained when breaker is opening with an inductive load connected) from the laboratory measurements when surge arresters, surge capacitors or RC-protections are installed as the protection devices in several different combinations.

As expected, the maximum magnitude of tov. when surge protection devices: surge capacitors and RC-protection are installed (together with surge arresters), are less than the base case (when only surge arresters are installed). When RC-protection is used the strike magnitude is generally half of that of the base case (see explanation in Sections 6.2.1 and 6.2.2). With surge capacitors, the steepness of the tov. is less which is due to the increased time constant (see explanation in Sections 6.1 and 6.1.2). As a result of these characteristics of surge capacitors and RC-protections, the number of strikes occuring are becoming less when the two surge protection devices are installed.

However, some inconsistencies can still be observed when for example the case with higher capacitance (installing 130 nF surge capacitors at transformer TX1 – Case ID C130-TX1) has more strikes than the case with lower capacitance (installing 83 nF surge capacitors at transformer TX1 – Case ID C83-TX1). The explanation of this could be the stochastic behavior of the breaker that will be further presented in the following Section 6.3.2.

Table 10 Summary of the quantifications of the strikes from the typical worst cases tested

Case ID	# strikes (ΔU > 5 kV and within $\dfrac{\Delta U}{\Delta t}$ > 5 kV/µs, phase a-b-c)	maxΔU (kV)	$\left(\dfrac{dU}{dt}\right)_{10\%-90\%}$ filtered (kV/µs)
Base Case	230-323	42-43	82-88
C83-TX1	129	25	42
C130-TX1	145	16.5	44
C130-BRK	190	21	52
R30C83-TX1	63	27	72,5
R20C83-TX1	50	25	67
R20C130-TX1	38	24	63
R30C83-TX1-C130-TX2	34	20	53
Point-on-Wave	-	-	-

6.3.2 Stochastic/random behavior of the breaker

Two aspects can be presented in relation to the inconsistencies within Table 10 (when e.g. the case with higher capacitance (installing 130 nF surge capacitors at transformer TX1 – Case ID C130-TX1) has more strikes than the case with lower capacitance (installing 83 nF surge capacitors at transformer TX1 – Case ID C83-TX1).

The first aspect is the stochastic behavior of the breaker (see Section 3.8.4). In the laboratory experiment, 2-6 shots have been performed on each case with exactly the same timing for taking into account this stochastic phenomenon. This aspect can be seen for example when the 5 shots on the base case are compared (see Table 7). In all these shots, the timing of opening the breaker is the same. However, it can be seen that the number of multiple strikes ranges from 230 strikes to 323 strikes, and some ranges are obtained also within the steepness of the tov.

Some statistical shots have been collected also in other cases with surge protections and RC protections. However, within this report, one shot has been selected based on visual inspection on these cases in which the quantification methods are applied and the results are shown in Table 8 and Table 9. The complete results of these cases could have been also in certain of ranges. These statistical shots are available and analysis on these shots can be performed in the future.

The second aspect is the worst timing hit when the breaker is opened. During the tests, it was always tried at best to hit the worst time for every shot made in all test cases (see Section 3.8.4). Opening an inductive load was tried to be performed when the current chopping level is at its highest. However, due to a combination of the stochastic behavior of the breaker operation and the limitation of visual inspection during the test, there is still a possibility that the timing hit when the breaker is opened in the case with 83-nF surge capacitors is not the-same-worst-case compared to the timing hit when the breaker is opened in the case of using 130-nF surge capacitors.

These two aspects can be actually improved in the future by collecting more statistical data (thus more shots) within every test of the breaker switching. This will however also be a time consuming process.

6.4 Point-on-Wave Control

No strikes are obtained when point-on-wave control is applied on the breaker operation, even when the breaker is opening with an inductive load connected. In the laboratory setup, when point-on-wave control is tested, the same laboratory as in the base case is used, only that the current monitoring devices is moved to the transformer TX1 terminals (from the breaker terminals) for practical reasons, which does not influence the behavior of the tested electrical circuit. Figure 86 shows the laboratory circuit used for the case of testing the point-on-wave control (Case number 9 in Table 2) and the typical results when breaker is opening with an inductive load connected is highlighted in Figure 87. As can be observed in Figure 87, no strike is obtained, thus any potential strike is basically prevented.

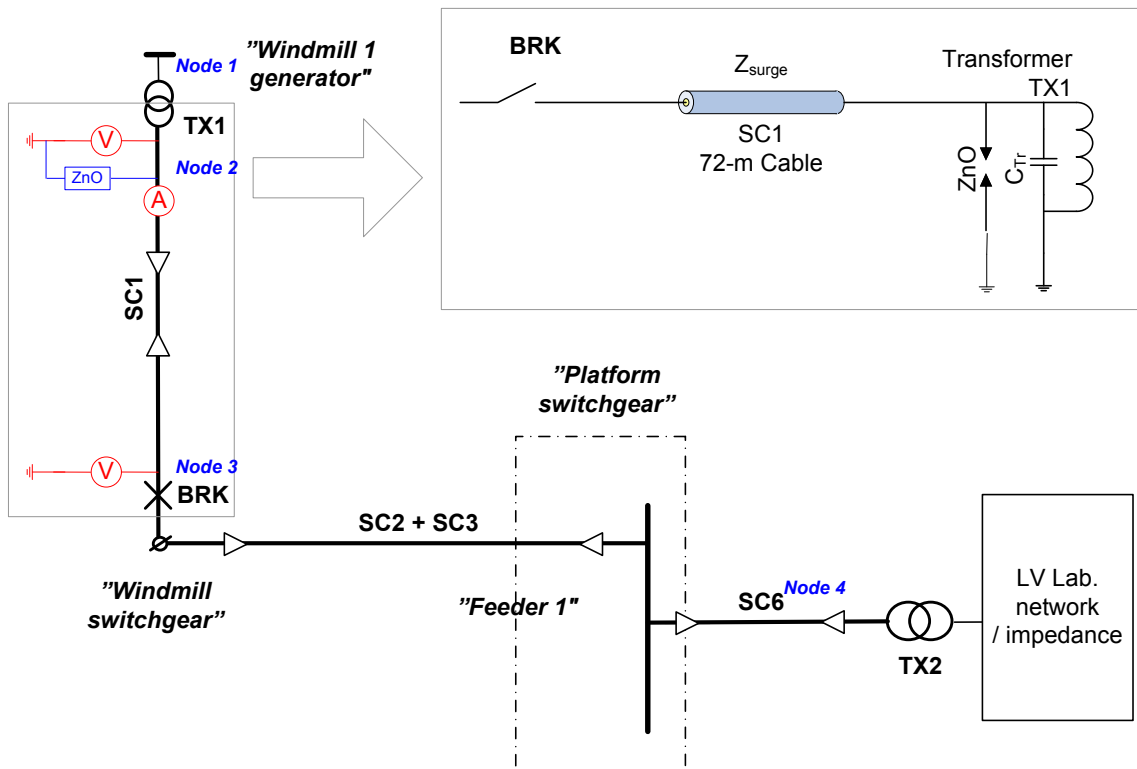| No	Case ID	ZnO	Surge Capacitor		RC-Protection	
		Location (installation)	Location (installation)	Parameter	Location (installation)	Parameter
9	Point-on-Wave	Node 2 (shunt)				

Figure 86: Laboratory setup and circuit for Case ID Point-on-Wave – only surge arresters shunted at the terminals of transformer TX1 (Note that the current monitoring devices have been moved to the transformer TX1 terminals (from the breaker terminals as in Figure 30)
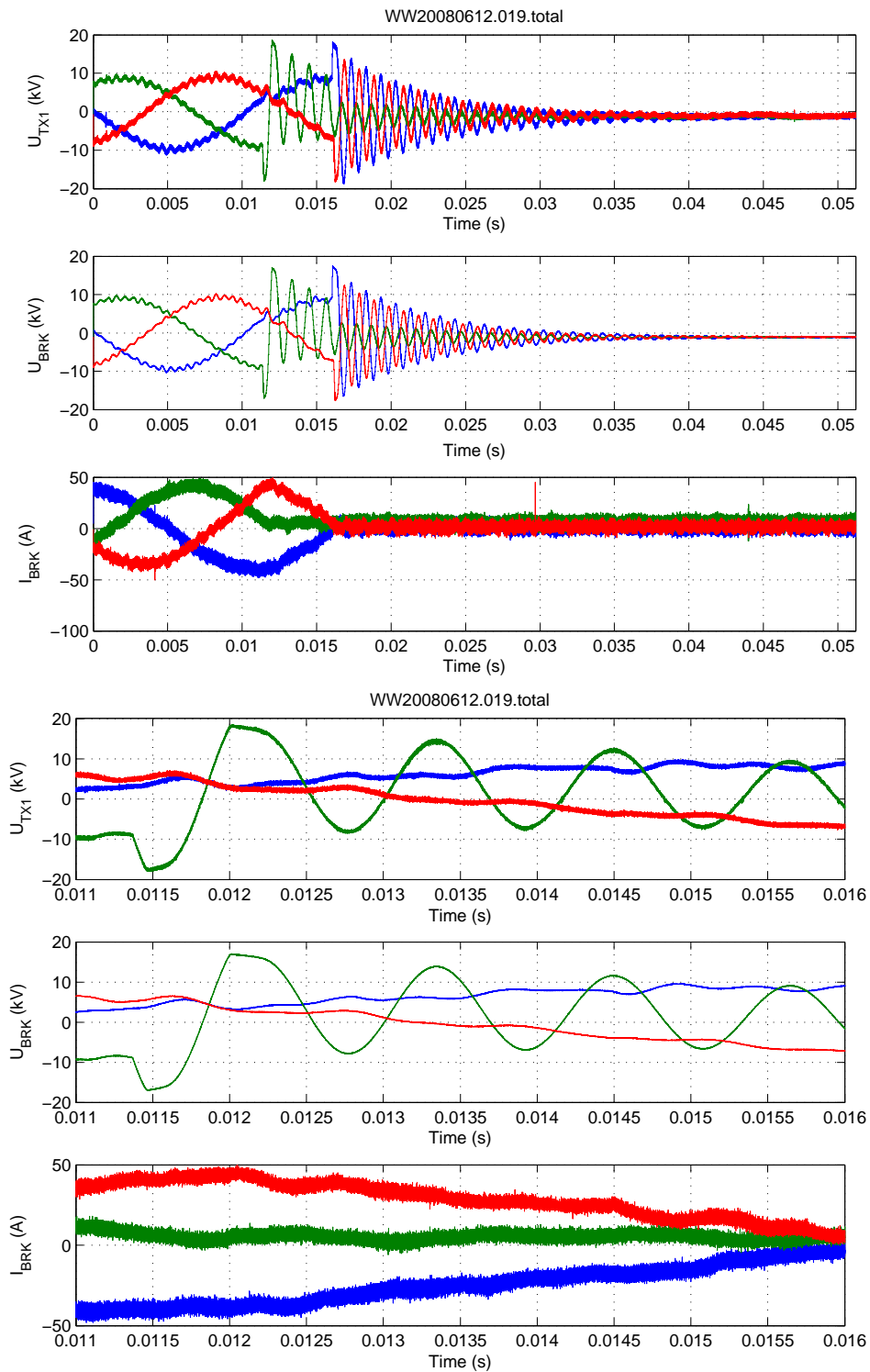
Figure 87 Measurement data from the Case ID Point-on-Wave: Opening the breaker with an inductive load connected

7 Summary of Results

7.1 Verification of Consistent Occurrence of Transient Overvoltages

Experiments verify the consistent occurrence of repetitive pre-strikes and re-ignitions determined by the electrical circuit and the point on wave of switching operations

Table 11 shows the summary of the worst strikes quantification obtained from the laboratory experiment when only surge arresters are installed as the protection devices.

Table 11 Summary of the worst strikes quantifications (only surge arresters installed)

Case (shot #)	# strikes (ΔU > 5 kV and within $\dfrac{\Delta U}{\Delta t}$ > 5 kV/µs, phase a-b-c)	Max ΔU (kV)	$\left(\dfrac{dU}{dt}\right)_{10\%-90\%}$ filtered (kV/µs)
0429.011	282	43	86
0429.012	264	43	85.5
0429.013	323	42	88
0429.014	274	43	87
0429.015	230	41.5	82.5

7.2 Summary of Surge Protection Devices Performances

All tested surge protection methods, namely the surge arresters, surge capacitors and RC-protections show mitigation effects:

1. Correctly applied surge arresters will always limit the maximum voltage magnitude but have no effect when the voltage swings are within a band in magnitude below the own corresponding protection level from negative to positive polarity. The protection level is always coordinated with the maximum temporary over- voltages during earth fault.

2. Surge capacitors can mitigate the transient steepness and magnitudes. Surge capacitors reduce the steepness effectively while located in any position between the breaker/switch and the objects in the load flow direction while switching. However, new combinations with existing circuit components can cause new resonant conditions with risk of oscillations and magnification.

3. RC protection (damped surge capacitors) mitigates transient magnitude.
   The resistance damp possible oscillations and prevents wave reflections by impedance matching and most of all significantly changes the high frequent current oscillations through the breaker, reducing the escalating magnitudes. However, the resistance allow a steep surge voltage to rise while the surge meets mainly the resistance. The capacitive part only act on about half of the step voltage magnitude due to voltage distribution between the cable wave impedance and the resistive part. RC protection is suitable for switching low impedance loads, e.g. stalling motors and should be located at the object of protection (e.g. at the transformer terminals).

None of the above removes the tov. completely. Furthermore, surge capacitors as well as RC protection require order engineering.

7.3 Measured Transient Overvoltages versus LIWL

In OHL systems, tov. often occur as a result of lightning strike and standard equipment test procedures are designed around the typical 1.2/50 μs impulse (LIWL = Lightning Impulse Withstand Level) due to fulmination. When the results of tov. measured in the cable laboratory is compared to this LIWL, Table 12, Figure 88 and Figure 89 are obtained.

Table 12 Standard LIWL [14] versus recorded breaker switching transients

	LIWL (at Un = 12 kV)	Surge Arresters	Surge Arresters + Surge Capacitors	Surge Arresters + RC Protection	Surge Arresters + RC Protection + Surge Capacitors
Steepness * (kV/μs)	62.5	82-88	42-52	63-73	53
Magnitude (kV)	75	42-43	17-25	24-27	20
Number of Strikes (#)	1	230-323	120-190	38-63	34

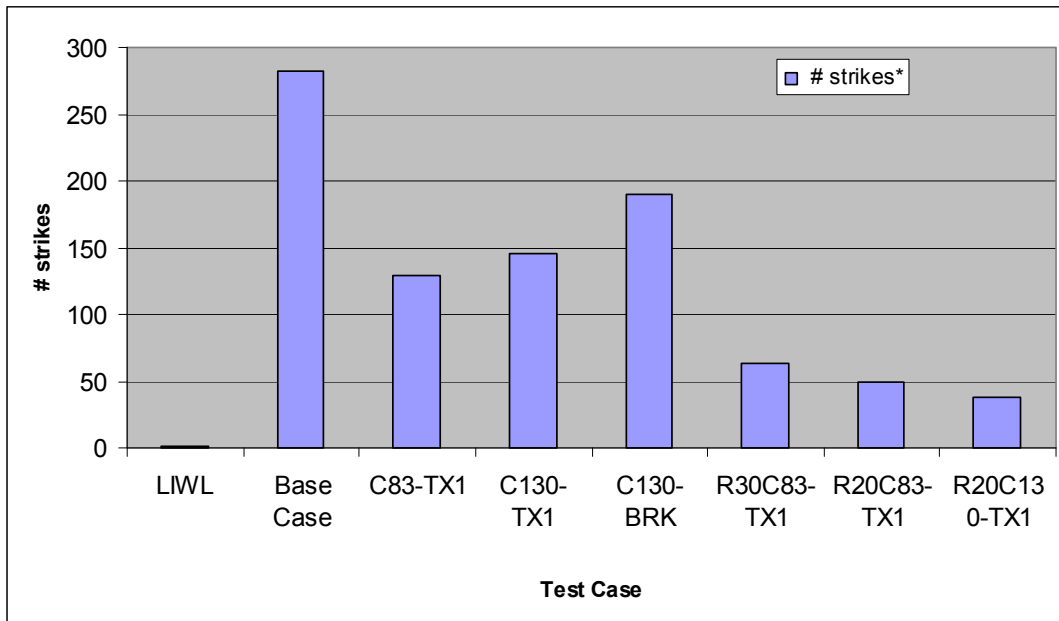$$* = \left(\frac{dU}{dt}\right)_{10\%-90\%} \text{-filtered}$$

Figure 88: Standard LIWL versus recorded breaker switching transients (number of strikes)
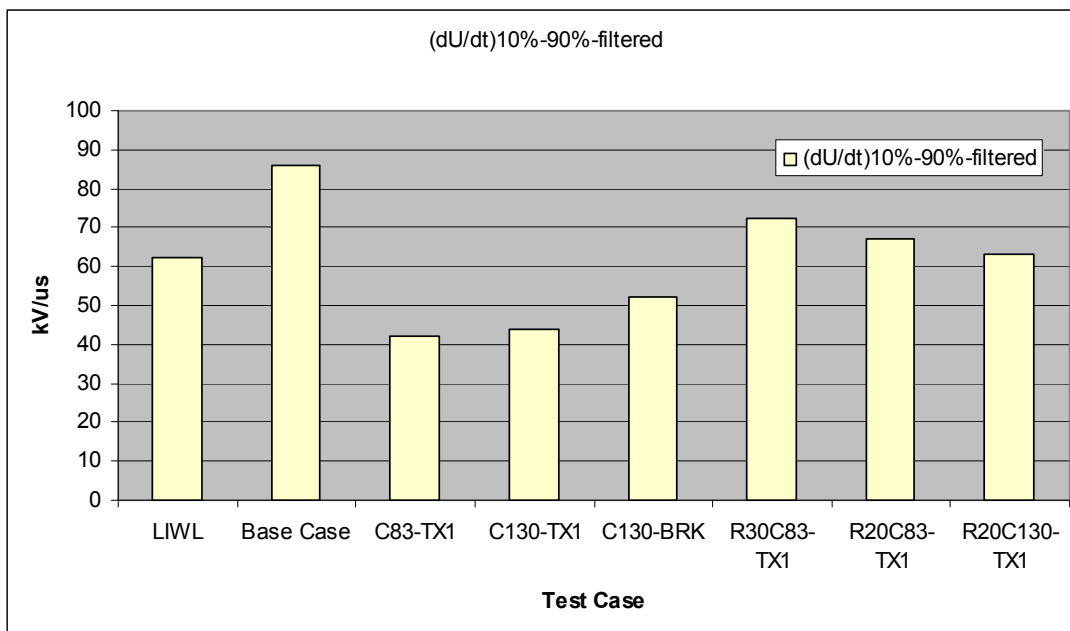

Figure 89: Standard LIWL versus recorded breaker switching transients (tov. rate-of-rise).

7.4 Breaker control relevance

"Point-On-Wave" control of the circuit breakers can prevent transient overvoltages.

8 Conclusions

An experimental laboratory has been establish at ABB Corporate Research for the study of switching transients occurring in cable systems such as wind parks. The transients are caused by the interaction between main electrical apparatus and cables within well-defined circuits and controlled parameters. Worst-case conditions can be tested without risk of hazard and process disturbance.

Experiments verify theoretical studies of transient overvoltages, also comprising the impact of stray-inductance loops. The results show consistent occurrence of repetitive pre-strikes and re-ignitions determined by the electrical circuit and the point on wave of switching operations. A typical electrical circuit for the occurrence of recurrent surges due to repetitive pre- and re-strikes is having a certain amount of cable on each side of the switch/breaker, long enough to preserve sufficient energy for the re-strikes.

- All tested surge protection methods, namely the surge arresters (e.g., ZnO), surge capacitors and RC-protections show mitigation effects.

- Correctly applied surge arresters will always limit the maximum voltage magnitude but have no effect while the voltage swings within a band in magnitude below the own corresponding protection level from negative to positive polarity. Without other mitigation measures applied, voltage steps can appear with up to 3 times higher rise-time than the maximum IEC standard impulse test. With the actual circuit, the number of recurrent surges can be from a few to several hundreds, and with a repetition frequency of typically 5-50 kHz where virtual current chopping will appear with the lower frequency.

- Surge capacitors and RC-protection show mitigation effects, however, the repetitive transients are not removed completely. Surge capacitors stand as an effective mitigation of the tov. steepness. The surge capacitor can be located anywhere down-streams the switch/ circuit breaker. The selection and dimensioning of mitigation method always requires some engineering

- Synchronized switching and point-on-wave control can prevent all tov. due to breaker operation.

It is found and tabled that none of the remedies completely removes the tov.:

- All mitigation methods still require qualified assessment of the effects of the corresponding transients.

- Transients must be considered in the dimensioning of the related components. It is therefore recommended to further investigate the insulation coordination of the components within large cable-based systems such as collection grids for wind parks.

- For park installations surge arresters (ZnO), surge capacitors as well as RC-protection require so-called order engineering.

In connection with this procedure, the created laboratory environment is an asset to handle hitherto unknown unknowns and to revive tacit knowledge. Furthermore, to support more studies of tov. in large cable-based collection grids for wind parks worldwide.

9 Remark

The authors are aware of other similar research activities on going and existing IEEE and CIGRE group active in the area, which may in due time lead to new standards appearing in the area.

10   Future Work

10.1   Single Pole Faults

The characteristics of earth faults involving arcing and intermittence could be important for the relevance and evaluation of prevention methods applied to the circuit breakers contra common mitigation methods.

10.2   Variation of Apparatus Types, Disconnector Operations

Disconnector operations are known to produce pre-strikes and re-ignitions which should be quantified and compared with different types of breakers.

10.3   The Impact of Multiple Reflection Points

Simulations indicate that multiple reflections cause additional repetition of the tov. arriving at a single point.

The cable system lab has been prepared with an extra feeders and tee-off adding up three reflection points. Most cases have been selected with the extra feeder disconnected, in order to start with a minimum of complexity while developing the basic understanding of the phenomena involved.

10.4   Switching with Generator Connected to Windmill Transformer

See Section 13.2.

- The effect of machine operation point and emf on the tov.
- Phase opposition as worse case of switching.

11 References

[1] J. P. Eichenberg, H. Hennenfent and L. Liljestrand, "Multiple re-strikes phenomenon when using vacuum circuit breakers to start refiner motors", Pulp & Paper Canada, vol. 98, no. 7, July 1997, pp. 32-36.

[2] J. P. Eichenberg, H. Hennenfent and L. Liljestrand, "Multiple re-strikes phenomenon when using vacuum circuit breakers to start refiner motors", Pulp & Paper Industry Technical Conference, 21-26 June 1998, pp. 266-273.

[3] T. E. Browne, "Circuit Interruption", Marcel Dekker, Inc., New York, 1984.

[4] L. van der Sluis, "Transients in Power Systems", John Wiley & Sons, Ltd, Chichester, 2001.

[5] T. van Craenenbroeck, H. de Herdt, J. de Ceuster, J.P. Marly, D. van Dommelen, R. Belmans, "Detailed Study of Fast Transient Phenomena in Transformers and Substations Leading to an Improved System Design", In Proc. 15th CIRED, Nice, France, 1999, 1.12.1–1.12.6.

[6] D. Paul, "Failure Analysis of Dry-Type Power Transformer", IEEE Transactions on Industry Applications, Vol. 37, No. 3, May/June 2001.

[7] M. Popov, "Switching Three-Phase Distribution Transformers with a Vacuum Circuit Breaker Analysis of Overvoltages and the Protection of Equipment", PhD Dissertation, Delft University of Technology, the Netherlands, 2002.

[8] ABB Handbook, "Distribution Transformer Handbook: IEC/CENELEC related specifications ABB Ident # 1LAC000003", 2003.

[9] F. H. Kreuger, "Industrial High Voltage", Delft University Press, 1992.

[10] ABB, "XLPE Cable Systems, User's Guide", ABB Power Technologies AB High Voltage Cables, Karlskrona.

[11] L. Liljestrand, A. Sannino, H. Breder, S. Johansson, "Transients in Collection Grids of Large Offshore Wind Parks", Wind Energy, Vol. 11, No. 1, 2008, pp. 45-61.

[12] A. Greenwood, "Electrical Transients in Power Systems", John Wiley & Sons, Inc., Second. Ed., New York, 1991.

[13] F. W. Grover, "Inductance Calculations: Working Formulas and Tables", D. van Nostrand Company, Inc., p. 35, 1946.

[14] IEC 60694, "Common Specifications for High-Voltage Switchgear and Controlgear Standards", Edition 2.2 2002-01 (In conjunction with of IEC 62271, "High-Voltage Switchgear and Controlgear", 2003).

12 Enclosure A: Impact of Stray-Inductance Loop on Surge Capacitors

12.1 General Impact

A closer look into the tov. obtained from measurement when surge capacitors are installed suggests that the voltage responses do not behave likes a pure RC-circuit because oscillations are observed as they should have been resulted from a circuit containing LC components.

Figure 90 shows the installation of surge capacitors at the transformer terminals in which the tov. are measured and shown in Figure 63 (Section 6.1.1). The grounding connection of the capacitors in this case – will be referred to setup 1 throughout this section – are connected to the grounding plate via the grounding connection shown in Figure 90. It is known that even a single, straight piece of wire has some self-inductance which can be important at high frequency. Loops with stray inductances are then developed, which is shown in Figure 91.
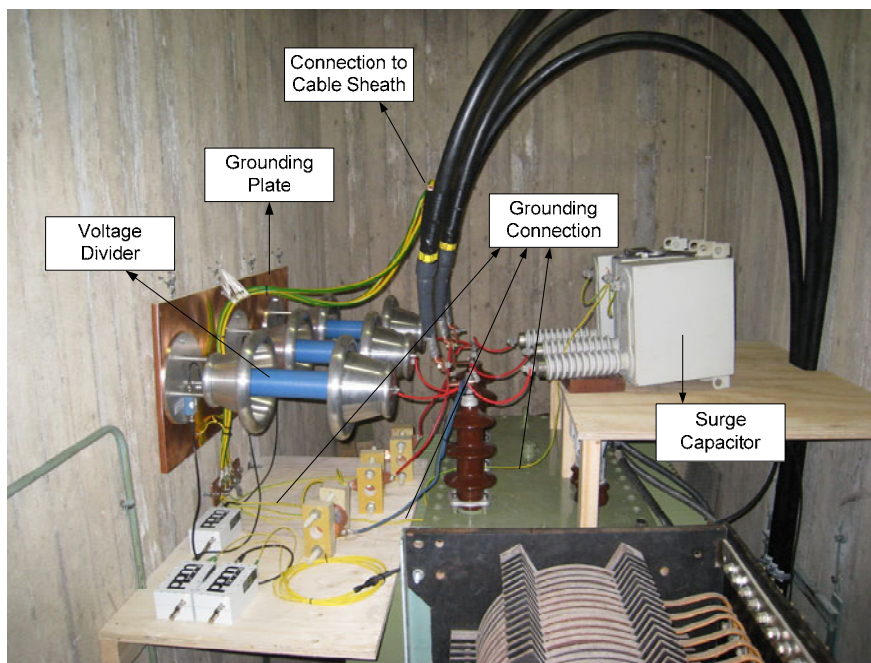

Figure 90: Photo of surge capacitors installation: Setup 1.
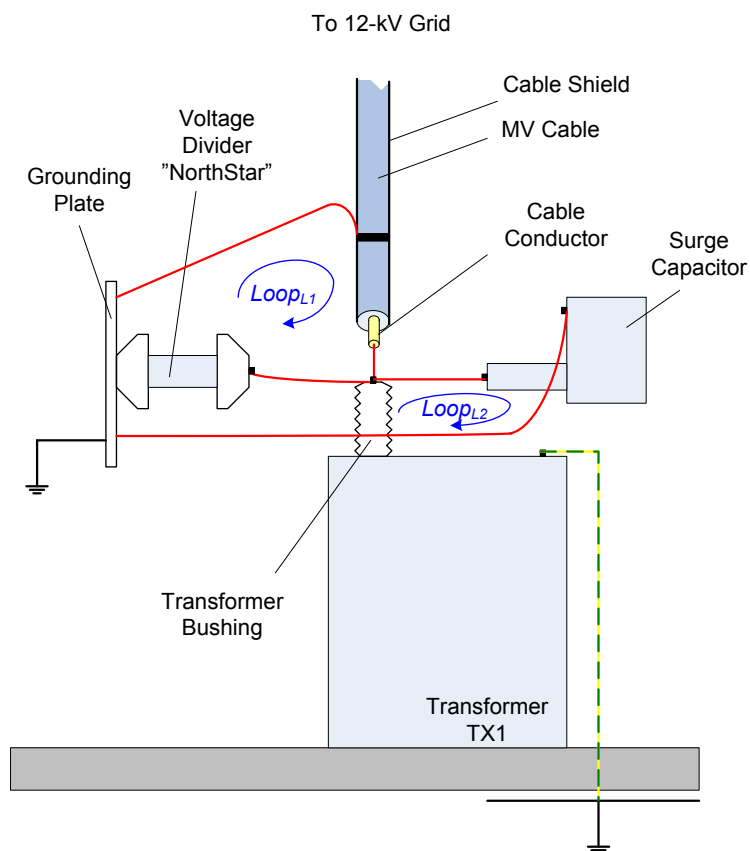
Figure 91: The sketch/illustration of setup 1 and the loops of stray inductances developed

For verifying this effect, simulation with PSCAD is performed. The circuit as shown in Figure 92 is used. The value of the stray inductance of the grounding wires connecting the surge capacitors within the PSCAD simulation is calculated using the following formula [13]:

$$L = 0.002l\left[\ln\left(\frac{2l}{r}\right) - 1 + \frac{\mu}{4}\right] \tag{7}$$

with l equal to the length of the wire, r the radius of the wire, μ the permeability of the wire material and L the self/stray inductance. The values of l and r are given in centimeters and the value of L is obtained in μH. For the circuit shown in Figure 92, the value of l equals 100 cm, r equals 0.3 cm and μ equals 1 have been used, and L equal to 1.29 μH is applied as the stray capacitance.

Figure 92: Modeling stray inductance within the installation of the surge capacitors

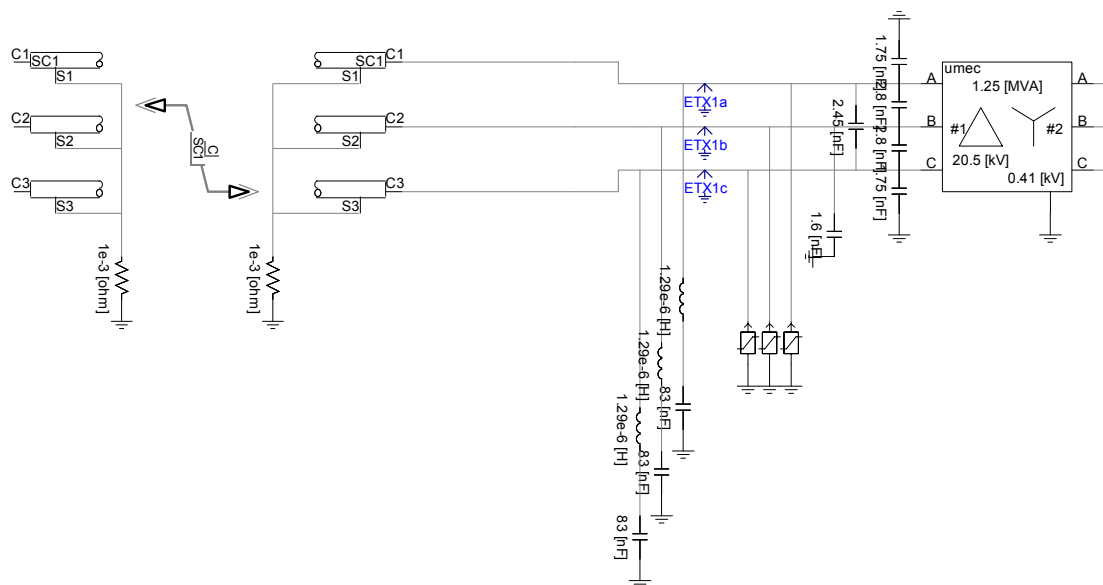The PSCAD simulation result is compared to the measurement. Figure 93 shows the comparison between the measurement and PSCAD simulation results - with stray inductance incorporated - when surge capacitors are installed with the capacitance equal to 83 nF.

Both results show a matching tov. steepness quite well especially in the beginning of the voltage step between t = 1 μs and t = 2 μs in Figure 93. This matching steepness is important since it represents the same time derivative of tov. obtained from both measurement and simulation. This tov. time derivative depends on the parameters within the circuit used in both measurement and simulation. It confirms that the measurement and simulation have been using identical circuits. To match the "full time-span" voltage response is on the other hand difficult and tedious, because the other values such as the voltage magnitudes, number of strikes etc. depends also on the instant of the switching-contact movement (in this case closing).

A remark can be made that with the stray inductance equal to 1.29 μH, tov. with a time derivative which is equal to 30% of the magnitude of its prospective value – when the capacitors were not used – can be obtained.
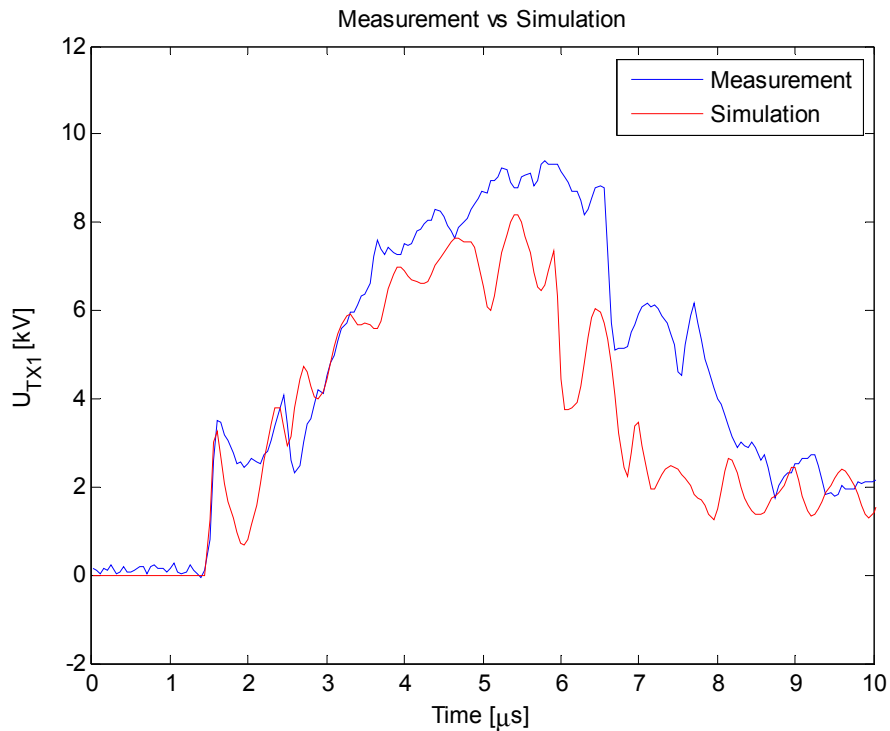
Figure 93: Comparison of measurement and PSCAD simulation results with stray inductance incorporated

12.2 Shorter Loop Inductance

A logical way to reduce the magnitude of the high derivative tov. in the beginning of the voltage step – when the surge capacitors are installed - is by reducing the stray inductance. One way to do this is by shortening the inductance loop.

This effect can be simulated in PSCAD by changing the values of the inductance L which is in series with the capacitance C shown in Figure 92. In Figure 94, the results when the value for the L is set as 0.129 μH, 0.065 μH or 0.032 μH is shown. As expected, the magnitude of the tov. in the beginning of the voltage step reduces when the value of the stray inductance is smaller.

Figure 94: tov. results from PSCAD simulation

To verify this effect by means of laboratory measurement, two setups of connecting the surge capacitors to the transformer TX1 terminals and the ground wire are tested, namely: setup 2-A and setup 2-B. The photos and the sketches/illustrations of these two setups can be seen in Figure 95 to Figure 98. The measurement results 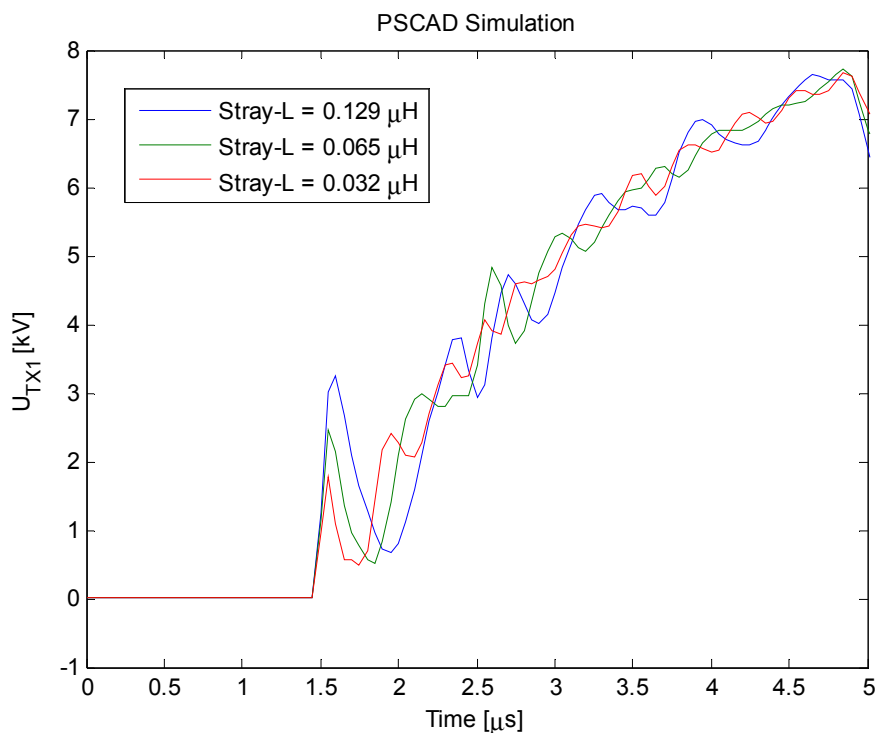from these setups 2-A and 2-B are compared to the result obtained from setup 1. The comparison is shown in Figure 99. As expected, since the inductance loops in both setup 2-A and 2-B (see Figure 96 and Figure 98) are smaller than in setup 1 (see Figure 91), the tov. magnitudes in the beginning of the voltage step are lower in setups 2-A and 2-B than setup 1. This is consistent with the obtained results from the PSCAD simulation (see Figure 94).

A remark should be made to the measurement result of setup 2-B. The noise obtained within this recording has been originated from external sources. The comparison of the tov. results from PSCAD simulation and the ones from measurement is further shown in Figure 100. For better visual inspection only the results from the PSCAD simulation with stray L = 0.125 μH and stray inductive L = 0.32 μH to the recorded measurement from setups 1 and 2-A are compared.

Figure 95: Photo of surge capacitors are installed with short loop in setup 2-A

Figure 96: The sketch of surge capacitors installed with short loop in setup 2-A

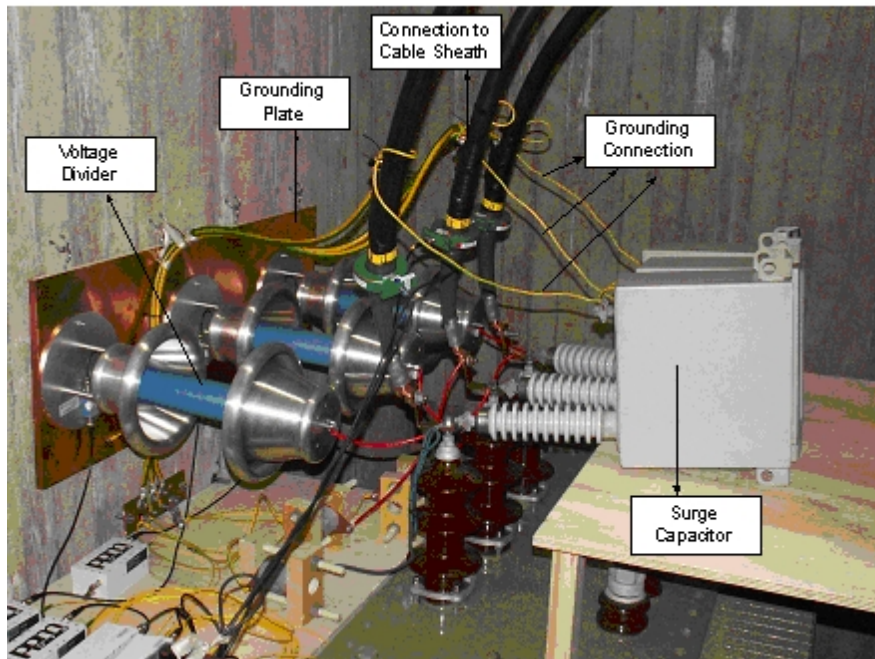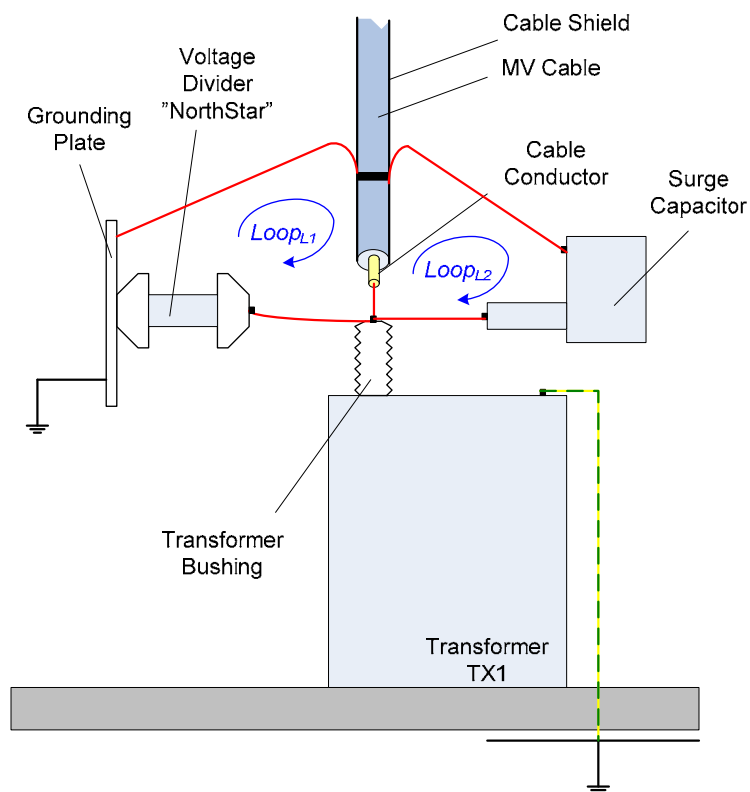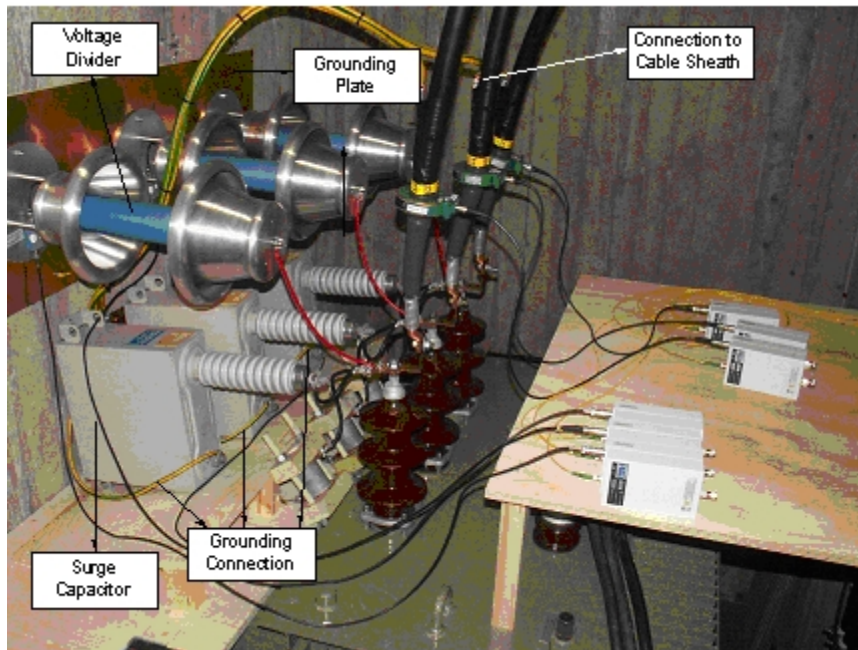*Figure 97: Photo of surge capacitors are installed with short loop in setup 2-B*
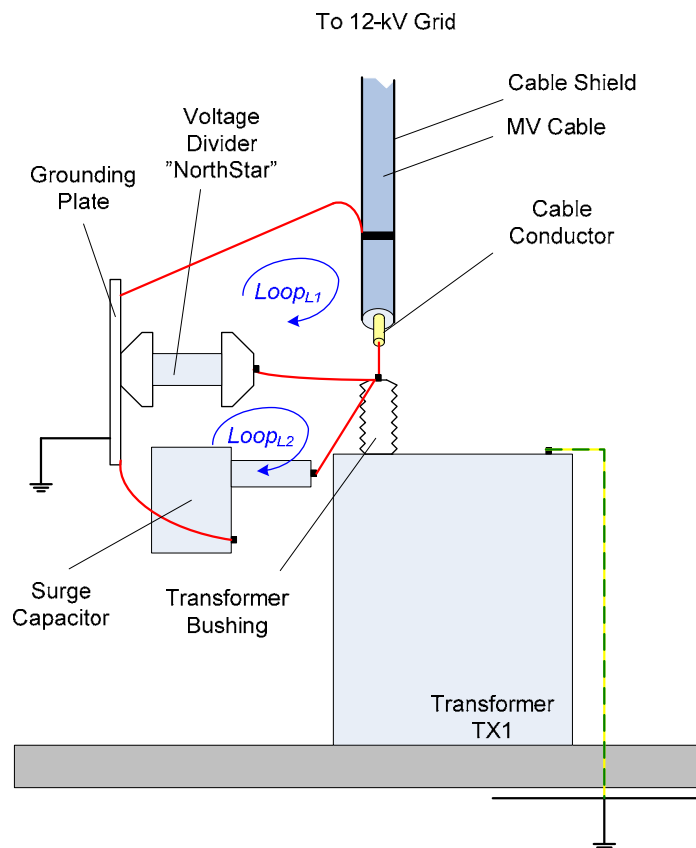
Figure 98: The sketch of surge capacitors installed with short loop in setup 2-B
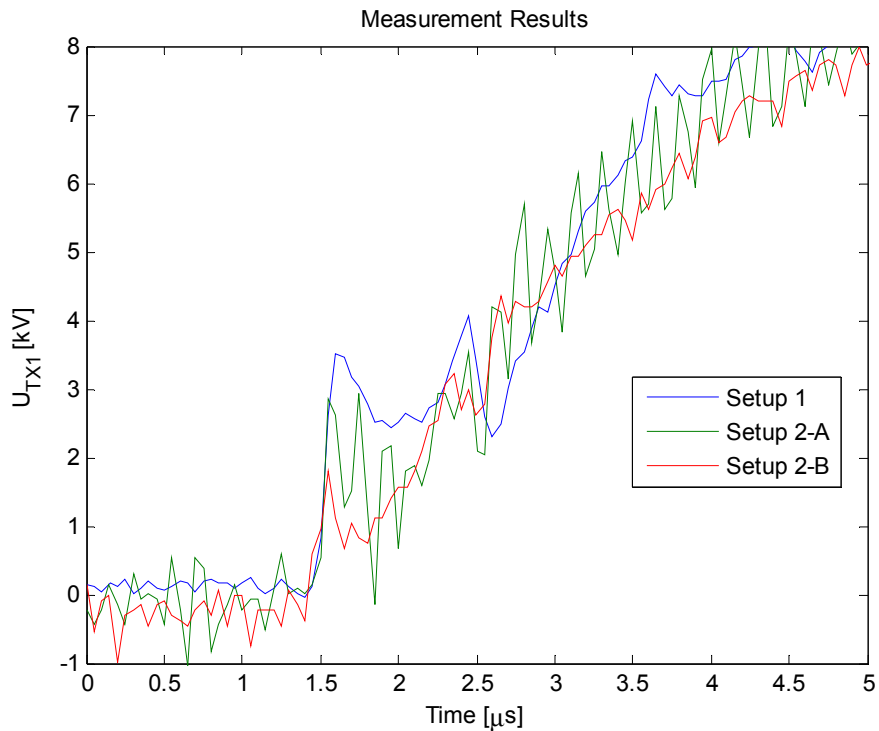
Figure 99: tov. recorded from measurement
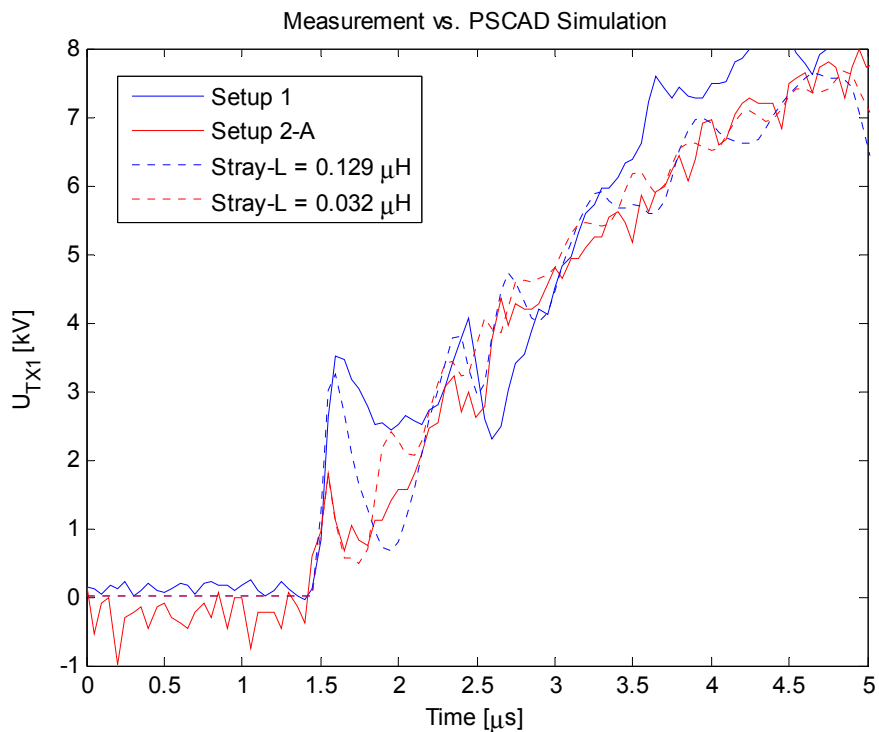
Figure 100: Comparing tov. from measurement with PSCAD simulation

12.3   PSCAD Simulation on Longer Inductance Loop

To further investigate the influence of this stray inductance, PSCAD is used to simulate the case where the stray inductance is higher. Two cases are then taken, the so called "case 5m" and "case 10 m". In both cases, 83 nF surge capacitors are installed; however they have different details as follow:

1. The case 5m is simulated by inserting a stray inductance equal to 8.06 μH to the PSCAD circuit shown in Figure 92. This 8.06 μH is obtained by applying (5) to a wire with 3 mm in diameter and 5 m in length.

2. The case 10m is simulated by inserting stray inductance equal to 17.5 μH to the PSCAD circuit shown in Figure 92. This 17.5 μH is obtained by applying (5) to a wire with 3 mm in diameter and 10 m in length.

The simulation results of the case 5 m and the case 10 m are displayed in Figure 101, and compared to the case when no surge capacitors are installed and the "ideal" case when surge capacitors (C = 83 nF) are installed without any inductance existed. As can be seen in Figure 101, with larger loops (e.g. equivalent to 5 to 10 m long wire), the magnitude of the tov. may reach up to 70% of its prospective value i.e. when the capacitors were not used.
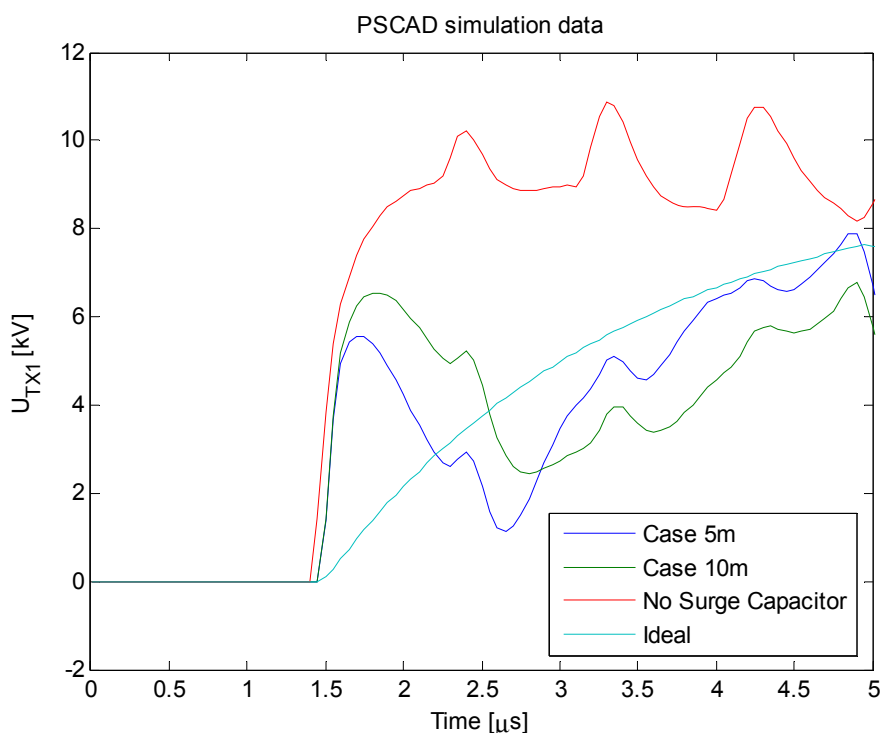
Figure 101: tov. from PSCAD simulation with different value stray inductance compared to cases with no surge capacitors installed and the ideal case when surge capacitors are installed without any stray inductance induced

13 Enclosure B: Concerns related to the Worst Cases (Section 2.4)

13.1 Operation Cases and Load Conditions

Normal operation in the SW1 point would be switching the medium voltage breaker in a correct sequence being coordinated with the LV side of the transformer. Closing operation will normally be performed with the transformer in no-load condition i.e. with open LV breakers/contactors. Normal breaking operations will also be performed with the transformer in no-load condition i.e. with open LV breakers/contactors, i.e. preceded by an LV opening operation.

However automatic trip or a manual operation during power flow from the actual windmill i.e. due to a fault or emergency can involve the interruption of a loaded transformer.

13.2 Phase Opposition between Network and Generator

Cases exist in theory while switching the medium voltage breaker in phase opposition to the generator side. Switching at points of phase opposition is not a normal operation and has not been covered by this study.

13.3 Interruption of Transformer Inrush Currents

Energizing a transformer through a cable involves a temporary saturation of the transformer iron core which causes inrush current peaks until the corresponding forced oscillation has been damped to steady state level. Tripping a breaker directly on closing could involve breaking the inrush current. Producing such a case requires operation of the windmill transformers at the nominal level of the transformer.

Inrush current cases could not be reproduced due to mismatch of the existing components in the laboratory, i.e. the transformers have been operated below their nominal level. This can be made after further investments in the laboratory and study object hardware.

13.4 Ground Fault Cases

System grounding and ground faults involve two major aspects regarding overvoltages, arrester protection level and arcing.

13.5 ZnO Protection Level

A gapless surge arrester shall be dimensioned to withstand the temporary overvoltages caused by an earth fault in the system. The temporary voltage during ground fault depends on the system neutral grounding impedance which also decides the minimum possible protection level for a certain diverted current defined by the V-I curve of the applied ZnO arrester. Consequently the neutral grounding impedance will decide the absolute voltage magnitude level for any switching surge occurring at the arrester terminals. Note that the voltage can still swing between the absolute levels of magnitude with opposite direction. In practice a 40 kV step can exist within the protection level band in a 12 kV system.

For these reasons a recommendation has been given to use low resistance neutral system grounding in windmill parks in order to enable lowest possible temporary over voltage level still providing current limitation. This solution is traditionally used in power generator installations.

The experimental laboratory provides an exception which does not require to follow the standard provisions regarding ground faults and safety rules. This is possible due to extra safety provisions and measures for the laboratory and the fact that the down scaled experimental installation has a low fault level. Consequently the actual ZnO protection level could be adjusted to simulate a possible resistance grounding approximately, i.e. at a lower level than given by the standard provisions.

Together with the artificial grounding and the selection of arrester block ratings and configurations, it has been possible to simulate the low resistance grounding with respect to the transient voltage swing without re-building or changing the transformers.

13.6 Open Arcs and Intermittent Earth Fault Situations.

The original plan was to study the effects of intermittent ground faults with possible repetitive re-strikes involved. This can be provided by a remotely controlled "bomb-dropping" of an open cable end into a water tray, all which has been prepared. However, the available windmill transformers being used in the experimental set-up are built as Y/D with the Delta- connected winding on the MV side. An artificial neutral grounding was provided during all experiments provided by three voltage transformer HV windings in delta connection, in order to define the neutral and to prevent dc charge of the system. However the artificial ground impedance was too high for any ground fault experiment.

A change to Y-connection is possible in the future, by rebuilding the transformer lid and provide an extra bushing or by substituting the transformers.

14   Enclosure C: Tables with All tov.-steepness-indicators defined in Section 4.2.4 recorded

Table 13 Summary of strikes indicators from the base case on all test routines (= Table 5)

Case	# strikes ($\Delta U > 5$ kV and within $\dfrac{\Delta U}{\Delta t} > 5$ kV/µs, phase a-b-c)	max ΔU (kV)	$\max\left(\dfrac{dU}{dt}\right)$		$\left(\dfrac{dU}{dt}\right)_{10\%-90\%}$	
			filtered kV/µs)	un-filtered (kV/µs)	filtered (kV/µs)	un-filtered (kV/µs)
Closing breaker at no load	3	10.5	27	42	13	16
Opening breaker at no load	3	7.5	19	35	12	13
Closing breaker with inductive Load connected	30	13	30	52	22	22
Opening breaker with inductive Load connected	282	43	114	211	86	82

Table 14 Base Case: Closing breaker at no load – statistical data collection (= Table **6**)

Case (shot #)	# strikes (ΔU > 5 kV and within $\frac{\Delta U}{\Delta t}$ > 5 kV/µs, phase a-b-c)	max ΔU (kV)	$\max\left(\dfrac{dU}{dt}\right)$		$\left(\dfrac{dU}{dt}\right)_{10\%-90\%}$	
			filtered kV/µs)	un-filtered (kV/µs)	filtered (kV/µs)	un-filtered (kV/µs)
0430.006	2	10.5	27	48	15	17
0430.007	2	11	28	47.5	19	21.5
0430.008	3	10.5	27	42	13	16
0430.009	3	10.5	27	44	14	17
0430.010	2	11	32	51	30	29

Table 15 Base Case: Opening breaker with an inductive load connected – statistical data collection (= Table 7)

Case (shot #)	# strikes (ΔU > 5 kV and within $\frac{\Delta U}{\Delta t}$ > 5 kV/µs, phase a-b-c)	max ΔU (kV)	$\max\left(\dfrac{dU}{dt}\right)$		$\left(\dfrac{dU}{dt}\right)_{10\%-90\%}$	
			filtered kV/µs)	un-filtered (kV/µs)	filtered (kV/µs)	un-filtered (kV/µs)
0429.011	282	43	114	211	86	82
0429.012	264	43	116	186	85.5	96
0429.013	323	42	109	197.5	88	102
0429.014	274	43	116.5	187.5	87	87
0429.015	230	41.5	112	180.5	82.5	84

Table 16 Summary of Strikes Quantifications on cases with Surge Protections: at breaker opening with an inductive load connected (worst cases) (= Table 8)

Case ID	# strikes ($\Delta U > 5$ kV and within $\dfrac{\Delta U}{\Delta t} > 5$ kV/μs, phase a-b-c)	max ΔU (kV)	$\max\left(\dfrac{dU}{dt}\right)$		$\left(\dfrac{dU}{dt}\right)_{10\%-90\%}$	
			filtered kV/μs)	un-filtered (kV/μs)	filtered (kV/μs)	un-filtered (kV/μs)
C83-TX1	129	25	50	128	42	191.5
C130-TX1	145	16.5	52	114	44	148
C130-BRK	190	21	57	131	52	87

Table 17 Summary of Strikes Quantifications on cases with RC-Protections: at breaker opening with an inductive load connected (worst cases) (Table 9)

Case ID	# strikes ($\Delta U > 5$ kV and within $\dfrac{\Delta U}{\Delta t} > 5$ kV/μs, phase a-b-c)	max ΔU (kV)	$\max\left(\dfrac{dU}{dt}\right)$		$\left(\dfrac{dU}{dt}\right)_{10\%-90\%}$	
			filtered kV/μs)	un-filtered (kV/μs)	filtered (kV/μs)	un-filtered (kV/μs)
R30C83-TX1	63	27	85	146	72,5	87
R20C83-TX1	50	25	81	168	67	101
R20C130-TX1	38	24	76	156	63	76
R30C83-TX1-C130-TX2	34	20	62	119	53	68

Table 18 Summary of the strikes quantifications from the typical worst cases tested (= Table 10)

Case ID	# strikes ($\Delta U > 5$ kV and within $\frac{\Delta U}{\Delta t} > 5$ kV/μs, phase a-b-c)	max ΔU (kV)	$\max\left(\dfrac{dU}{dt}\right)$		$\left(\dfrac{dU}{dt}\right)_{10\%-90\%}$	
			filtered kV/μs)	un-filtered (kV/μs)	filtered (kV/μs)	un-filtered (kV/μs)
Base Case	230-323	42-43	109-116	180-211	82-88	82-102
C83-TX1	129	25	50	128	42	191.5
C130-TX1	145	16.5	52	114	44	148
C130-BRK	190	21	57	131	52	87
R30C83-TX1	63	27	85	146	72,5	87
R20C83-TX1	50	25	81	168	67	101
R20C130-TX1	38	24	76	156	63	76
R30C83-TX1-C130-TX2	34	20	62	119	53	68
Point-on-Wave	-	-	-	-	-	-

Table 19 Summary of the worst strikes quantifications (only surge arresters installed)
(= Table 11)

Case (shot #)	# strikes ($\Delta U > 5$ kV and within $\frac{\Delta U}{\Delta t} > 5$ kV/μs, phase a-b-c)	max ΔU (kV)	$\max\left(\dfrac{dU}{dt}\right)$		$\left(\dfrac{dU}{dt}\right)_{10\%-90\%}$	
			filtered kV/μs)	un-filtered (kV/μs)	filtered (kV/μs)	un-filtered (kV/μs)
0429.011	282	43	114	211	86	82
0429.012	264	43	116	186	85.5	96
0429.013	323	42	109	197.5	88	102
0429.014	274	43	116.5	187.5	87	87
0429.015	230	41.5	112	180.5	82.5	84

Table 20 Standard LIWL [14] versus recorded breaker switching transients
(= Table 12)

	LIWL (at Un = 12 kV)	Surge Arresters	Surge Arresters + Surge Capacitors	Surge Arresters + RC Protection	Surge Arresters + RC Protection + Surge Capacitors
Steepness */ **/*** /**** (kV/μs)**	62.5	110-116/180-211/82-88/82-102	50-57/114-131/42-52/87-192	76-85/146-168/63-73/76-101	62/119/53/68
Magnitude (kV)	75	42-43	17-25	24-27	20
Number of Strikes (#)	1	230-323	120-190	38-63	34

* = $^{\max\left(\frac{dU}{dt}\right)}$-filtered;   ** = $^{\max\left(\frac{dU}{dt}\right)}$-unfiltered;   *** = $\left(\frac{dU}{dt}\right)_{10\%-90\%}$-filtered;   **** = $\left(\frac{dU}{dt}\right)_{10\%-90\%}$-unfiltered